US Army Corps
of Engineers
Construction Engineering
Research Laboratories

USACERL Technical Report 97/84
June 1997

CONSTRUCTION PRODUCTIVITY ADVANCEMENT RESEARCH (CPAR) PROGRAM

Development of High-Performance Lightweight Concrete Masonry Units

by

Steven C. Sweeney, Pamalee A. Brady, Maher K. Tadros,
Gary L. Krause, Joan D. Bowser, Babrak Amiri, Savita M. Kulkarni,
Ahmed E. Magzoub, Say-Gunn Low, Amin Einea,
Magdi A. Khalifa, and Ervall Staab

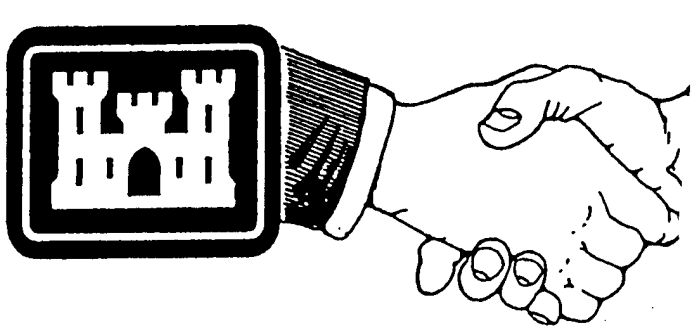

A Corps/Industry Partnership To Advance
Construction Productivity and Reduce Costs

USER EVALUATION OF REPORT

REFERENCE: USACERL Technical Report 97/84, *Development of High-Performance Lightweight Concrete Masonry Units*

Please take a few minutes to answer the questions below, tear out this sheet, and return it to USACERL. As user of this report, your customer comments will provide USACERL with information essential for improving future reports.

1. Does this report satisfy a need? (Comment on purpose, related project, or other area of interest for which report will be used.)

_____

_____

_____

2. How, specifically, is the report being used? (Information source, design data or procedure, management procedure, source of ideas, etc.)

_____

_____

3. Has the information in this report led to any quantitative savings as far as manhours/contract dollars saved, operating costs avoided, efficiencies achieved, etc.? If so, please elaborate.

_____

_____

4. What is your evaluation of this report in the following areas?

   a. Presentation: _____

   b. Completeness: _____

   c. Easy to Understand: _____

   d. Easy to Implement: _____

   e. Adequate Reference Material: _____

   f. Relates to Area of Interest: _____

   g. Did the report meet your expectations? _____

   h. Does the report raise unanswered questions? _____

i. General Comments. (Indicate what you think should be changed to make this report and future reports of this type more responsive to your needs, more usable, improve readability, etc.)

_____

_____

_____

_____

_____

_____

5. If you would like to be contacted by the personnel who prepared this report to raise specific questions or discuss the topic, please fill in the following information.

Name: _____

Telephone Number: _____

Organization Address: _____

_____

_____

6. Please mail the completed form to:

Department of the Army
CONSTRUCTION ENGINEERING RESEARCH LABORATORIES
ATTN: CECER-TR-I
P.O. Box 9005
Champaign, IL 61826-9005

REPORT DOCUMENTATION PAGE

Form Approved
OMB No. 0704-0188

1. AGENCY USE ONLY *(Leave Blank)*	2. REPORT DATE	3. REPORT TYPE AND DATES COVERED
	June 1997	Final

4. TITLE AND SUBTITLE
Development of High-Performance Lightweight Concrete Masonry Units

5. FUNDING NUMBERS
CPAR FAD 90-080398,
dated 27 June 1990
WU LR0

6. AUTHOR(S)
Steven C. Sweeney, Pamalee A. Brady, Maher K. Tadros, Gary L. Krause, Joan D. Bowser, Babrak Amiri, Savita M. Kulkarni, Ahmed E. Magzoub, Say-Gunn Low, Amin Einea, Magdi A. Khalifa, and Ervall Staab

7. PERFORMING ORGANIZATION NAME(S) AND ADDRESS(ES)
U.S. Army Construction Engineering Research Laboratories (USACERL)
P.O. Box 9005
Champaign, IL 61826-9005

8. PERFORMING ORGANIZATION REPORT NUMBER
TR 97/84

9. SPONSORING / MONITORING AGENCY NAME(S) AND ADDRESS(ES)
Headquarters, U.S. Army Corps of Engineers
ATTN: CEMP-ET
20 Massachusetts Ave. NW
Washington, DC 20314-1000

10. SPONSORING / MONITORING AGENCY REPORT NUMBER

11. SUPPLEMENTARY NOTES
Copies are available from the National Technical Information Service, 5285 Port Royal Road, Springfield, VA 22161.

12a. DISTRIBUTION / AVAILABILITY STATEMENT
Approved for public release; distribution is unlimited.

12b. DISTRIBUTION CODE

13. ABSTRACT (Maximum 200 words)

Masonry construction continues to predominate in U.S. military construction and other sectors, but there has been little improvement in masonry structural technology for several decades. Without improvements in materials and productivity, the cost of masonry construction will significantly increase. To help keep masonry construction affordable, the U.S. Army Construction Engineering Research Laboratories (USACERL) initiated a Cooperative Research and Development Agreement with the University of Nebraska Center for Infrastructure Research to develop a lightweight high-strength concrete masonry unit (CMU).

The objective of this research was to merge high-strength concrete and lightweight concrete technologies to produce a high-performance lightweight CMU up to 50 percent lighter than normal-weight units while maintaining or improving structural characteristics. The work produced a new type of high-strength lightweight CMU that can be manufactured using industry-standard equipment and meets or exceeds all performance-based requirements for block masonry. Using expanded shale aggregates and an optimized unit shape as the primary innovative components, the high-performance lightweight CMUs weigh about 8.6 kg and have average net compressive strength of 4000 lb/in.^{2} The minimum void gradation of the expanded shale was modified to provide high strength, good durability, and a smooth, uniform texture.

Details on mix design and optimized block shape are provided.

14. SUBJECT TERMS
Construction Productivity Advancement Research (CPAR)
concrete
masonry

15. NUMBER OF PAGES
144

16. PRICE CODE

17. SECURITY CLASSIFICATION OF REPORT	18. SECURITY CLASSIFICATION OF THIS PAGE	19. SECURITY CLASSIFICATION OF ABSTRACT	20. LIMITATION OF ABSTRACT
Unclassified	Unclassified	Unclassified	SAR

Foreword

This study was conducted for Headquarters, U.S. Army Corps of Engineers under "Construction Productivity Advancement Research (CPAR); Work Unit LR0, High-strength Ultralight CMU"; Funding Authorization Document (FAD) 90-080398 dated 27 June 1990. The technical monitor was Charles Gutberlet, CEMP-ET.

The work was performed by the Engineering Division (FL-E) of the Facilities Technology Laboratory (FL), U.S. Army Construction Engineering Research Laboratories (USACERL). The USACERL principal investigator was Steven C. Sweeney. Larry M. Windingland is Acting Chief, FL-E, and Donald F. Fournier is Acting Operations Chief, FL.

Dr. Michael J. O'Connor is the Director of USACERL.

Contents

List of Figures and Tables

Figures

Tables

1 Introduction

1.1 Background

The masonry industry has seen little change or improvement in structural technology for several decades. While new steel alloys, high-strength bolts, and high-strength concretes were being developed, masonry materials and construction remained the same. However, masonry construction has continued to predominate in military construction. Without improvements in materials and productivity, the cost of masonry construction will significantly increase.

Worker productivity is an important driver of masonry construction costs. The masonry trade is appealing for several reasons. Because masonry construction is so efficient, salaries are often higher than for other trades. Common cold-weather construction techniques allow masons to work during seasons when other tradespeople are usually laid off. However, there is one significant drawback that keeps many prospective young masons from entering the trade: the standard modern concrete masonry unit (CMU) weighs approximately 38 lb, and the burden of lifting these blocks can become very tedious and tiring. After only relatively few years on the job some masons must retire prematurely due to physical disabilities related to the heavy lifting of masonry blocks. Others suffer crippling back and shoulder injuries before retirement. Such hazards of the masonry trade could be substantially reduced with the widespread adoption of lightweight CMUs by the U.S. construction industry.

Lightweight aggregates for masonry have been on the market for several years, and many concrete block manufacturers offer a standard lightweight block. However, the lightweight units available on the market so far have been handicapped by low net compressive strengths—usually below 2000 psi. An even bigger problem has been their high water absorption and low durability. These problems have prevented standard lightweight blocks from gaining wide acceptance in the U.S. construction industry. To reap the potential cost benefits offered by lightweight CMUs, an improved design and material composition is needed that exhibits strength, absorption, and durability characteristics comparable to the standard normal-weight CMU.

To help keep masonry as a viable and economic means of construction in the United States, the U.S. Army Construction Engineering Research Laboratories (USACERL) initiated a Cooperative Research and Development Agreement (CRDA) to develop a lightweight and durable high-strength CMU in partnership with the University of Nebraska Center for Infrastructure Research. The project was funded and coordinated under the Army Corps of Engineers Construction Productivity Advancement Research (CPAR) program.

1.2 Objectives

The objective of this research was to merge the high-strength concrete and lightweight concrete technologies to produce a high-performance lightweight CMU up to 50 percent lighter than normal weight units while maintaining or improving structural characteristics. In addition, the unit was intended to be compatible as possible with existing block-making equipment to facilitate implementation in the market.

1.3 Approach

The work was divided into two phases. In the first phase, optimization of the masonry unit shape was conducted. Finite element analysis was used to perform stress analysis and refine the shape of the unit. Next, a basic mix was developed using fly ash and silica fume with cement and lightweight aggregates. Optimization of the mix was performed by producing several trial mixes in the laboratory. The specimens were tested for compressive strength. The optimum amounts of cementitious material and fly ash in the mix were determined based on the laboratory test results. Lightweight aggregates, with a maximum size of 3/8 in. (9.525 mm), were blended together to give the minimum void gradation for high-strength and better texture. The optimized shape and mix proportions were used to produce units commercially. A unit weighing 18 lb (8.2 kg) and with an average net compressive strength of 3500 lb/sq in. (24.1 MPa) was produced.

Many difficulties were faced in commercial production of the units during the first phase. Analysis of these problems led the researchers to:

- Change the aggregate gradation and reduce the maximum size of the aggregate.
- Use a high dosage of admixtures to improve the workability of the mix.
- Increase the feed and vibration time.

- Carefully monitor the amount of water added to the mix to avoid stickiness and lumpiness.

The second phase of the work focused on overcoming the initial problems faced during commercial production of the new CMUs. The effects of different types of aggregate, cementitious material, and admixture on the strength of both lightweight and normal-weight units were investigated. Durability tests of the new units were conducted. Cost and manufacturing productivity of the units were also evaluated.

1.4 Scope

This report summarizes numerous studies to determine the optimum configuration and materials for a new type of lightweight high-performance CMU. Two alternative units were developed:

1. a CMU formed in an optimized A-configuration and made of normal-weight high-strength materials (normal-weight high-performance unit)
2. a CMU formed in the same optimized A-configuration but made of lightweight materials (lightweight high-performance unit).

1.5 Metric Conversion Factors

U.S. standard units of measure are used throughout this report. A table of metric conversion factors is presented below.

1 in.	=	25.4 mm
1 ft	=	0.305 m
1 ft^2	=	0.093 m^2
1 ft^3	=	0.028 m^3
1 yd^3	=	0.7646 m^3
1 oz	=	28.35 g
1 lb	=	0.453 kg
1 psi	=	6.89 kPa
°F	=	(°C × 1.8) +32

2 Unit Shape

2.1 Introduction

This chapter discusses the shape optimization of an 8 x 8 x 16-in. CMU.

Concrete masonry units are fabricated in many different shapes. The conventional shape of the normal-weight unit is shown in Figure 2.1.* This two-voided shape has been used for many years. Nevertheless, there are some drawbacks to this shape. When the units are laid in the running bond, the cells do not line up, and this creates difficulties in grouted masonry construction. In addition, due to the closed cells, masons must lift the units over pre-placed reinforcing bars, essentially "threading" them over the reinforcement. These drawbacks are eliminated by modifying the shape of the high-performance CMU.

2.2 Practical Considerations for Shape Design

The standard 8 x 8 x 16-in. CMU shown in Figure 2.1 is the most widely used unit in U.S. masonry construction. Recently, this shape has been developed into an open-end block (A-block) as shown in Figure 2.2. The unit meets all the ASTM C 90 dimensional requirements. One benefit of this A-configuration is the elimination of the need to lift a block and "thread" it over pre-placed vertical reinforcement. In addition to increasing productivity, this feature also reduces the number of reinforcement lap splices and improves the cell size and alignment for grouting. For these reasons, the A-block configuration was used as the basis for optimizing the shape of the high-performance block.

Before the block shape was optimized analytically, the vertical cell alignment of successive block courses was evaluated for the commonly used running bond pattern of masonry construction (Figure 2.3). Results of this study indicated that the center web of the existing A-block configuration should be shifted 5/8-in. from the centerline towards the closed cell. This shift resulted in perfect alignment of the cells for improved grouting.

---

* Figures and tables are located at the end of the chapter in which they are first discussed.

Placement of joint reinforcement between blocks was also considered. Manufacturers of joint reinforcement indicated that it can be placed within a 7/8-in. mortar bed with adequate mortar cover for corrosion protection. Web and face shell thickness of 7/8-in. were therefore assumed in the preliminary design of the high-performance block.

2.3 Analytical Study

After the general shape and preliminary dimensions of the block were established, the shape optimization study was conducted. The main criterion of the shape optimization study was to use the least possible amount of material while maintaining the same margin of safety against breakage due to grout pressure as a unit that meets ASTM C 90 standards. The shape design of the 16-in. open-end unit was performed with the general purpose finite element analysis (FEA) computer program, ANSYS (ANSYS, Inc., Canonsburg, PA 15357).

2.3.1 Analysis Assumptions

The FEA was meant to provide relative performance data for the proposed unit as compared with a standard open-end unit meeting ASTM C 90 requirements. Parameters used in the optimization process were based on the results of a previous study of an open-end unit that satisfied ASTM C 90 dimensional requirements. The assumptions for this analysis are as follows:

1. Minimum thickness of face and web shells is 7/8 in.
2. Restraint at bed and head joints due to mortar and adjacent units is ignored.
3. Grout is assumed to be totally fluid, with an equivalent fluid unit weight of 140 lb/ft^3.
4. Grout height was assumed to be 3.7 ft; that corresponds to a grout pressure of 3.6 psi.
5. The allowable tensile stress of masonry in flexure is:

$$= \frac{7.5\sqrt{f'_m}}{SF} \qquad \text{[Eq 2-1]}$$

where f'_m is the compressive strength of CMU and SF is the safety factor.*

* Equation 2-1 is identical to the allowable tensile strength for plain concrete set by ACI subcommittee 318 (ACI 318-95). There is no ASTM limit on tensile strength of CMU, so Equation 2-1 is used to predict the tensile strength of the block. While Section 2412(c) 4B of the UBC limits the modulus of rupture of a partially grouted masonry wall to 2 times the square root of f'_m and less than 125 psi, it was assumed these limits were applicable only to masonry assemblies and account for the relatively weak mortar joint. The "pure" masonry units themselves would have a modulus of rupture comparable to other concrete materials. The validity of this assumption will be evaluated by experimental test results.

6. Masonry compressive strength is 4000 psi, above the minimum compressive strength of 1,900 psi required by ASTM standards.

Assuming a safety factor of 1.33, the tensile strength of the new shape was 357 psi using Equation 2-1.

2.3.2 Minimum Web Thickness

ASTM C 90 requires 8 x 8 x 16-in. units to have a minimum equivalent web thickness of 2.25 in. per foot. For partially grouted walls, C 90 states: "equivalent web thickness doesn't apply to the portion of the unit to be filled with grout. The length of that portion shall be deducted from the overall length of the unit for the calculation." Applying these provisions to a partially grouted wall using the optimized 8 x 8 x 16-in. open-end units with a grout spacing of 6 ft, the minimum equivalent web thickness required is calculated as follows:

$$\frac{2.25 \text{ in. thickness}}{16 \text{ in.}} \times \frac{(72 \text{ in.} - 8 \text{ in.})}{6\text{-ft length section}} = \frac{9.0 \text{ in.}}{6\text{-ft wall section}}$$

The amount of equivalent web thickness provided by the new blocks is 9 (webs), or 9 × 7/8 in., which equals 7.88 in. over a 6-ft length. This thickness does not meet the ASTM requirement. A similar calculation shows that the minimum web thickness requirement is met if a 32 in. grout spacing is specified.

This calculation does not give enough credit to the presence of grout. For example, the new shape with 6-ft grout spacing has larger total web thickness (15.88 in.) than the standard ungrouted sample (13.50 in.). When comparing a wall containing the optimized units and 6-ft grout spacing with an ungrouted wall containing the standard units, no apparent loss in out-of-plane shear resistance or in pure axial load capacity exists. However, until ASTM C 90 is revised to recognize this type of comparison, testing according to the following section must be conducted to confirm the unit strength. ASTM C 90 does, however, permit the use of the optimized A-configuration when all cells are fully grouted.

2.3.3 Block Prototype Dimensions

Results of a preliminary analysis of the block shape indicated a maximum tensile stress of 530 psi located at the junctions between the middle web and the face shells. The section was redesigned by adding 7/8-in. haunches in this region, permitting stress redistribution. Dimensions of the haunches were obtained from

the optimization routine of the computer program based on the allowable tensile stress. Figure 2.4 shows the modeling of one-half of the block and the corresponding stress contours when the model is subjected to 3.6 psi of grout pressure. The optimized dimensions of the block are shown in Figure 2.5.

2.4 Shape Optimization and Final Design

The preliminary shape of the unit was established prior to detailed stress analysis. An open-end (A-shape) unit was selected to facilitate construction without the need for "threading" the unit through pre-placed vertical reinforcement. A 7/8-in. minimum thickness was used for both cross-webs and face shells, taking into consideration the production of the unit, placement of horizontal reinforcement, and laying of the unit at the site. The middle web was positioned to align vertically so that the grout can easily fill unit cells, and the mortared cross webs can provide adequate dams to prevent grout from filling adjacent cells in a partially grouted wall.

Two-dimensional FEA was conducted to determine critical stress regions and magnitude of tensile stresses. Analysis results showed that fillets were required in high tensile stress regions to redistribute the stresses.

Testing was conducted to establish the compressive strength, tensile strength, and flexural strength of the optimized unit. The strength evaluation of the units is presented in Chapter 4. Issues on the transportation, handling, durability, and texture of the new unit were also addressed and summarized in Chapter 6.

Based on these evaluations, a final block was designed with modifications for several practical requirements. A wider head joint was provided and mortar grooves on both ends of the unit were added. The face shell thickness of 7/8 in. (22.23 mm) was insufficient for making grooves for a good head joint, so the thickness was gradually increased from 7/8 in. (22.23 mm) to 1-1/4 in. (31.75 mm), for a 2- 9/16 in. (65.1 mm) length of face shell near the open end. Due to these modifications, the volume of the unit increased by 2 percent. This modified shape is shown in Figure 2.6.

In addition to the 16-in. blocks, 24-in. long units were also produced. A survey was conducted to get opinions of masonry contractors about 24-in. masonry units. The response to this survey was very encouraging, so it was decided to produce 24-in. units using the new high-performance lightweight and normal-weight mixes. The shape of the 24-in. unit is shown in Figure 2.7.

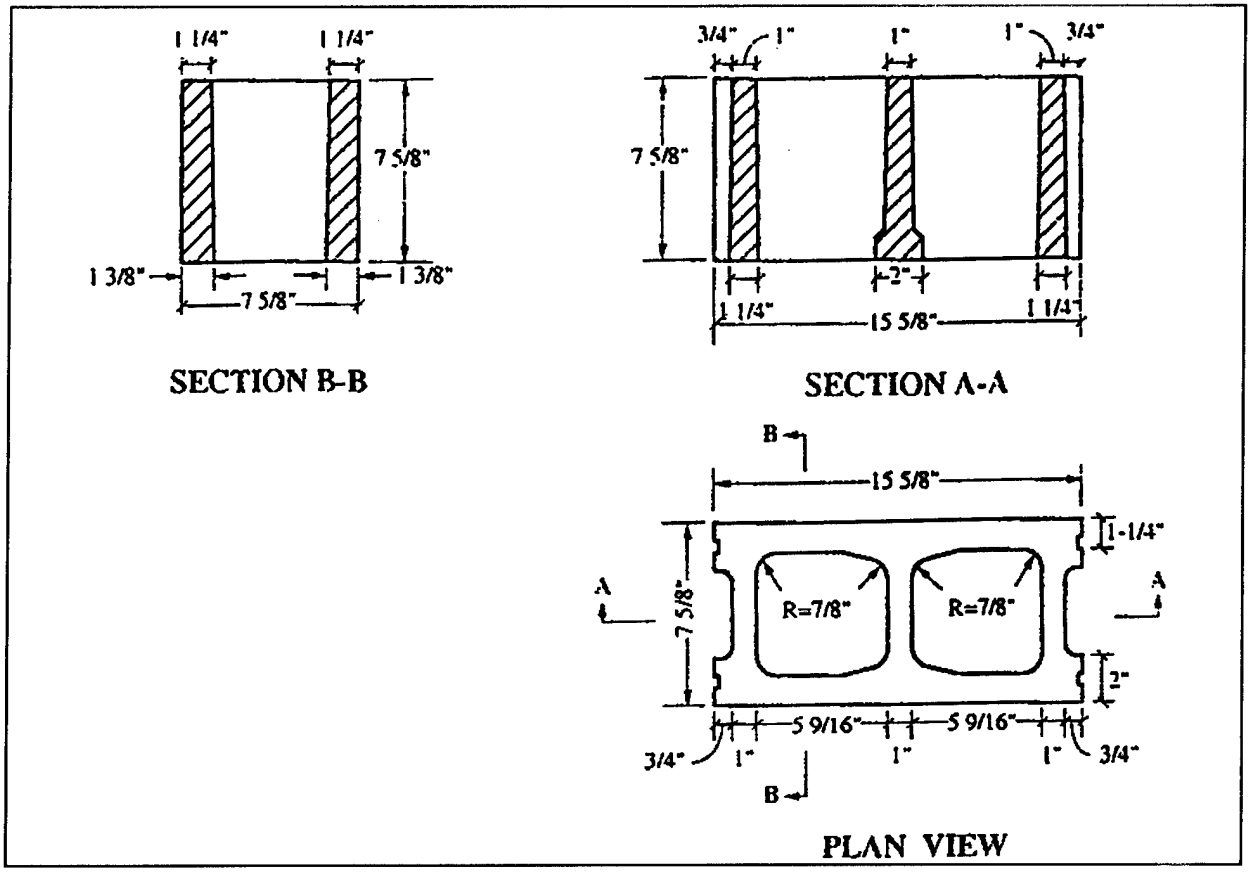

Figure 2.1. Standard 8 x 8 x 16-in. normal weight CMU (formblock).

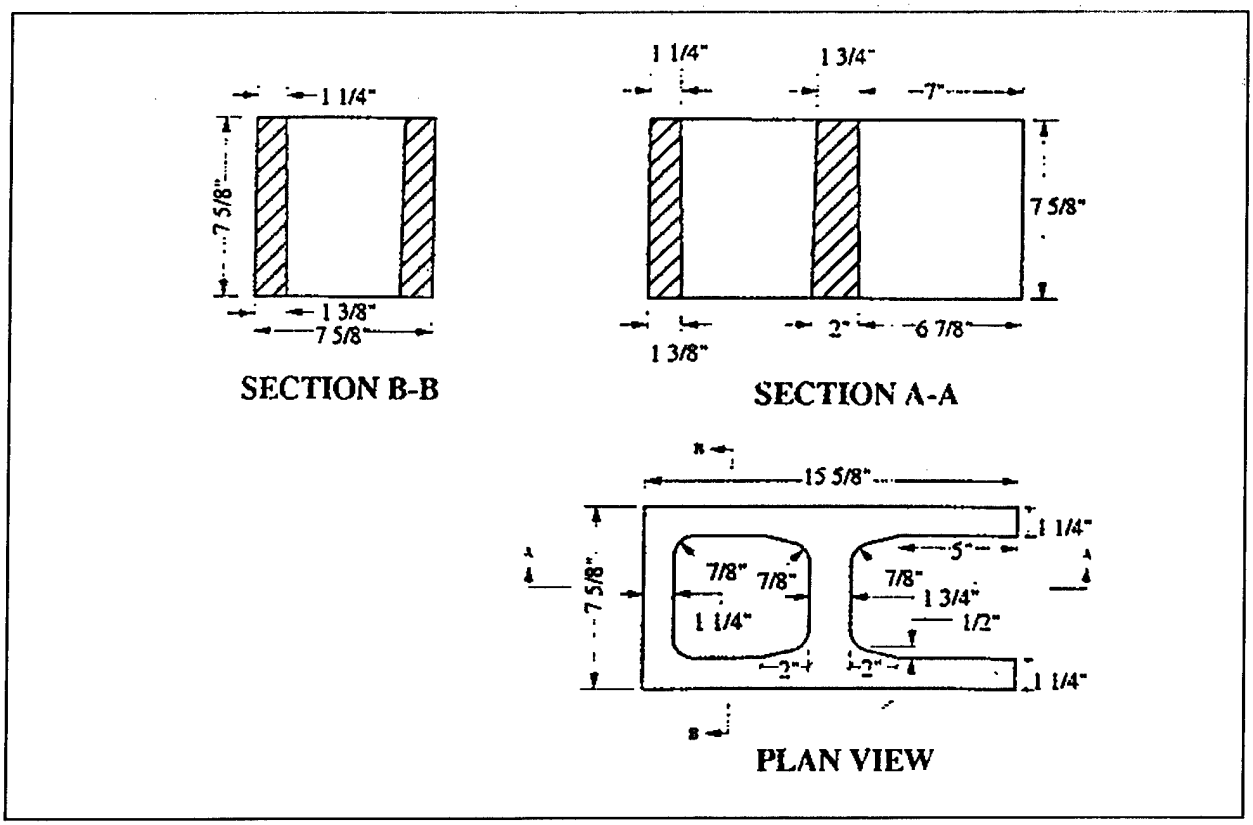

Figure 2.2. Standard 8 x 8 x 16-in. open-end CMU (A-block).

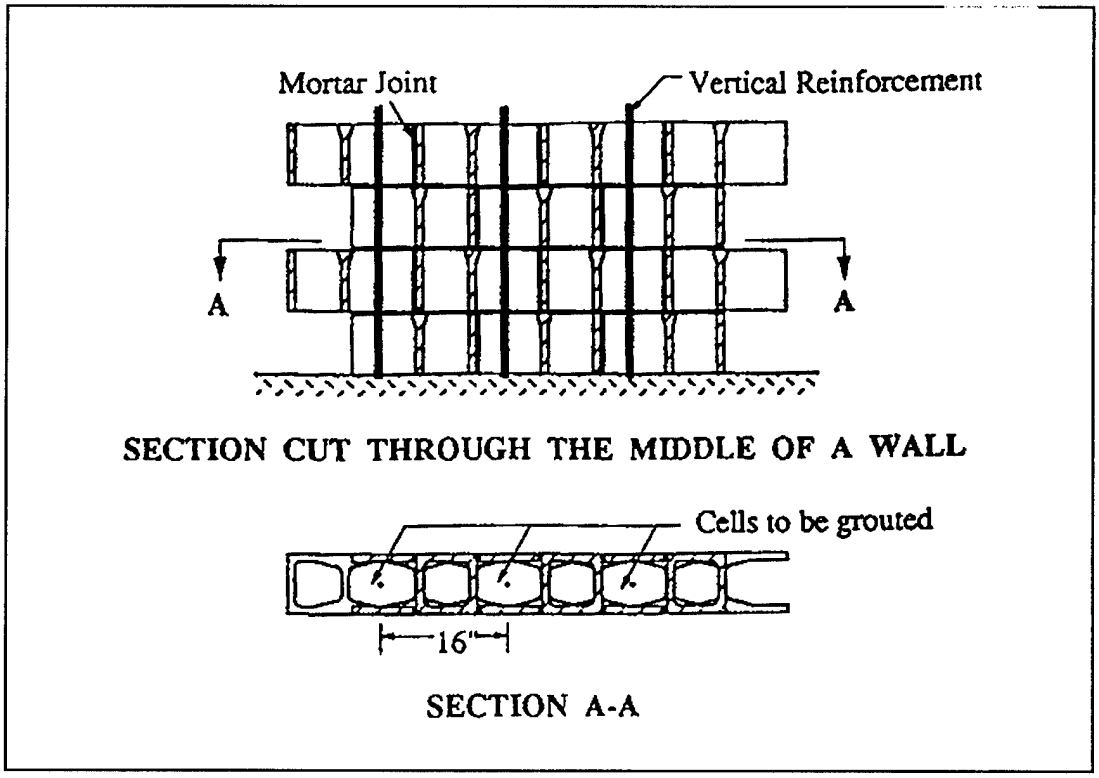

Figure 2.3. Indexing of 8 x 8 x 16-in. CMU.

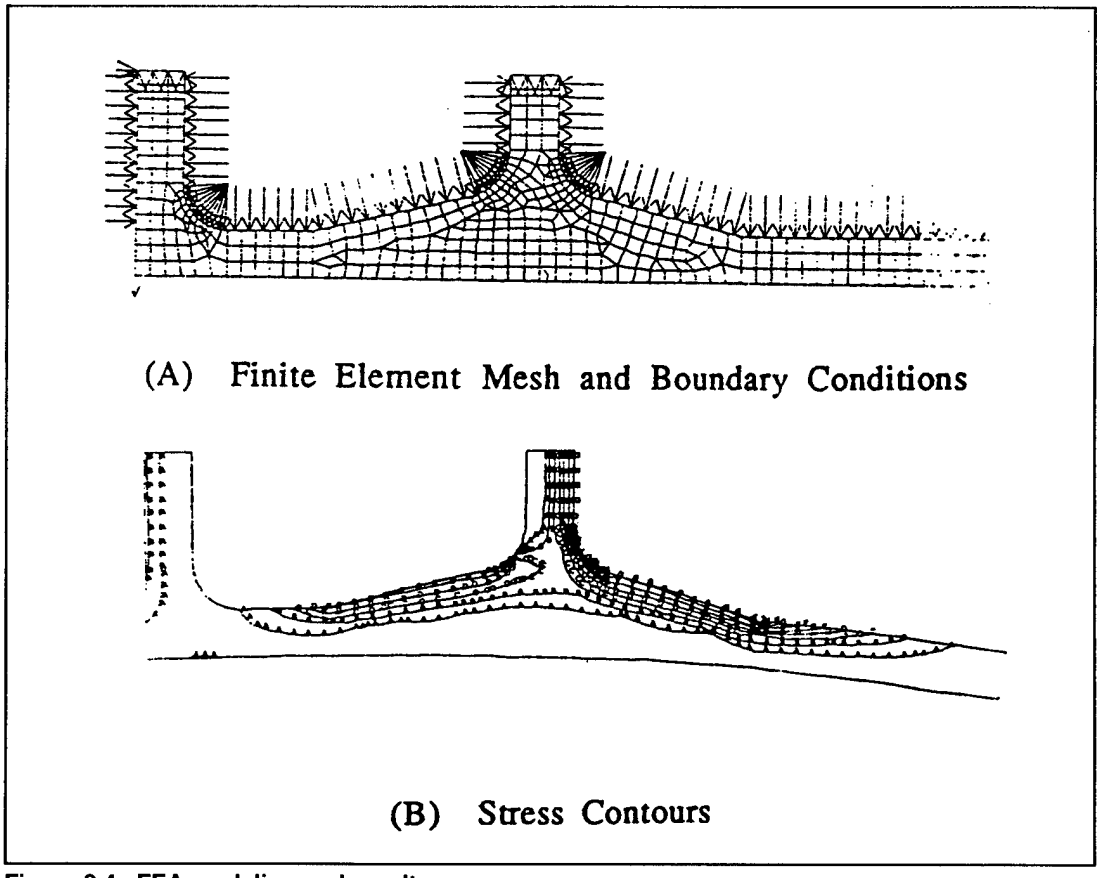

Figure 2.4. FEA modeling and results.

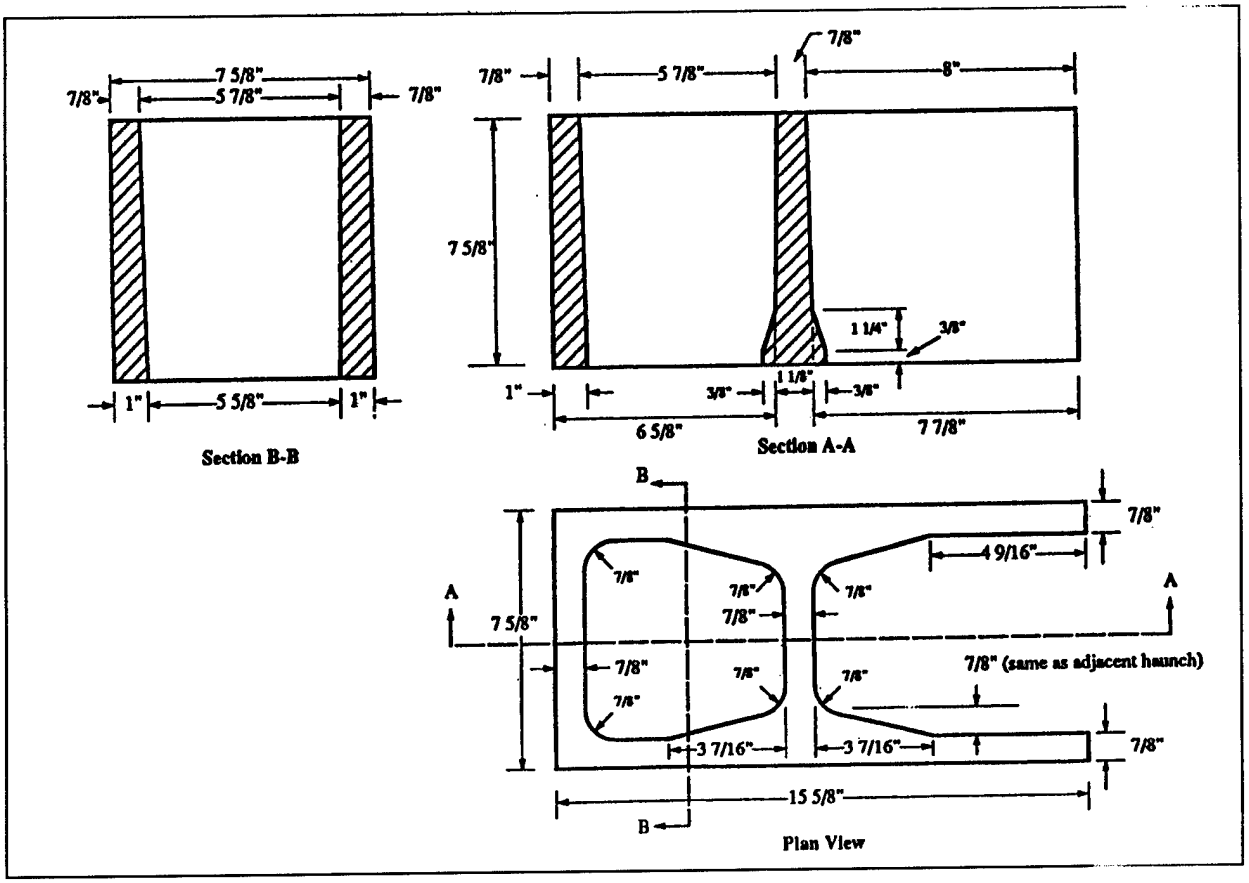

Figure 2.5. Optimized block dimensions.

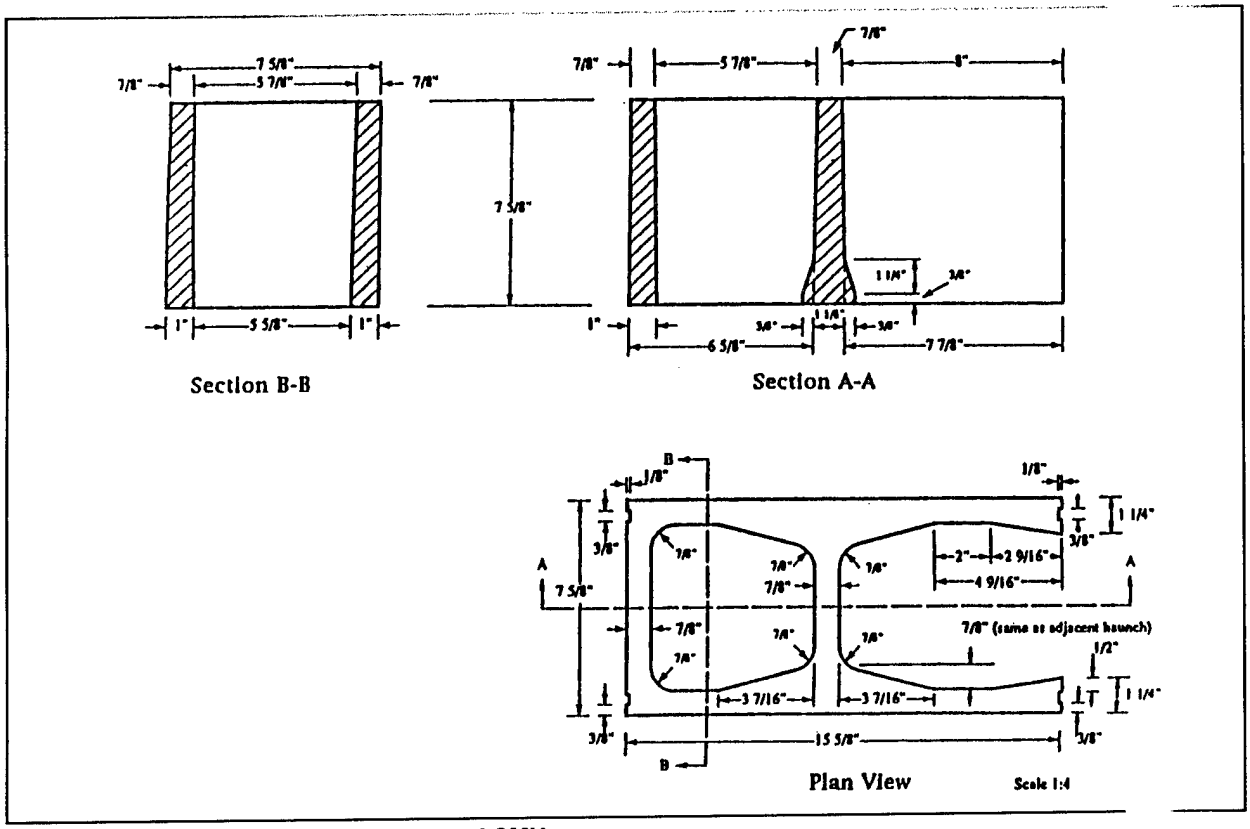

Figure 2.6. Modified optimized A-shape of CMU.

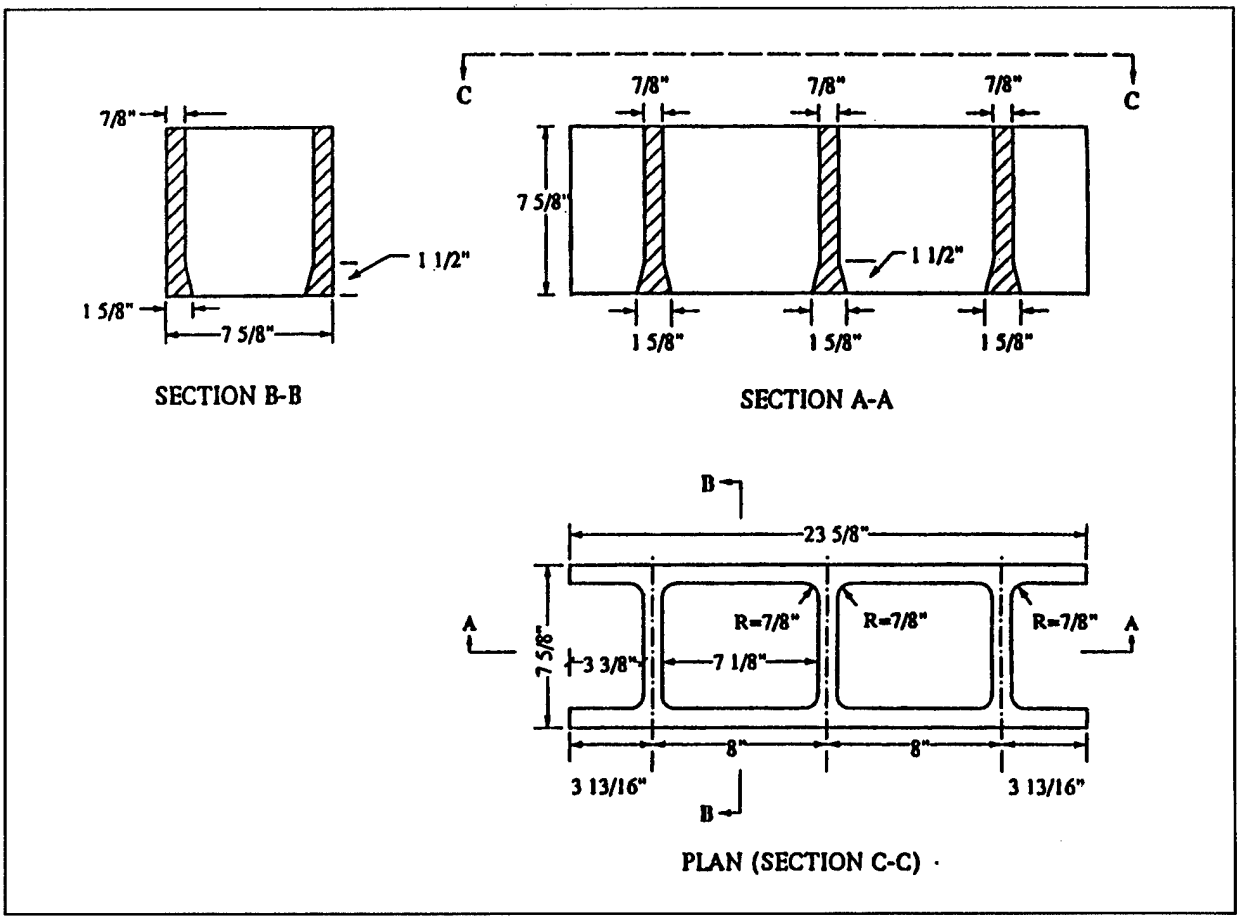

Figure 2.7. Shape of 24-in. CMU.

3 Mix Design and Optimization

3.1 Introduction

This chapter discusses the evaluation of materials that make up a typical concrete block mix: aggregate, cementitious material, and admixtures. The basic mix design, mix optimization, and the final design mixes for high-strength normal-weight and lightweight CMUs are described.

Mix design for lightweight CMUs was a primary focus of this work. The research evaluated the aggregates and cementitious material content of the mix to achieve a high-strength block with good texture. Several different proportions were tried to find the optimum percentage of the total cementitious material for the mix. Also, the minimum void gradation of aggregate was used initially, anticipating that it would give the densest and the strongest possible unit. However, trial mixes showed that this gradation was not practical and the mix, being rich in cementitious material, needed admixtures for improvement. Final mix design was based on evaluations of the workability of the mix in commercial production, strength tests results described in Chapter 4, and a durability study described in Chapter 6.

3.2 Proportioning and Mixing Processes

Material proportioning is done using either the specific gravity method or the volumetric method. Though the specific gravity method provides more control, the volumetric method is used in practice. In the specific gravity method the ingredients are proportioned as percentages of the total weight of the batch based on the specific gravities of the ingredients. In the volumetric method the amount of each ingredient is determined according to its volume in the batch as a percentage of the total volume of the batch. The volumetric method of proportioning was used throughout the development of mixes for the high-performance CMU.

Proper mixing of all materials is one of the major factors in determining the quality of the resulting mix. Very little information was available on the benefits of proper mixing procedures. Such questions as how much water should be added, when should the water be added, when and how should the cement be added, and should

the fine aggregates be placed in the mixer first, were some of the major points of discussion. A portion of the present research was devoted to answering these questions. The resulting mixing procedure for a lightweight concrete mix is as follows:

1. Charge the mixer with all lightweight aggregates.
2. Add 1/2 to 2/3 of total mixing water.
3. Mix for approximately 30 seconds.
4. Add all cementitious material, e.g., cement, fly ash, etc.
5. Add the measured quantity of admixtures.
6. Add water as required.
7. Continue mixing for 2 minutes.

Other observations were made about factors affecting the mixing process:

- If mixing time is increased, the fine materials begin to form balls. Therefore, the importance of mixing for only 2 minutes after the water is added should be stressed.
- The water to be added in the mix is determined from the machinability of the mix. The amount of water required for complete hydration of the cementitious materials is much more than that added to the mix, but if water required for complete hydration of the cementitious materials is added, then the mix is not machineable. Admixtures solve this problem; a water enhancer allows water to be added so that complete hydration may occur without increasing the slump and making the mix sticky.

3.3 Cementitious Materials

Cementitious materials that are used to produce CMUs include different types of Portland cement, fly ash, silica fume, and hydrated lime. All these materials have different chemical compositions, and the amount of each material used affects the properties of the final mix. The difference in fineness of these materials is also an important consideration when using different types of cementitious material in one mix. Some of the physical and chemical properties of the various materials were evaluated and are discussed in the next sections. The effect of using these various cementitious materials on the strength development was examined, and the results are discussed in detail in Chapter 4.

3.3.1 Portland Cement

Portland cement is the most important and basic constituent of concrete. Types I, IA, III, and IIIA Portland cement are typically used in masonry production. Types III and IIIA are preferred when increased plasticity and high degree of compaction are desired. In this research, Type III cement was used. Type III cement has the same chemical and physical properties as Type I cement, but it is ground finer than Type I and gives high early strength. The chemical composition of Type III cement is typically 56 percent C_3S, 15 percent C_2S, 12 percent C_3A, 8 percent C_4AF, 3.9 percent $CaSO_4$, 1.3 percent free CaO.

3.3.2 Fly Ash

Fly ash is a coal combustion byproduct obtained from coal-fired power plants, so it is readily available at very little cost. Depending on hauling costs, it is generally economical to use as a cement additive. The chemical composition and quality of fly ash may differ greatly by the type of coal burned, pulverization, burning process, fly ash accumulation technique, and storage. Fly ash is classified by ASTM as either F or C. Class F fly ash is normally produced from burning anthracite or bituminous coal and has pozzolanic properties, but little or no cementitious properties. Class C fly ash is produced from burning lignite or sub-bituminous coal and has both pozzolanic and cementitious properties. The chemical composition of Class C fly ash is typically 45 percent SiO_2, 20–25 percent Al_2O_3, 5–10 percent Fe_2O_3, 5–15 percent CaO. In general, Class F fly ash is available in the eastern United States and Canada while Class C fly ash is available in the western United States and Canada. Class C fly ash was used in the design of mixes for this study. Specifications for fly ash are covered by ASTM C 618-89. Methods for sampling and testing are found in ASTM C 311-88.

Fly ash reacts in hydrating Portland cement with the lime that is liberated by the hydration of tricalcium silicate (Ca_3S) and dicalcium silicate (Ca_2S), and forms additional Ca-S-H which precipitates in the pores of the cement paste. Replacing Portland cement with fly ash reduces the short-term compressive strength when cured at 20 °C. Higher temperatures at early stages of strength development can substantially reduce this early age strength loss (Idorn 1982).

Fly ash has been used in concrete for strength improvement, heat reduction, better handling, placing, and finishing, as an admixture to improve characteristics of concrete in aggressive environments, and to improve workability in silica fume concrete (Ukita and Ishii 1991). Masonry units with Class C fly ash contents in the range of 20–30 percent of the total cementitious material will show equivalent or

higher strengths than units containing only Portland cement. Proper use of fly ash will also improve unit durability. Use of either Class F or Class C fly ash produces units with better resistance to freeze-thaw cycles than those without this material. Fly ash can also be used as a replacement for fine aggregates.

3.3.3 Silica Fume

Silica fume is a processed byproduct obtained during production of silicon metal and ferro-silicon alloys. When used in concrete it offers reduced alkali-silica reaction, improved resistance to sulfate attack, reduced heat of hydration, improved durability, increased long-term compressive strength, reduced permeability, improved workability, and reduced bleeding.

Different types of silica fumes are available. One difference among silica fume types is the percentage of silicon in the product, which varies from 44–96 percent. Silica fume also varies according to the type of alloys in the material. One plant may produce multiple products, and the compositions of the byproducts vary with the composition of the main products, causing slight variations in the chemical composition of silica fume.

Silica fume particles are spherical in shape and have a wide range of sizes. Silica fume is a much finer material than Portland cement—approximately 100 times finer than other supplementary materials used in concrete technology. It physically fills the voids between cement particles. It is not easy to determine the particle size distribution of such a fine material. The high specific surface area of condensed silica fume in concrete causes high pozzolanicity and high water demand.

In addition to increasing the rate of hydration of tricalcium silicate (Ca_3S), silica fume combines with the lime formed as a reaction product of cement hydration. The addition of silica fume reduces the pH of the solution in the system. Plain cement paste shows a pH of about 13.9, and the passivity of mild steel is maintained at a pH of greater than 11.5. However, the addition of 10–20 percent silica fume gives pH values of 12.5.

Silica fume may take the form of condensed silica fume or silica fume cement in concrete mixes. The chemical composition of the condensed silica fume is generally 85–92 percent SiO_2, 0.5–3 percent Fe_2O_3, 1–3 percent alkalis, 1–2 percent carbon, and minor amounts of Al_2O_3, CaO, and MgO. From the chemical composition it is clear that condensed silica fume contains more than 85 percent amorphous SiO_2. Condensed silica fume is an extremely reactive pozzolan that chemically produces additional calcium silicate hydrate gel when added to concrete. Condensed silica

fume is available commercially in the United States in several different forms such as dry, densified dry, and slurried. Though the use of silica fume is very advantageous, the material is expensive.

Silica fume cement is a new type of cement in which 7.5–10 percent (by weight) of powdered silica fume is mixed with Portland cement. This pre-blended cement, identified as silica fume cement Type 10SF, was used to produce high-performance CMUs for this study. Type 10SF cement is manufactured by Lafarge Canada, Inc. Its chemical composition is generally 26.2 percent SiO_2, 4 percent Al_2O_3, 3.1 percent Fe_2O_3, 58.9 percent CaO total, 0.9 percent free CaO, 2.7 percent SO_3, 2.6 percent MgO, 0.80 percent Na_2O.

The condensed silica fume can be used successfully to enhance the quality of masonry units. The resulting reduction in absorption, increased strength, and greater resistance to freezing and thawing makes the unit more desirable. However, the masonry units with condensed silica fume are darker in color compared with conventional units.

3.3.4 Hydrated Lime (Calcium Hydroxide)

Hydrated lime, $Ca(OH)_2$, is a very reactive chemical. The chemical composition of hydrated lime used in this research was typically 97.0 percent available calcium hydroxide, equivalent to calcium oxide (CaO) 73.5 percent, and chemically combined water 23.5 percent, calcium carbonate 2.0 percent, magnesium hydroxide ($Mg(OH)_2$) 0.26 percent, calcium sulphate ($CaSO_4$) 0.02 percent, silicon dioxide (SiO_2) 0.6 percent, ferric oxide (Fe_2O_3) 0.05 percent, aluminum oxide (Al_2O_3) 0.24 percent, sulfur trioxide (SO_3) 0.01 percent, carbon dioxide (CO_2) 0.88 percent, and mechanical moisture (H_2O) 0.65 percent. When hydrated lime and a pozzolan react together, a compound having lower solubility and good cementitious properties is formed. Thus, higher strength is achieved. Additionally, this composition helps the mix to fall easily into the mold and be consolidated.

3.4 Aggregates

Lightweight aggregate selected for producing quality lightweight CMUs must satisfy the following requirements:

- It must be or must have the potential to be widely produced throughout the United States.
- It must be cost-effective—about 2 to 3 cents per pound.

- It should preferably be made from waste products or recycled resources.
- It must meet ASTM C 331-87[4] for lightweight aggregate.

Lightweight aggregate comes in two types—natural and artificial. Pumice, scoria, and cinder fall into the first category; expanded shale, expanded clay, and expanded slate are examples of the second category. Since natural lightweight aggregate is not abundant in large quantities everywhere, artificial lightweight aggregates were evaluated in this study. Artificial lightweight aggregates also have the advantage of controlled quality and strength. Expanded shale, AggreCel™, expanded clay, 3M Macrolite™, and Poraver™ were considered in this research. As most block producers use some type of normal weight sand as fine aggregate in their block mixes, natural sand and gravel (i.e., normal weight aggregate) was also evaluated. Properties important to the development of a high-strength lightweight block are discussed below. Evaluation of the aggregate types for these properties are summarized.

3.4.1 Properties of Aggregates

Aggregate properties such as unit weight, moisture content, water absorption, crushing strength, and gradation are very important in determining the properties of the CMU. The aggregates that were used in production of the units were tested in the laboratory to evaluate their properties. The tests were performed in accordance with ASTM procedures. The test results are discussed in the various sections pertaining to the aggregates.

Lightweight aggregates used to produce CMUs have unit weights in the range of 40 to 70 lb/ft^3 (641 to 1121 kg/m^3). The maximum value allowed by ASTM C 331-87 for the delivered unit weight of aggregate in a dry, loose condition is 65 lb/ft^3 (1041 kg/m^3). Unit weights of all aggregates used in this research are calculated by following the shoveling procedure given in the ASTM C 29-78. These unit weights, also called bulk density, are used in proportioning the different mixes.

Artificially produced aggregates have a great capacity to absorb water from the mix. This is because the lightweight aggregates are produced by expanding naturally available aggregate materials. The process creates numerous air pockets in the aggregate that make it absorptive. To overcome this problem, the aggregate is pre-wetted. By pre-wetting, the water demand of the lightweight aggregates is satisfied before coming into contact with the cementitious materials in the mix. In addition, pre-wetting is one of the most effective means of minimizing segregation. It has been estimated that about one-half to two-thirds of the total mixing water will

completely saturate all the lightweight aggregate. The water absorption property of the aggregate is determined in accordance with ASTM C 127-88.

All aggregates used were tested for moisture content following ASTM C 566-84. Since lightweight aggregates are produced artificially, they are always air-dry in their natural state with a small amount of absorbed moisture from the surrounding atmosphere. Normal weight aggregate, such as sand and gravel, contains 1–2 percent moisture, depending on the method of recovery and storage.

Crushing strength can be a useful guide for estimating the resistance of an aggregate to breakage and abrasion during handling and mixing. There is no designated test which can be used to calculate crushing strength of aggregate alone. The Los Angeles abrasion test (ASTM C 131-81) could be used for testing coarse aggregate, that is retained above the no. 4 sieve, to determine resistance to degradation. Section 4 of ASTM C 131-81 discusses the significance and use of this test and notes that, "The results do not automatically permit valid comparisons to be made between sources distinctly different in origin, composition, or structure. This test can be used as an indicator of the relative quality or competence of various sources of aggregate having similar mineral composition." As an indirect measure of aggregate strength, aggregates can be used with the same mix proportion and the units tested for compressive strength. By this method, performance of aggregate within the mix can be evaluated. This latter method was used to evaluate the crushing strength of the aggregate for application in high-strength lightweight CMUs.

Crushing strength and gradation are related aggregate properties. A friable aggregate could easily break down to give a grading entirely different from that established on a trial mix basis. Gradation is of particular importance for the successful manufacture of quality CMU. Strength, weight, and texture of the unit are affected by a change in the gradation. Good grading also exerts a major influence on the moldability and cohesiveness of the mix and helps freshly molded units to resist cracking and breakage in handling. Gradation, surface, and shape characteristics of aggregate influence workability which in turn affects green block stability, breakage, and speed at which block can be molded. Block weight and green block stability are affected by the amount of fines (finer than #50) in the aggregate. Generally greater aggregate sizes provide stronger mixes, provided that the aggregate is well graded. The maximum size depends on the minimum section thickness of the block (National Concrete Masonry Association 1955). A well graded blend will have fewer voids because the space between large particles will be filled by smaller ones; this helps transfer the applied load properly among particles. Moreover, since there are fewer voids, the block will be less permeable and more durable. A smooth texture can be obtained from mixes that have larger particles

in them only if they have enough fines to fill the gap between the larger sizes. The ASTM C 136-84 test procedure was followed in performing the sieve analysis of the different aggregates.

3.4.2 Aggregate Evaluation

As noted previously, properties of all aggregates were evaluated in the laboratory. Five different types of aggregates were used to produce high-strength CMUs. As the aggregate type changed, the strength and durability of the CMUs changed. Units produced in the laboratory were first evaluated for texture, and then tested for compressive strength and durability.

For an impermeable mix, it is very important to have minimum voids in the mix. Thus, the denser the mix, the less permeable is the unit. The minimum void gradation curve plots as a straight line when plotted on the gradation chart raised to 0.45 power (Figure 3.1), whereas it results in an S shape on the semi-log plot. Proper gradation plays an important role in determining the amount of cement to be used. The evaluation of different aggregates on this basis is discussed in the following sections.

3.4.2.1 Evaluation of expanded shale. Expanded shale is the most widely used type of lightweight aggregate. It is obtained by heating the shale to about 2000 °F to form tiny air bubbles in the material. It is produced by different manufacturers across the country under different names such as Haydite, Buildex, Stalite, etc. The density of expanded shale varies from 45 to 72 pounds per cubic foot (pcf). For this work, expanded shale was supplied by Buildex, Inc., Ottawa, KS.

The unit weight and water absorption are given in Table 3.1. The commonly used gradations of this aggregate were studied and the minimum void gradation was designed. As stated above, the objective of the gradation design was to achieve the strongest and the most durable CMU possible. When the CMUs were produced using the minimum void gradation, the texture of the units was very coarse and unacceptable.

A completely different gradation was developed in the plant, which consisted of less cementitious materials and lower water content. These units had a smooth and uniform texture. While the texture of the units was acceptable, the units had too little compressive strength when evaluated. The gradations of these two mixes were modified to design an optimum gradation for texture and strength. The percent of coarse material, i.e., 1/4 in. (6.35 mm), as well as fines, i.e., no. 50 and no. 100, from the aggregate blend was reduced. The coarser aggregate gives a poor

texture and excess fines make the mix sticky and less machineable. Fly ash was added to make-up for the lack of fine aggregate and to provide higher strength. The units produced with this new gradation were expected to give good texture, higher strength, and lower absorption.

This designed gradation was sent to the aggregate manufacturer for review. It was not possible to get the exact gradation for the expanded shale aggregate because the manufacturing process made it difficult to completely eliminate the fines. The gradation shown in Table 3.2 was used to produce all of the remaining test units.

3.4.2.2 ***Evaluation of other aggregates.*** Natural sand and gravel, commonly known as block sand, are used to produce high-strength normal-weight units. Sand and gravel provide the best gradation to produce a unit with a smooth, uniform texture. However, its heavy weight is a major disadvantage in producing a quality CMU. The properties of this aggregate were evaluated in the laboratory and the results are given in Tables 3.1 and Table 3.3.

AggreCel™ is produced and supplied by the Greengrove Corporation, Brooklyn Park, MN. This aggregate is produced using paper mill sludge and specific ash. The unit cost for this aggregate is much less than other lightweight aggregates because of the low cost of the raw materials and the energy-efficient method of production. The unit weight and water absorption of this aggregate, as evaluated in the laboratory, are shown in Table 3.1. The absorption of this aggregate is higher than the absorption of the other lightweight aggregates tested in this study. This aggregate was blended to have the designed gradation, as shown in Table 3.3. The texture of the units produced using this aggregate was smooth and uniform.

Expanded clay was supplied by Big River Industries, Inc., Livingston, AL. It is one of the common lightweight aggregates used in the United States. Test results for unit weight and water absorption of expanded clay are given in Table 3.1; sieve analysis gradation of the aggregate is given in Table 3.3. This aggregate contained a very high percentage of fine material, passing the no. 50 sieve, as well as coarse material, retained above the no. 4 sieve. The fines made the mix dusty and sticky while the coarse material gave poor texture. The aggregate retained above the no. 4 sieve was removed to give a better texture. While the texture was improved, the strength was lowered.

A newly manufactured product called 3M Macrolite™ ceramic sphere is produced and supplied by the 3M Company, St. Paul, MN. It is the lightest aggregate among all lightweight aggregates that were used in this research. It is a microcellular lightweight aggregate having almost spherically shaped particles. The aggregate

is produced by expanding glass at very high temperatures. The test results are given in Table 3.1. Compared to other aggregates, the 3M aggregate had very low absorption and unit weight. This aggregate is available in five different sizes. The sizes that were best suited for the designed gradation were chosen. A gradation very close to the designed gradation was achieved, as shown in Table 3.3. The unit weight of this aggregate blend was 26.5 lb/ft^3 (425 kg/m^3).

Poraver™ is produced by the Dennert Poraver GMBH, Schlusselfeld, Germany. The aggregate material is supplied by the company's Construction Technology Division, Rosemont, PA. It is also a microcellular lightweight aggregate produced from recycled glass, with each grain almost spherical in shape. Laboratory test results (Table 3.1) showed that absorption of this aggregate is very high compared to other lightweight aggregates, so it was not used to produce any CMUs in the laboratory. Table 3.3 gives the gradation of the four different grain sizes, ranging from 0.0098 –0.63 in. (0.25–16 mm).

3.5 Admixtures

Admixtures are widely used in the production of high-strength CMUs. There are two types of admixtures—chemical and mineral. Admixtures significantly contribute to increased compressive strength, improved workability, and durability of the mix. Most of the admixtures used are superplasticizers to help in the demolding of the block. Also, the amount of water that can be used in a block mix is limited and usually is less than the amount needed for full hydration of cementitious material. Therefore, some admixtures are used to allow more water in the mix while still maintaining zero slump.

3.5.1 Plasticizers

A plasticizer makes the mix plastic and helps to consolidate and easily remove the masonry unit from the mold. Krete Plast™ is a specialized plasticizer formulated to achieve the highest performance in no-slump concrete production. Advantages include superior lubricity, large increase in plasticity of the mix, and reduction in the amount of water needed for hydration. Ultra Mix™ is a combination of densifier and plasticizer. When this admixture is used in the mix, the units produced have a smeared surface.

3.5.2 Water Enhancers

Water enhancers allow more water in the mix without increasing slump. Krete Mix™ is an integral admixture formulated to tighten texture and reduce machine part wear while helping to disperse fines and integral colors, especially for zero slump concrete. Other advantages include uniform plasticizing action and minimizing efflorescence.

3.5.3 Admixture Combinations

Combinations of plasticizers along with other admixtures have become common to achieve optimum performance at low cost. Improvements in strength gain, and workability are possible with optimized combinations. When using a combination of admixtures, each should be dispensed individually in a manner approved by the manufacturer.

3.6 Mix Designs

3.6.1 Basic Mix Designs

Trial mixes for normal-weight and lightweight units were first produced in the laboratory. High-strength normal-weight mixes were produced using normal-weight sand and gravel aggregate. The mixes used in producing normal-weight units are shown in Table 3.4. The texture of the units produced from each of the trial mixes was better than the texture of conventional normal-weight units. Mixes W12 and W18 were selected for strength, durability, and cost optimization.

For the lightweight masonry units, the optimum amounts of cementitious material and fly ash in the mix were determined based on compressive strength test results. Expanded shale aggregate with a maximum size of 3/8 in. (9.525 mm) was blended to give the minimum void gradation for high-strength and good texture. The initial two lightweight mix designs were designated W4 and W11(old). Their compositions are shown in Table 3.5. The mix proportions were used to produce units commercially in the Watkins Block Company, Inc., Omaha, NE. Units produced using mix W4 had high-strength but unacceptable texture while those produced using mix W11(old) had lower strength but better texture. The following modifications were made to optimize the mix:

1. Revise aggregate gradation and reduce the maximum size of aggregate.
2. Use a high dose of admixture to improve workability.

3. Monitor the amount of water added to the mix to avoid stickiness and lumpiness.
4. Alter the ratio of aggregate to cementitious materials.
5. Increase the feed and finish times.

Mix designs were optimized and several commercial productions of modified mixes were undertaken.

3.6.2 Optimized Mix Designs

Normal-weight mix W20, based on modifications to W12, produced units with exceptional strength, better absorption, and good texture. As the cost of the units was too high, the mix was again modified and the final mix design produced is designated W23. Commercial production of units based on this mix design was successful.

Lightweight mixes W11' and W16 were produced with the same proportion of ingredients as W4 and W11(old) respectively, with a new aggregate gradation and increased admixtures (Table 3.6). W17 was also produced based on W16, with the aggregate pre-coated with a waterproofing admixture. Mix W16 exhibited particularly good texture. Based on strength and cost analyses several additional mixes were designed to achieve higher strengths with the desired texture.

The third commercial production of a lightweight mix with the optimum amount of hydrated lime proved unworkable when water was added. A modified mix W24 was developed to address this problem. The mix was workable and had a satisfactory texture. The units had sharp corners.

3.6.3 Effects of Specific Material Components on Mix Design

3.6.3.1 Influence of cement-aggregate ratio. Cement-aggregate ratio is the weight of cement to the weight of aggregates. For lightweight aggregates the recommended ratio is 1:6, but from the trial mixes it was found that more cementitious material was required to coat all the lightweight aggregates. The optimal cement aggregate ratio was determined to be 1:4. Cement-rich mixes frequently have very high water demands. Therefore, special precautions were necessary to provide adequate water so that sufficient hydration could occur. Otherwise, steam curing at elevated temperatures for longer periods of time would be required for complete hydration.

3.6.3.2 Significance of water in the mix. While working with the lightweight aggregates, more water was required for making a mix in the laboratory than was

required in the plant. The water requirement of aggregates changes depending on the condition of aggregates at the time of mixing. If the aggregates are wet at the time of mixing, less water is required, regardless of the mix. Also, water demand changes as the cementitious materials are changed. Adding more water to the mix affects the texture and moldability of the unit.

Although logical, it is not advisable to consider absolute volume of water to calculate total water volume of the mix. In the plant, the amount of water added to the mix is determined from the machinability of the mix. The lightweight mixes W11' and W11'+ with expanded shale had the same mix proportions, except for the amount of water. In mix W11'+ more water was added to examine its effect. The units produced from this mix had coarse texture and lower strength.

When silica fume is used separately in the mix, the water demand of the mix increases dramatically. This can be seen by comparing the two normal-weight mixes, W12 and W14. Both of these mixes had the same proportions of ingredients, except that in mix W14 pre-blended silica fume cement was replaced by Type-III cement and silica fume. In mix W14, 3 gallons more water were added than that to mix W12 to get the same workability. For a normal-weight mix, 3 more gallons of water would have given the mix a high slump. However, excellent units having average strengths of about 9000 lb/in^2 (62 MPa) were produced from mix W14.

In the normal-weight mixes W20 and W23, the same amount of water was added. These mixes were produced at two different times. The mix W23 was proportioned similar to the mix W20, except the total amount of cementitious material was reduced by 15 percent. Also, pre-blended silica fume cement was replaced by Type-III cement and silica fume. The 15 percent reduction in the cementitious materials should have reduced the total water added to the mix. However, the reduction in cementitious materials did not reduce the total water in the mix, because the use of silica fume increased the water demand.

3.6.3.3 ***Effect of different admixtures.*** The aggregates required for optimum texture, durability, and strength tend to absorb high amounts of water, which in turn makes the lightweight CMU too absorptive. To overcome this problem in the lightweight unit, a waterproofing admixture was used to pre-coat the lightweight aggregates. When the proctor specimens produced in the laboratory were tested for absorption, a 20 percent decrease in absorption was observed, whereas the CMUs showed only a 6 percent decrease in absorption. Therefore, more research is needed to optimize the percentage of admixtures used.

Fiber mesh (Harborite 300™) has been used in concrete to control shrinkage cracking. To study its effect on CMUs, this material was used as an admixture in the mix W19. The units produced from this mix had fibers protruding on all the surfaces. The units were not pleasing in appearance and the strength was not very high.

Combinations of plasticizers along with other admixtures have become common in order to achieve optimum performance at low cost. Improvements in strength gain, and workability are possible with optimized combinations. When using a combination of admixtures, each should be dispensed individually in a manner approved by the manufacturers.

3.6.4 *Final Mix Design*

Using mix workability as the primary evaluative criterion, mix W24 was selected for the final design of high-strength lightweight CMUs and mix W23 was selected for the final design of normal-weight optimized units.

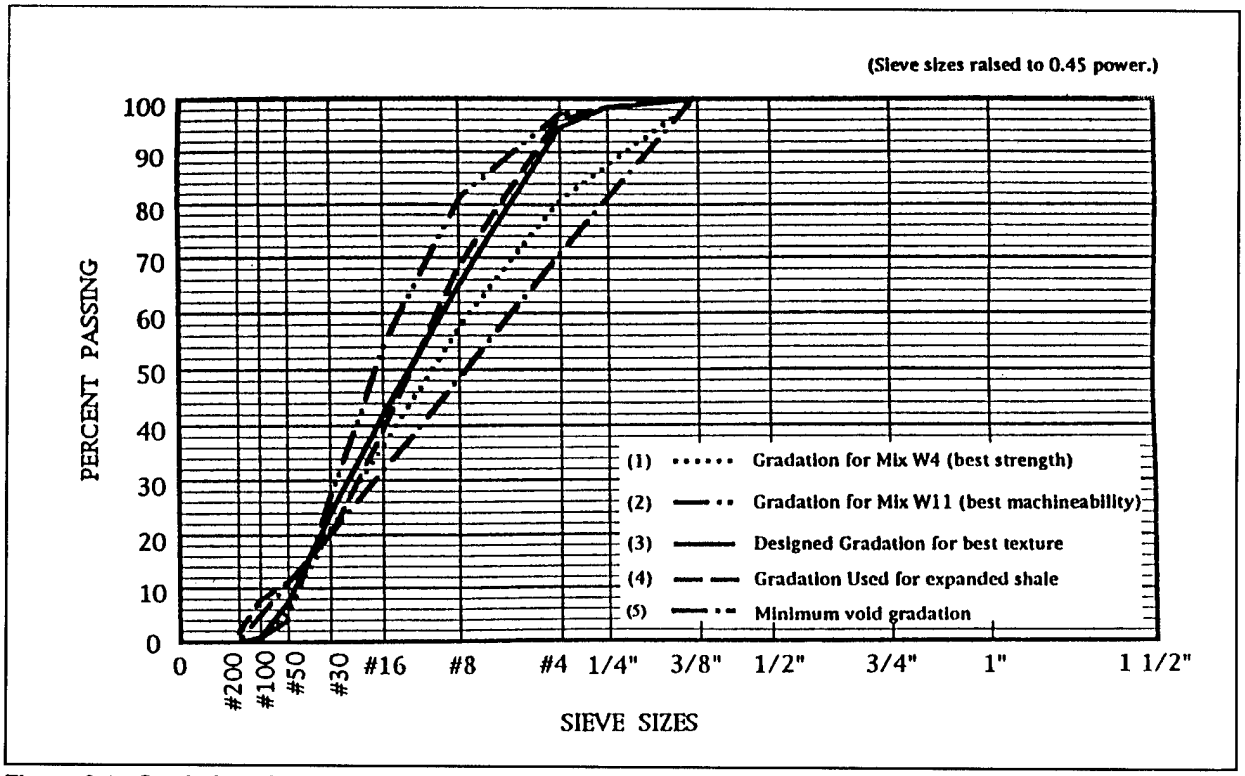

Figure 3.1. Gradation chart showing designed gradation.

Table 3.1. Properties of aggregates.

Material	Shoveled unit weight lb/ft^3 (kg/m^3)	Water Absorption (%)
Expanded shale	56 (897)	12
Sand and gravel	98 (1570)	1
AggreCel™	60 (961)	26
Expanded clay	42 (673)	20
ML357	22 (352)	2
ML714*	26 (417)	3
ML1430	27 (433)	4
ML3050	32 (513)	4
P4-10**	11 (175)	32
P2-4	12 (200)	41
P1-2	14 (225)	37
P0-1	22 (360)	82

* ML = 3M Macrolite™ Ceramic Sphere
** P = Poraver™

Table 3.2. Gradation for expanded shale.

Sieve size	3/8 in.	1/4 in.	#4	#8	#16	#30	#50	#100	#200
% passing	100	98	96	68	37	21	11	7	0

Table 3.3. Gradation of other aggregates.

Sieve size	3/8 in.	1/4 in.	#4	#8	#16	#30	#50	#100	#200
% Sand and Gravel passing	100	97	89	70	58	41	14	1	0
% AggreCel™ passing	100	98	94	66	43	25	8	1	0
% Expanded Clay passing	100	93	86	71	47	31	20	13	3
% ML* passing	100	96	93	62	40	29	0	0	0
% Poraver 4-10 passing	88	90	13	6	4	0	0	0	0
% Poraver 2-4 passing	100	100	100	52	2	1	0	0	0
% Poraver 1-2 passing	100	100	100	98	41	2	0	0	0
% Poraver 0-1 passing	100	100	100	100	100	22	1	0	0
* ML = 3M Macrolite™ Ceramic Spheres									

Table 3.4. Identification of normal-weight mixes.

Mix No.	Description
W12	Normal-weight mix, proportion of ingredients same as Mix W11', increased dosage of admixtures.
W13	Normal-weight mix, proportion same as Watkins' standard block mix.
W14	Normal-weight mix, proportion of ingredients same as Mix W12, use of Type-III cement plus condensed silica fume instead of pre-blended silica fume cement, increased dosage of admixtures.
W15	Normal-weight mix, proportion same as Watkins' standard dry-block mix.
W18	Normal-weight mix, proportioned as paver mix.
W19	Same Mix W18 with fiber mesh (Harborite 300) used as an admixture.
W20	Normal-weight mix, proportioned in between W12 and W18, increased dosage of admixture.
W23	Normal-weight mix, proportion of ingredients same as Mix W12, pre-blended silica fume cement replaced by Type-III cement plus condensed silica fume, all cementitious materials reduced by 15 percent.

Table 3.5. Identification of lightweight mixes.

Mix No.	Description
W11'	Lightweight mix, proportion of ingredients same as Mix W11(old), new gradation for aggregates, increased dosage of admixtures.
W11'+	Same Mix W11' with added more water.
W11'-PC	Lightweight mix, proportion of ingredients same as Mix W11', new gradation for aggregates and aggregates are pre-coated with waterproofing admixture, increased dosage of admixtures
W16	Lightweight mix, proportion of ingredients same as Mix W4, new gradation for aggregates, increased dosage of admixtures.
W16+	Same Mix W16 with added more water.
W17	Lightweight mix, proportion of ingredients same as Mix W16, new gradation for aggregates and aggregates are pre-coated with waterproofing admixture, increased dosage of admixtures.
W21	Lightweight mix, proportioned in between W11' and W16 , increased dosage of admixtures.
W22	Lightweight mix, proportion of ingredients same as Mix W16, new gradation for aggregates, silica fume cement replaced by Type-III cement plus condensed silica fume, 12 percent of fly ash replaced by hydrated lime.
W24	Lightweight mix, proportion of ingredients same as Mix W16, new gradation for aggregates, silica fume cement replaced by Type-III cement plus condensed silica fume, 8.5 percent of fly ash replaced by hydrated lime.
W25	Lightweight mix, proportion of ingredients same as Mix W16, new gradation for aggregates, silica fume cement replaced by Type-III cement plus condensed silica fume.

Table 3.6. Proportions of initial lightweight mixes.

Mix No.	Expanded Shale lb/yd^3	Silica Fume Cement lb/yd^3	Fly Ash lb/yd^3	Krete Plast fl oz	Krete Mix fl oz
W4	Coarse 740 Fine 901	462	528	---	---
W11 (old)	Medium 1500 Fine 500	462	200	7	ultramix - 17

4 CMU Strength Tests

4.1 Introduction

This chapter describes the comprehensive test program conducted to evaluate the strength of concrete blocks representative of different mix designs for normal-weight and lightweight quality CMUs. The main parameters investigated were compressive strength, flexural strength, tensile strength, and the stress-strain relationship. The strength of the newly developed unit was compared with standard normal-weight CMUs. Current masonry strength testing methods specified by codes were examined and alternate test methods were explored with the objective of unifying and simplifying the masonry, mortar, and grout test assemblage.

The compressive strength of masonry, f'_m, is the most important parameter in reinforced masonry design. This parameter is used to obtain modulus of elasticity, modular ratio, modulus of rupture, shear modulus, allowable bending compressive stress, and allowable axial compressive stress. It is the basis for establishing the load-carrying capacity of a structural element and the reinforcement required by the design methods.

4.1.1 Test Standards

Unlike the compressive strength of concrete, f'_c, there is as yet no uniformly accepted procedure for establishing masonry compressive strength, f'_m, or for defining it. The masonry prism is the most widely used test specimen for determining the compressive strength of masonry. The prism is made of masonry unit, mortar, and sometimes grout, all of the same constituent materials as used in construction. The masonry units are laid up in stack bond as specified by ASTM E 447 and tested in compression. Typical height-to-thickness ratios of prisms range between 2–5. Codes and standards used in the United States and Europe for determining the compressive strength of masonry are described below.

The Uniform Building Code (UBC 1991) provides the following three methods for verifying the specified compressive strength of masonry:

Masonry prism testing—UBC section 2405(c)1. Prisms are made with the actual materials used in the structure's construction. The prism should be built in stack bond in accordance with ASTM E 447. A prism should be a minimum of two units in height with the height-to-thickness ratio in the range of 2–5.

Masonry prism test record—UBC section 2405(c)2. The UBC allows f'_m to be based on previous testing history. The code states that when there is a representative masonry prism test record of at least 30 masonry prism tests conducted in accordance with UBC standard No. 24-26, the specified compressive strength may be selected on the basis of this record.

Unit strength method—UBC section 2405(c)3, Table No. 24-C. The specified compressive strength of masonry, f'_m, may be selected from tables that are based on the strength of the masonry unit and the mortar used.

Other codes provide tables and/or test methods. ACI 530-92/ASCE 5-92/TMS 402-92 (ACI 1992) recommends the use of a table of masonry strengths for different shape factors and for the compressive strength of the masonry unit and mortar. The British code (BS 5628 Part 1) differentiates between the fully bedded mortar and face-shell mortar construction of masonry. It states that when hollow blocks are laid with mortar only on the outer shells of the block, the value of the compressive strength should be reduced by the ratio of the bedded area to the net area of the block. Alternately, the British code recommends testing of wall specimens (at least two identical panels) of 1.20–1.80 m (3.93–5.90 ft) in length, with a minimum cross-sectional area of 0.125 m^2 (1.34 ft^2) and 2.40–2.70 m (7.87–8.86 ft) in height. The construction and bond of the test wall should correspond to the masonry to be evaluated.

Because experimental test methods for evaluating masonry compressive strength are difficult to perform due to equipment requirements, designers typically assume values of f'_m from code tables (UBC 1991; ACI 1992). These tables conservatively estimate f'_m as low as 1500 psi for inspected construction and 750 psi for non-inspected construction. These assumptions result in the perception that masonry is a low-strength product that does not compete with a 4000 psi normal concrete strength product.

4.1.2 Test Phases

Proctor molded specimens of solid concrete blocks were developed from the initial mix designs, W4 and W11 (old). See Chapter 3 for the composition of the mix designs. The strength of these specimens was evaluated experimentally and based on the results of the tests; block ingredient proportions were optimized. Additional samples of blocks were then made using the optimized mixes, with a block-making machine. Compressive testing of machine-made solid concrete blocks was conducted. From the trial mixes produced in the laboratory, the optimum amounts of admixtures, Krete Mix™ and Krete Plast™, were selected.

Based on both strength and texture, the best mixes were chosen and used to produce 16-in. CMUs in the optimized A-shape in commercial block manufacturing. The mixes chosen were W11', W16, and W17. Modifications to the mixes occurred during production to increase the machinability, thereby reducing production time and improving the texture of the block. These changes led to a lighter block that had better texture but lower strength than the blocks made from the original mix. They were steam cured for 2 hours at a temperature of 180 °F. They were saw-cut to give specimens 8 x 8 x 8 in. (20.32 x 20.32 x 20.32-cm) in size and tested for 14- and 28-day compressive strength and durability.

Based on the strength and cost analysis, further modifications to the mix were made to create mix W21, from which 24-in. units were produced. The units were cut into 8 x 9 x 8-in. specimens and tested for 28-day strength and durability. The mixes were again refined to give higher strength and better durability. The third commercial production used the lightweight mix W22 with the optimum amount of hydrated lime. As was found in the laboratory, adding water made the mix sticky and unworkable. Using less water gave an almost dry mix. A new mix, designated W24, decreased the amount of hydrated lime. From this mix, 16-in. and 24-in. units were produced. The mix was workable and had a satisfactory texture. The units had sharp corners.

4.2 Compressive Strength Evaluation

4.2.1 Test Specimens

Prisms represent the primary specimen tested to assess the compressive strength of high-strength lightweight CMU construction. Components of the prisms were also evaluated including hollow units (8 x 8 x 8 in.) and (8 x 8 x 9 in.), coupons, cored cylinders, grout prisms (4 x 8 x 4 in.), grout cylinders, and mortar cylinders.

All specimens were made and tested in accordance with ASTM specifications for masonry. Cored cylinders were used as an alternate method of determining the compressive strength of grouted masonry. A brief description of the specimen types follows.

As some of the units were open-ended with irregular shapes or too long for the test machine's bearing block and platen, the units were sawed according to ASTM C 140 to remove any face shell projections. The resulting specimens were (8 x 8 x 8 in.) sawed from 16-in. units and (8 x 8 x 9 in.) sawed from 24-in. units as shown in Figure 4.1. These specimens were used to assess the mix strengths as they were developed.

Hollow units differed in their sizes and cross-sectional areas due to the variation of the shell thickness resulting from the shape optimization procedure. As shown in Figure 4.2, coupons were cut from the face-shell of each unit in accordance with ASTM C 140 to unify the dimensions for determining the strength of the unit material. The coupon size had a height-to-thickness ratio of two to one before capping, and length-to-thickness ratio of four to one. The compressive strength of the coupon was considered to be the net area strength of the whole unit.

Hollow units were grouted using a grout batch for masonry walls. After 28 days, specimens were obtained by drilling cores out of the grouted units. As shown in Figure 4.3, cores were drilled vertically through the unit at the grouted cell to include part of the face shell and/or the web. All specimens were capped with sulphur before testing. Core specimens were used to simulate the compression zone of a typical masonry wall subjected to bending forces. Tested cores would also indicate the quality of bonding between the grout material and the unit from its failure mode.

To establish the compressive strength of grout used, two types of grout specimens were made for testing: 4-in. diameter cylinders and (4 x 8 x 4-in.) prisms. The prisms were made using the tested concrete masonry units to form the mold in accordance with ASTM C 1019. Grout specimens were cured and sulphur capped before testing. Mortar cylinders were made in accordance with ASTM C 270-91 specifications.

As shown in Figures 4.4 and 4.5, two types of masonry prisms were made: hollow and grouted. The size of the prisms depended on the type of unit tested. For 8 x 8 x 16-in. units the prism size was 8 x 8 in. in cross-section and 16-in. high. For the 24-in. units the size of the prism was 8 x 9 in. in cross section and 16-in. high. The prism was constructed by placing a half unit at top and bottom of a whole unit to

provide two mortar joints as recommended by ASTM E 447. All prisms are built by professional masons. Mortar used was representative of that used in construction and met the requirements for Type N of ASTM C 476-61. Full mortar beds, with a bedding thickness approximately 3/8 in., was used in building all prisms. The prisms were sealed in moisture-tight plastic sheets to cure. After a period of 7 days, they were grouted and mechanically vibrated. After completing grouting, the moisture-tight plastic sheets were drawn back around the prisms and resealed. Prisms were capped with sulphur meeting the requirements of ASTM C 140-91.

4.2.2 Test Procedure

Figure 4.6 shows a schematic diagram of the test setup for testing prisms. A 2-in. thick steel plate was placed between the bearing block and the specimen to transfer loads to the specimen. A hydraulic test machine (Baldwin model 40 BTE) was used to apply the axial compression. The capacity of the machine is 440 kips. Load was applied at a continuously increasing magnitude until the specimen failed.

4.2.3 Test Results

This section discusses the compressive test results of grouted and ungrouted prism specimens constructed of CMUs of the final mix designs, W24 for lightweight blocks and W23 for normal-weight blocks.

The number and type of specimens tested are summarized in Table 4.1. Of particular interest are the test results of the hollow units, and the hollow and grouted prisms. Table 4.2 summarizes the test results of hollow 8 x 8 x 8-in. and hollow 8 x 8 x 9-in. specimens. The results have a coefficient of variation ranging from 0.07 to 0.10, which shows a high uniformity. The high-performance optimized normal-weight unit yielded a strength of 5.47 ksi, that is 13 percent stronger than the standard normal-weight unit, and double the ASTM C 140 requirement for standard normal-weight units (2.75 ksi). The lightweight 16-in. units yielded a strength of 3.69 ksi, that is 94 percent stronger than the ASTM C 90 requirement (i.e., 1.9 ksi) for units made of lightweight material.

Results for tests of hollow unit prisms are shown in Table 4.3. High-performance normal-weight units remained the strongest, with an average strength of 4.68 ksi, 20 percent stronger than standard normal-weight units. Lightweight units yielded an average strength of 3.2 ksi for 16-in. units and 3.17 ksi for the 24-in. units, dropping 15 percent from their corresponding sawed specimens. Test results, shown in Table 4.4, for grouted prisms were not as good as those for hollow prisms. There was a very high coefficient of variation for all types of units. Strength of all

units dropped about 40–50 percent with the exception of grouted prisms made from the lightweight 16-in. units. Grouted prisms of these units had the highest strength of those tested and were only 4 percent weaker than their corresponding hollow prisms. The grout and the block in lightweight prisms acted homogeneously due to the strong bonding between the block and the grout which enhanced the strength and produced more ductile behavior of the prism. This case is unlike those of the other prisms where bond failure was the major failure mode.

The failure of hollow prisms in compression began with cracks in the center blocks at a load approximately 90 percent of ultimate. This was followed by instability and collapse of the face shells. Grouted prisms failed gradually. First, vertical cracks began in the middle and near the corners of the center block at a load approximately 70 percent of ultimate. These cracks were due to the lateral tensile stresses introduced by the expansion of the grout. The cracks propagated across the bed joints and through the prism. At failure, splitting occurred in most of the prisms where there was an incompatibility or weak bonding between the grout and unit material. No damage was apparent in the grout for those specimens which failed with splitting. Prisms which had stronger bonding did not experience any slippage between the grout and the block and failed in shear.

4.3 Flexural Strength Evaluation

In practice, most masonry walls are subjected to a combination of axial loads, from the roof and upper walls, and to lateral loads, due to soil pressure, wind, and seismic activity. Eccentric loads induce moments in structural elements in addition to moments due to lateral load. However, some walls may be subjected to pure lateral loading. Examples of these walls are free-standing walls, such as garden walls, fences, and triangular gables during construction, before restraint from the roof. These walls are fixed at the base and subject to loads perpendicular as well as parallel to the wall plane. To establish the flexural strength of lightweight units, four beams were tested in a simply supported condition to simulate a wall subjected to only lateral loads.

4.3.1 Test Specimens

Four beams were constructed: two of the standard normal-weight units and two of lightweight 16-in. units. The beams were constructed by professional masons and built in a vertical position for ease and to simulate actual construction conditions. The two ultra light high-performance specimens were built at a construction site and transported to the structural laboratory for testing.

The specimens, built to simulate wall elements built in stack bond, were one unit wide with a wall height of 8 ft, 0 in. The units were fully bedded with type N mortar and the thickness of the bedding was 3/8 in. All the beams were under-reinforced to avoid any brittle failure with a No. 5 steel reinforcing bar placed in the center of each cell and secured using wires hooked to the mortar joints at three equally spaced locations along the beam height. After waiting 7 days for the mortar joints to harden, plywood forms were placed around the specimens. Grout was then poured and vibrated in three stages. Transportation of the two lightweight specimens from the construction area caused some breakage on the face shells that was repaired upon arrival at the laboratory.

4.3.2 Test Procedure

Figure 4.7 is a schematic diagram of the beam test setup. After curing, the beams were tilted into a horizontal orientation and placed on simple supports located 6 in. from each end of the wall length. Loading of the beams was introduced by two hydraulic jacks. The travel limit of the jack was 4 in. Deflection and cracking were recorded for each load increment. All specimens were loaded to failure to determine the ultimate load capacity. The specimens were tested 28 days after construction was completed.

4.3.3 Test Results

Failure in the beam specimens was initiated at a very early stage of loading by bed joint cracks in the tension zone. From these points the cracks spread over the block units themselves. This indicates that the masonry specimens acted homogeneously. With increasing load the initial cracks opened widely and crushing of the face shell in the compression zone was observed. The location of crushing was near the point of load application, also in an area of maximum bending moment. This failure mode occurred for all beam specimens.

The data generated from the specimens were analyzed to determine the compressive strength of masonry, f'_m. Based on the load-deflection curve of Figure 4.8, the load causing yielding of steel is determined by observing the change of slope. This load was averaged for the two specimens of each type. Beyond this yield point a large deflection is observed with a small increase in the load for all specimens. The specimens exhibited good ductility in these tests on the order of 2 to 3.

Four lengths of steel reinforcing bar were cut from supplementary material. The specimens were tested to assess their tension behavior, and developed a yield stress of 71 ksi. Using various values of f'_m, obtained from different masonry unit

strengths, and the reinforcing steel strength, the load capacity of each type of specimen was predicted using a strength design approach. A strength reduction factor and load factor of 1.0 were used. Using the same material properties, the working stress method was used to evaluate the specimen load capacities. As shown in Table 4.5, the predicted load capacity underestimated the actual load capacity of the specimens. The compressive strength determined using the working stress method and the results of the flexural tests was much higher than the strengths determined from the other specimens.

4.4 Stress-Strain Relationship

The stress-strain relationship provides the means of assessing the material modulus of elasticity. The modulus of elasticity of masonry is an important engineering property affecting the modular ratio in the working stress design method and thereby the calculation of the allowable moment from the transformed member section. It is also used to determine the element stiffness and the associated deflections of members subjected to loading.

4.4.1 Test Specimens

Four hollow prisms and four grouted prisms were chosen from each type of masonry unit, lightweight and normal weight, to assess the materials' stress-strain relationship. The prisms were capped with sulfur to assure accurate measurement of the strain. Coupons measuring 3 x 3 in. were cut from the face shell of each type of specimen as well.

4.4.2 Test Procedure

The prism specimens were placed in a 440-kip capacity load frame and tested in axial compression. A Demec gauge was used to measure the strain; the device had an accuracy of 0.8×10^{-5} strain. The measurements were taken by fixing the Demec gauge on two locator pins glued on the test prism 8 in. apart. Strain readings were taken at every 5 kip load step until the first crack developed.

The coupon specimens were tested similarly. Axial compression was applied until failure by using a MTS machine with displacement control. Strain readings were taken over the central position of the 3 x 3 in. coupons using 20 mm strain gauges.

4.4.3 Test Results

Stress-strain curves for all specimens are shown in Figures 4.9 through 4.12. Coupon specimens were stronger and stiffer than the hollow and grouted prisms. This result might be due to the absence of the negative effects of mortar and grout. Hollow prisms were stiffer than grouted prisms for all specimens except the lightweight 16-in. unit. The good quality of bonding between the grout and the lightweight unit material contributed to this result.

The average secant modulus of elasticity was calculated to be between $0.05f'_m$ and $0.33f'_m$ from the stress-strain curve in accordance with UBC Sec 2405(f). Coupons cut from optimized normal-weight units yielded a modulus of elasticity of 4,800,000 psi which was the highest of all specimens and 22 percent higher than the elastic modulus of standard normal-weight units. Coupons from lightweight 16-in. and 24-in. units had the same average modulus of elasticity which was found to be 2,003,000 psi.

4.5 Validity of Prism Test

The masonry prism is the test specimen specified by most codes for determining the compressive strength of masonry. A hollow prism is used to determine f'_m for ungrouted construction while a grouted prism is used to determine f'_m for grouted and partially grouted construction. Results of tests with prisms produced a coefficient of variation as high as 18 percent, that indicates a large inconsistency in strength results. Strength tests of grouted prisms gave much lower values than those of ungrouted prisms, and the strength of ungrouted prisms was lower than the strength of the coupon or hollow unit.

In practice, masonry walls are subjected to a combination of gravity loads and lateral loads. The gravity load is minimal compared to the lateral load due to soil pressure, seismic activity, or wind loads. Beams were tested to simulate a strip of a wall subjected to lateral load. The beams were analyzed to determine the compressive strength in the compression zone. The beam strength was found to be four times the compressive strength of grouted prism made from the same materials. The mode failure of the beam was crushing of the face shell in the compression zone at the maximum bending moment area. On the other hand, the failure of the hollow prism was a sudden failure due to stability and collapse of the face shell. The failure mode for grouted prism was splitting of the face shell due to the expansion of the grout. Therefore, prism tests underestimate the actual flexural strength available in masonry walls and do not simulate its failure mode. Moreover, prism

specimens are impractical due to their heavy weight and need for special laboratory equipment that is not always available in commercial laboratories.

Behavior of the prism when subjected to axial compression is complicated due to its composite nature. The prism consists of masonry unit, mortar, and sometimes grout. Each of these individual materials has its own structural properties that affect the overall behavior of the assemblage when subjected to loading. The literature review presented in Chapter 2 shows the complexity of the three-dimensional behavior of the prism and the numerous factors affecting its compressive strength.

Grout typically is used in masonry construction to strengthen masonry wall and to increase its load-carrying capacity. However, the results presented in Chapter 3 indicate that grout has a negative effect on the strength of the prism regardless of its size, geometry, or unit type.

All grouted prisms yielded poor strength results, dropping 40–50 percent from their corresponding hollow prisms. In an extreme case a masonry unit with 5.7 ksi was filled with grout having 6.7 ksi strength, but the resulting grouted masonry had strength of only 2.75 ksi. Drysdale and Hamid yielded similar results in an experimental program conducted to assess the behavior and characteristics of masonry prisms. They believed that the incompatibility of the deformation characteristics between grout and masonry unit contributed to the premature failure of grouted prisms.

Researchers have attempted to improve the efficiency of grouted prisms by adjusting some of these parameters affecting its compressive strength. Shrive and Josseb indicated that the performance of grouted masonry can be improved by minimizing the taper of webs and face shells to reduce bending effects and lateral tensile stresses caused by the stiffer grout during loading. They also suggested the use of nonshrinking grout, which has the same deformational compatibility as the masonry unit.

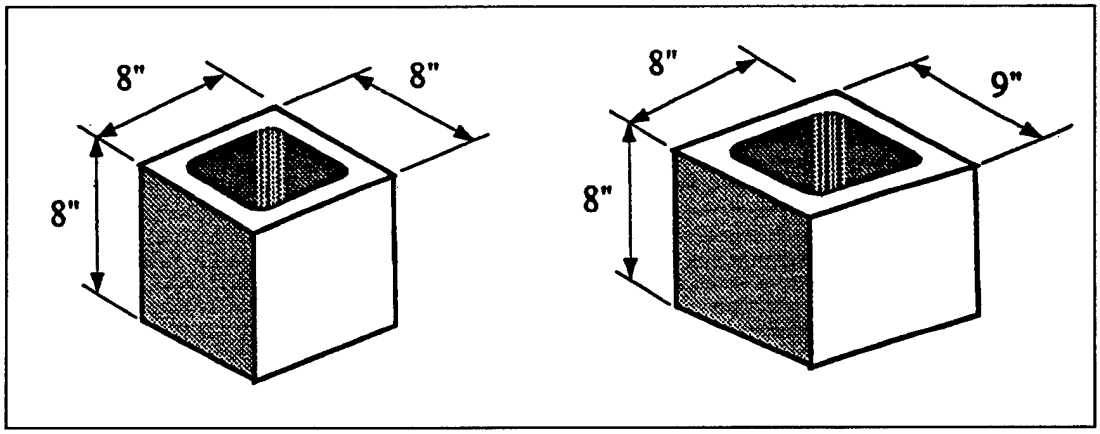

Figure 4.1. Hollow unit specimen.

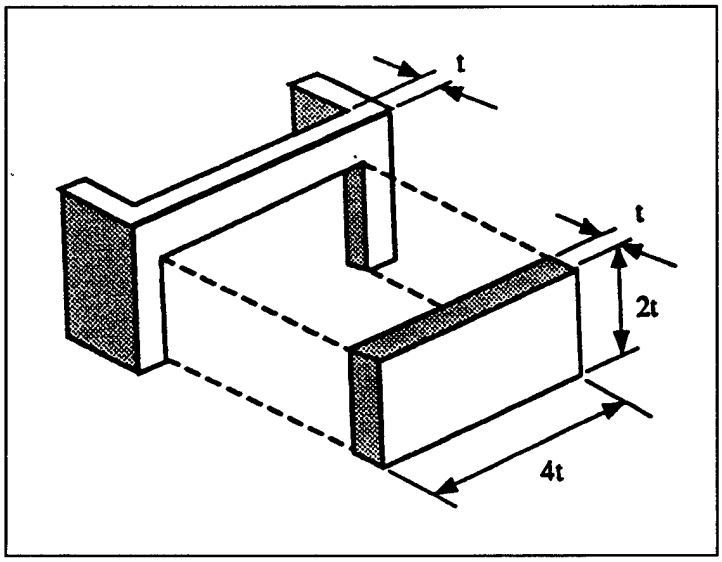

Figure 4.2. Coupon specimen.

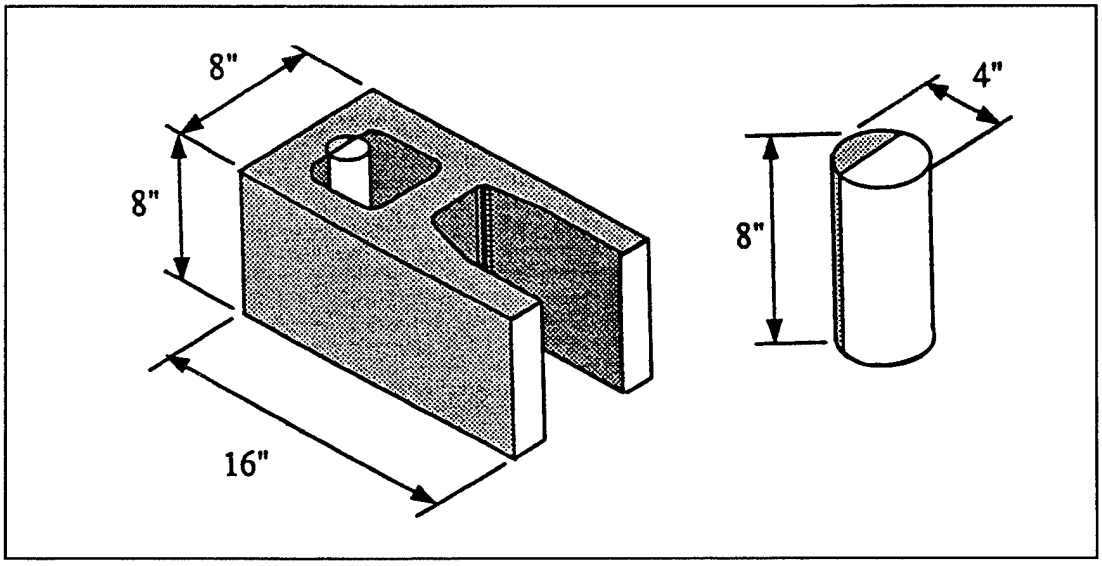

Figure 4.3. Cored cylinder specimen.

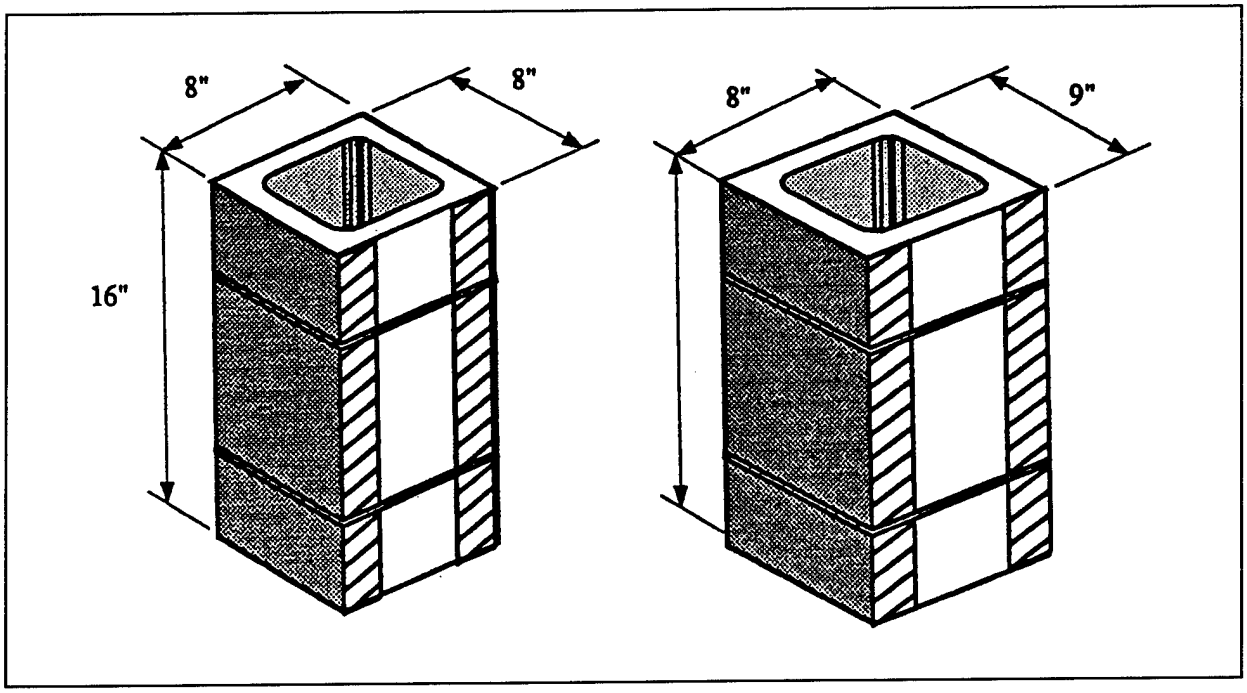

Figure 4.4. Hollow prism specimen.

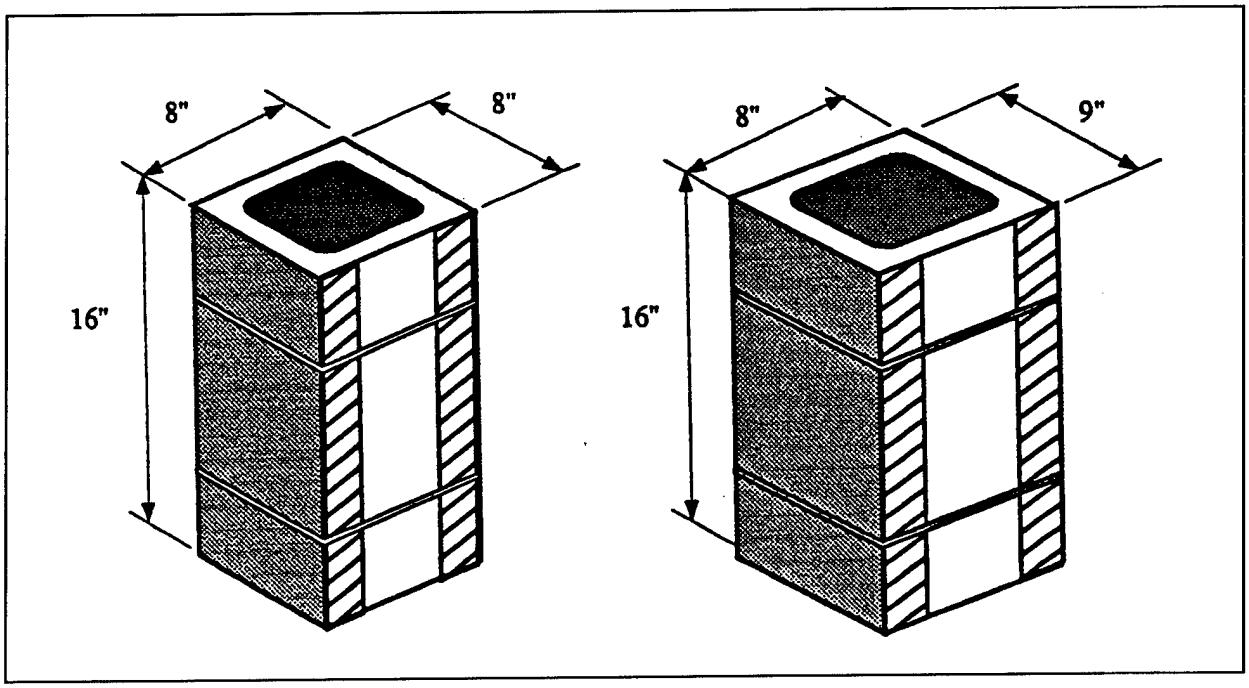

Figure 4.5. Grouted prism specimen.

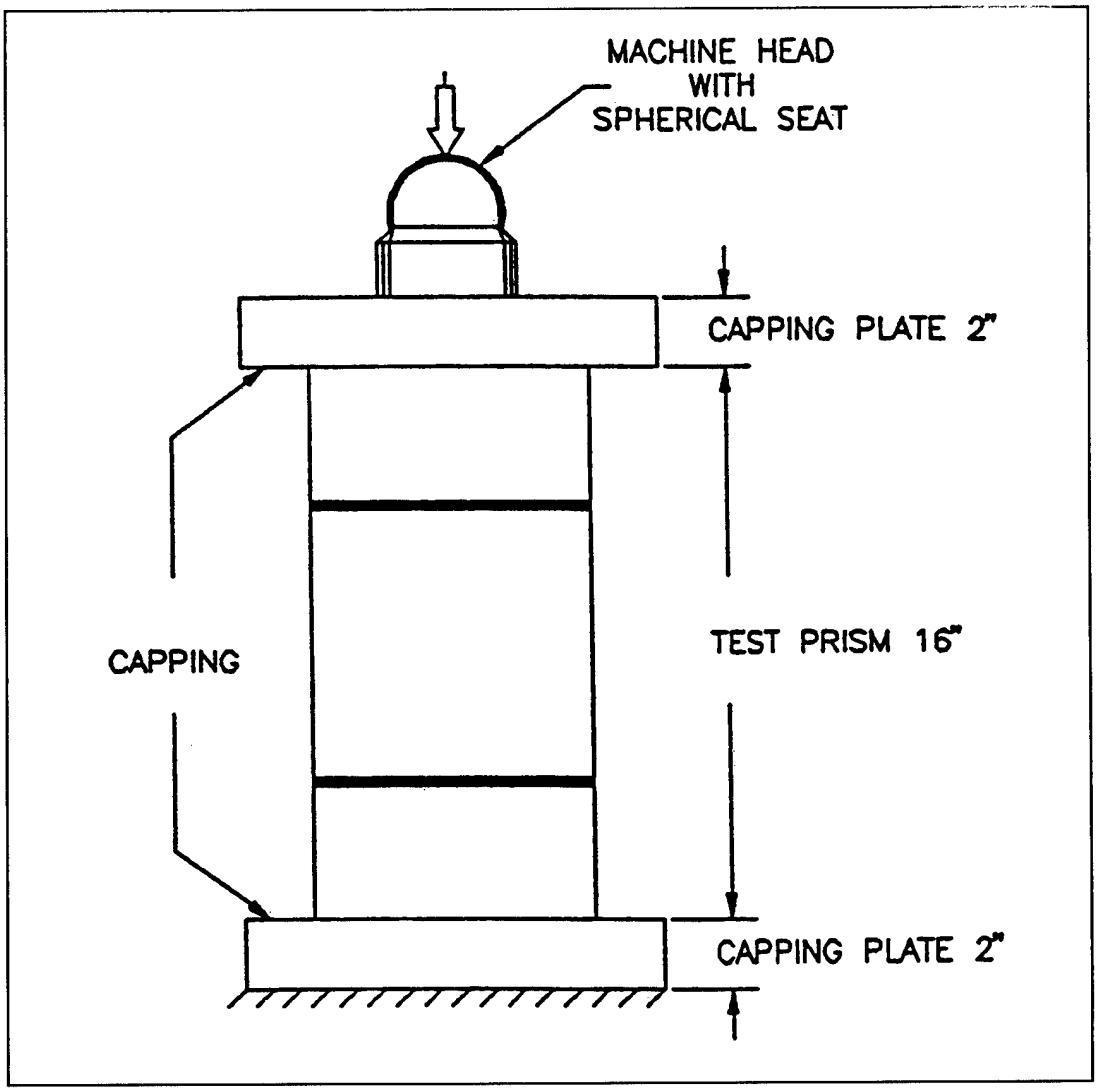

Figure 4.6. Schematic test setup of prism.

Table 4.1. Final testing program.

Specimen	Dimension (WxHxL-in.) or (DxH-in.)	Total Number of Specimens	Specifications
Hollow Unit	8x8x8, 8x8x9	110	ASTM C 140
Coupon	tx2tx4t	120	ASTM C 140
Hollow Prisms	8x16x8, 8x16x9	116	ASTM E 447
Grouted Prisms	8x16x8, 8x16x9	113	ASTM E 447
Cored Cylinders	4x8, 3.5x7	88	-
Grout prisms	4x8x4	20	ASTM C 1019
Grout Cylinders	4x8	3	-
Mortar Cylinders	4x8	3	ASTM C 780

t : Thickness of face-shell

Table 4.2. Compressive strength of hollow unit specimens.

Specimen Type	Mix Number	Dimension (WxHxL-in.)	Number of Specimens	Average Strength (ksi)	C.O.V.[5]
LWT-16[1]	W24	8x8x8	30	3.69	0.07
LWT-24[2]	W24	8x8x9	30	3.21	0.10
OPNWT[3]	W23	8x8x8	30	5.47	0.09
STNWT[4]	-	8x8x8	19	4.87	0.09

[1] Ultra Light High-performance 16-in unit
[2] Ultra Light High-performance 24-in. unit
[3] High-performance Optimized Normal Weight
[4] Standard Normal Weight
[5] Coefficient of variance

Table 4.3. Compressive strength of hollow prisms.

Specimen Type	Mix Number	Dimension (WxHxL-in.)	Number of Specimens	Average Strength (ksi)	C.O.V.[5]
LWT-16[1]	W24	8x16x8	30	3.20	0.12
LWT-24[2]	W24	8x16x9	30	3.17	0.13
OPNWT[3]	W23	8x16x9	30	4.68	0.10
STNWT[4]	-	8x16x8	26	4.58	0.16

[1] Ultra Light High-performance 16-in unit
[2] Ultra Light High-performance 24-in. unit
[3] High-performance Optimized Normal Weight
[4] Standard Normal Weight
[5] Coefficient of variance

Table 4.4. Compressive strength of grouted prisms.

Specimen Type	Mix Number	Dimension (WxHxL-in.)	Number of Specimens	Average Strength (ksi)	C.O.V.[5]
LWT-16[1]	W24	8x16x8	25	3.01	0.18
LWT-24[2]	W24	8x16x9	30	1.58	0.13
OPNWT[3]	W23	8x16x8	29	2.76	0.10
STNWT[4]	-	8x16x8	29	2.75	0.16

[1] Ultra Light High-performance 16-in unit
[2] Ultra Light High-performance 24-in. unit
[3] High-performance Optimized Normal Weight
[4] Standard Normal Weight
[5] Coefficient of variance

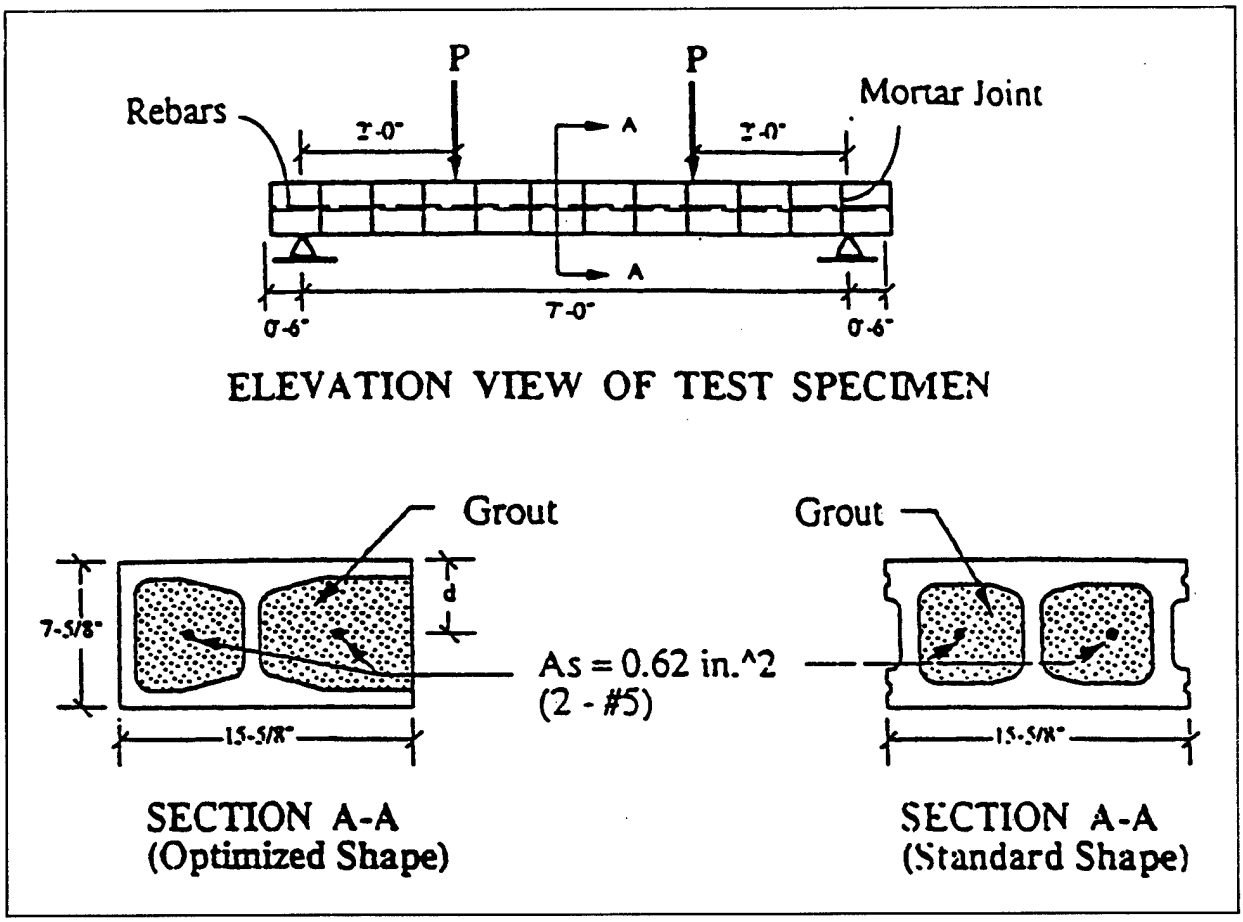

Figure 4.7. Schematic of beam test.

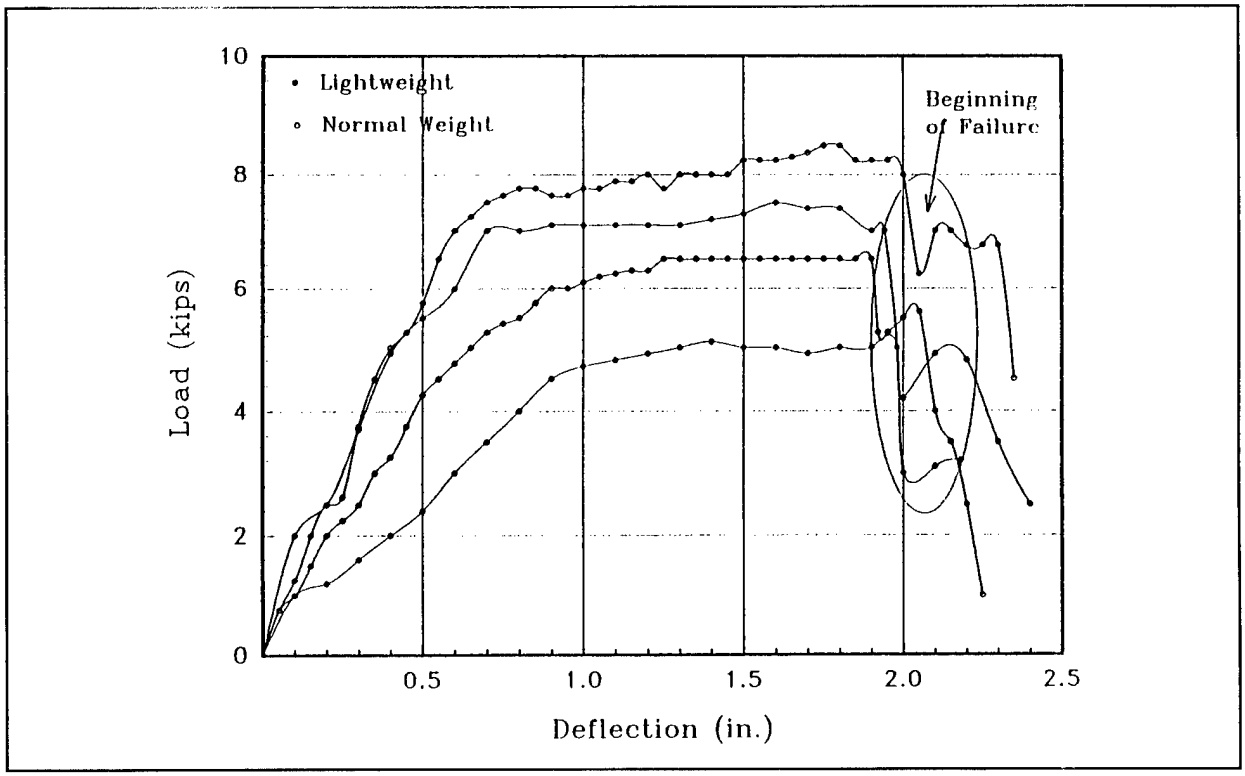

Figure 4.8. Load-deflection curves of reinforced masonry beams.

Table 4.5. Analytical and experimental load capacity for simply supported masonry beam.

Specimen Type	Size WxHxL (in.)	Compressive Strength (psi)		Calculated Load Capacity P, (lb)			
				Working Stress		Ultimate Strength	
		STNWT[2]	OPLWT[3]	STNWT[2]	OPLWT[3]	STNWT[2]	OPLWT[3]
Grouted Prism	8x16x8	2470	1460	3221	2078	5001	3897
Hollow Prism	8x16x8	4800	2470	5293	3221	5775	5001
Hollow Unit	8x8x8	-	3390	-	4109	-	5434
Cored Cylinder	4x8	4580	4680	5119	5199	5736	5754
Beam	16x8x84	7983[1]	6166[1]	-	-	-	-

[1] Predicted compressive strength using working stress method.
[2] Standard Normal Weight (P=7500 lb)
[3] High-performance Optimized Lightweight (P=6302 lb).

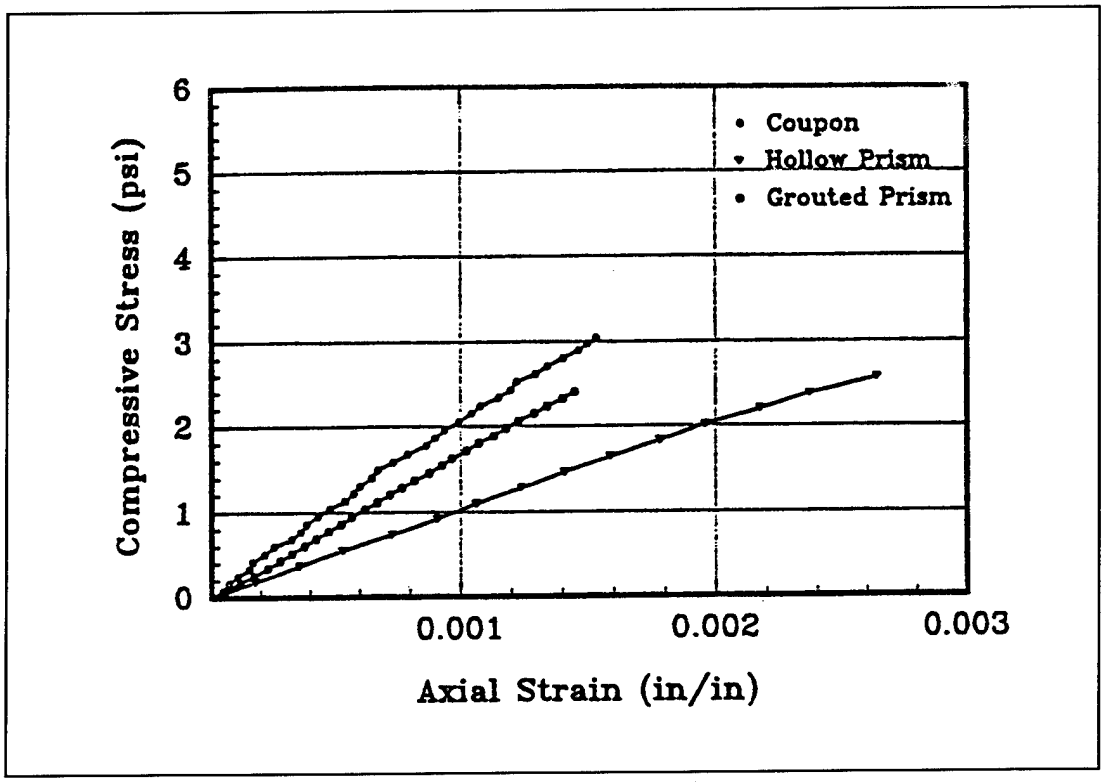

Figure 4.9. Stress-strain relationship of lightweight 16-in. unit.

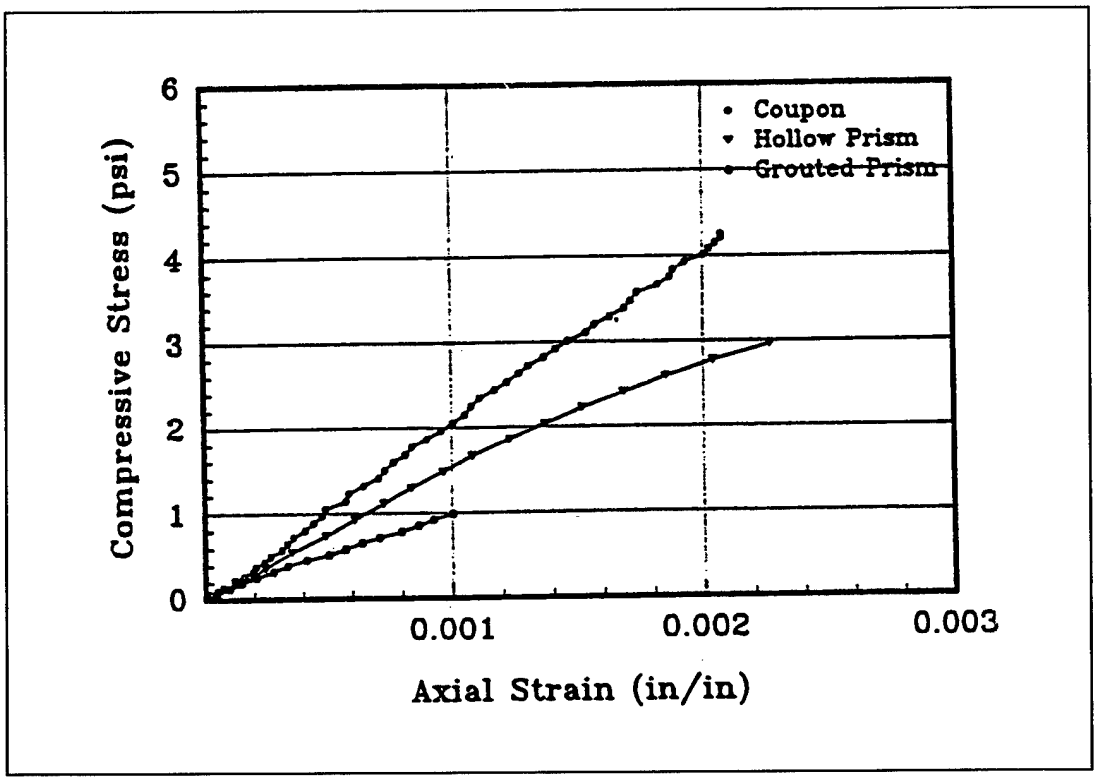

Figure 4.10. Stress-strain relationship of lightweight 24-in. unit.

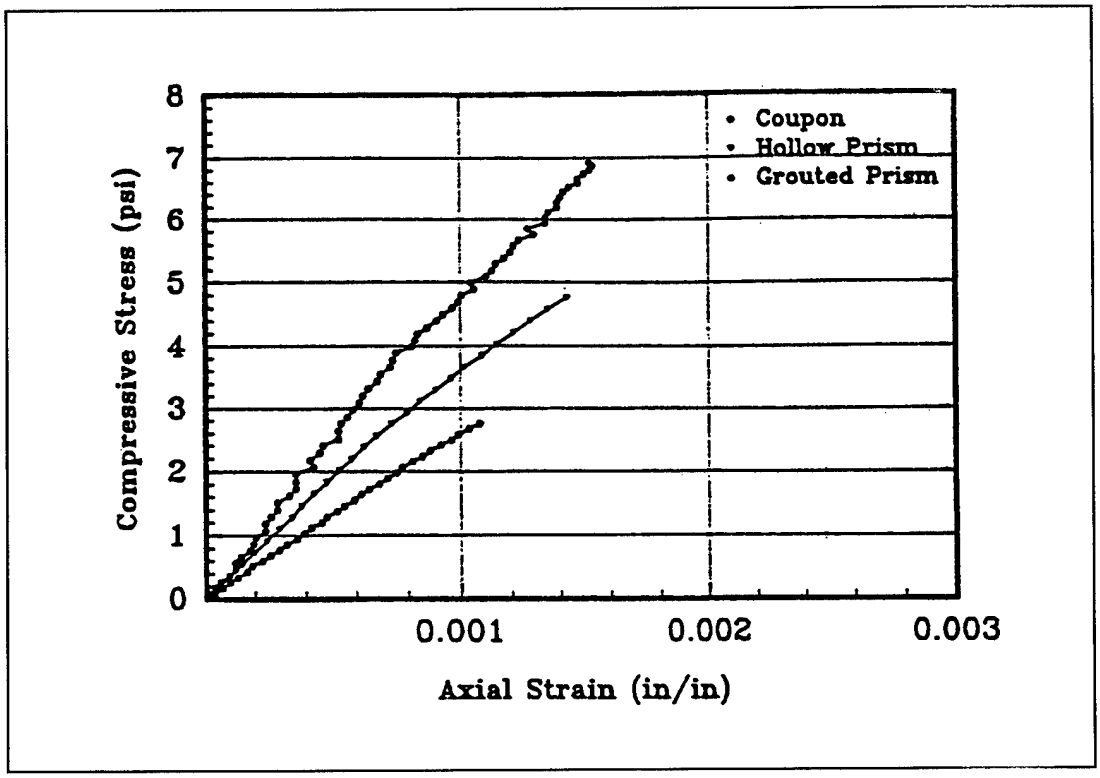

Figure 4.11. Stress-strain relationship optimized normal weight unit.

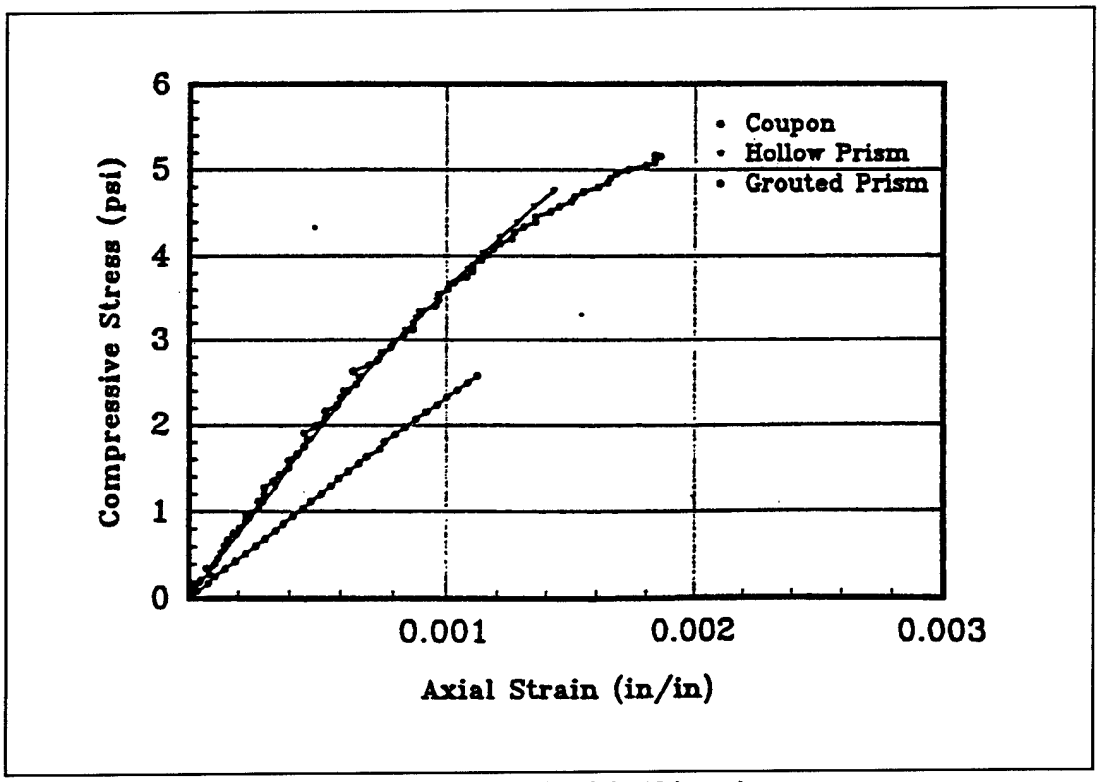

Figure 4.12. Stress-strain relationship of normal weight 16-in. unit.

5 Shear Wall Testing

5.1 Introduction

Two static in-plane shear wall tests were conducted at USACERL. The purpose of these tests was to evaluate the in-plane load resistance capability of reinforced wall constructed with the ultra light high-performance units. These loading conditions represent those that could be encountered during earthquakes and high winds in buildings where the masonry acts as the lateral load resisting system. The objective of this limited test series was to compare behavior between the ultra light and normal-weight high-performance blocks and to identify any problems with the performance of the ultra light units.

5.2 Test Structures

5.2.1 Wall Design

Static tests were performed on partially grouted reinforced walls. One ultra light block and one normal-weight block wall were tested. Each wall had the same configuration, measuring a nominal 56-in. long (in the direction of loading), 64-in. high, and 8-in. thick. A 9-gauge ladder-type joint reinforcement was placed after the first, third, fifth, and seventh courses of blocks. Vertical reinforcement consisted of three #4 bars spaced at 24 in. on center, resulting in one bar in the center cell and one bar in each cell at either outer edge of the wall. High-slump grout was placed only in the vertical cells which contained reinforcement. A typical test wall is shown in Figure 5.1.

5.2.2 Base Beam

The wall was constructed on a large reinforced concrete base beam that was securely bolted to the structural load floor. The base beam had three #4 reinforcing bar dowels epoxied at 24 in. on center to serve as lap splices for the reinforcement in the wall. The surface of the base beam was roughened to enhance bond between the first mortar bed joint and the base beam. The base beam is also shown in Figure 5.1.

5.2.3 Load Beam

A second large reinforced concrete beam was epoxied and anchored to the top of the test walls to provide vertical constraint to the wall and accommodate the loading actuators. When the test walls were originally grouted, the three cells were filled to just below the top of the seventh course of masonry. Threaded J-bolts were grouted into the top of the test walls, filling the cells full, with the J-bolts extended up through holes on the load beam. High-strength epoxy was used to bond the top course of masonry to the load beam. After the grout had cured and prior to testing, the J-bolts were tightened to provide additional strength to the connection between the load beam and the walls. The load beam is shown in Figure 5.1.

5.2.4 Vertical Load Beam Restraint

Vertical restraint was applied at each end of the load beam through the use of structural rods pinned at each end to act as links. Anchor plates were bolted to each end of the load beam and two more were welded to steel plates that were bolted to the load floor. The link itself consisted of special swivel eye bolts connected at each end that vertically pinned each end of the load beam to the anchor plate on the floor. A turnbuckle style steel pipe in the center of the link was used to adjust the link to exact length and to induce a nominal vertical downward force to the load beam prior to testing. Detail of the vertical restraint is shown in Figure 5.2.

5.3 Testing Procedure

5.3.1 Loading

Loading was accomplished through two 50-kip actuators applied in parallel to the load beam. The actuators were connected to each of two large corbels on each side of the load beam. Swivels were located between the load beam and the actuator to reduce the possibility of inducing torsion to the actuators. The actuators were connected to a steel load resisting frame that was bolted to the load floor. The load apparatus is shown in Figure 5.3.

Running two actuators in parallel requires a control system that will keep the actuators in balance. The initial test plan was to have the primary or master actuator operate in stroke or displacement control with the secondary or slave actuator operating to balance the loads between the two. This set-up worked poorly, resulting in significant torsion being induced in the first test of the first wall.

Subsequent use of stroke control for the master actuator and stroke control to maintain parallel displacements in the slave actuator worked very well.

The load scheme for these tests was a series of actuator displacement cycles of increasing magnitude until the ultimate load of the test wall had been obviously achieved. The displacement cycle is shown in Figure 5.4. This displacement represented the stroke of the actuator and not the actual displacement of the wall. The reaction frame used was not rigid, therefore significant displacement occurred in the reaction wall as well during testing. Absolute displacements of the shear wall were measured from a separate fixed reference frame.

5.3.2 Instrumentation

A diagram of the instrumentation for these tests is shown in Figure 5.5. In addition to the load and stroke measurements for each actuator, there were five absolute displacements measured to the fixed reference frame, six relative displacements on the test specimens, and two strain measurements on each of the outermost vertical reinforcing bars.

Absolute displacements are labeled AD #1 through AD #5 in Figure 5.5. AD #1 detected any slip of the base beam on the load floor. AD #2 through AD #4 measured the actual deformation in the wall at the bottom course of masonry, the mid height of the wall, and at the top course of masonry, respectively, and AD #5 measured the actual displacement history of the load beam.

Relative displacements are labeled RD #1 through RD #6 in Figure 5.5. RD #1 measured vertical strain in the north end of the wall, RD #2 and RD #3 measured diagonal strains in the wall, and RD #4 measured vertical strain in the south end of the wall. RD #5 and RD #6 measured any gaps that occurred between the wall and the base beam at the south and north ends of the wall, respectively.

The two reinforcing bars placed in the outermost cells of the shear walls were instrumented at mid height with two strain gauges. The strain gauges on the bar at the north end of the wall are labeled S1N and S2N, and the gauges on the south end of the wall are S3N and S4N, as shown in Figure 5.5.

5.4 Numerical Analysis for Shear Strength

The maximum shear was calculated using a Matsumura shear equation revised by S.G. Fattal of the National Institute of Standards and Technology (Shultz 1994).

Fattal studied test results from three programs for partially grouted masonry infill in shear. A total of 72 specimens were included in the study. Fattal performed a parametric study of variables and revised the Matsumura equation as follows:

$$V_p = k_o k_u [(0.5/(r + 0.8)) + 0.18] f_m^{0.5} f_{yv}^{0.5} \rho_v^{0.7} + 0.011 k_0 \gamma \delta f_{yh} \rho_h^{0.31} + 0.012 k_o f_m + 0.2q \quad \text{[Eq 5-1]}$$

where: V_p = ultimate shear strength (kN)
k_o = 0.8 for partially grouted walls
k_u = 0.64 for partially grouted concrete masonry
r = h/L, aspect ratio of wall
h = height of wall (mm)
L = length of wall (mm)
f_m = compressive test of masonry prisms (MPa)
f_{yv} = yield strength of horizontal reinforcement (MPa)
ρ_v = vertical reinforcement ratio
γ = 0.60 for partially grouted concrete masonry
δ = numerical coefficient boundary condition effects, assume 0.8
f_{yh} = yield strength of horizontal reinforcement (MPa)
ρ_h = horizontal reinforcement ratio
q = nominal axial stress in the wall (MPa)

The factor δ is 0.6 for a cantilever wall and 1.0 for a wall with an inflection point at mid-height. However, deflection and strain data indicated that the double curvature inflection point condition was not completely achieved in these tests; therefore, a value of 0.8 for δ was assumed.

The only difference between the two tests performed at USACERL was the compressive strength of the masonry, f_m. Table 5.1 lists all of the variables and the resulting ultimate shear strength predicted by Equation 5-1. The maximum shear force predicted for the tests of the partially grouted lightweight and normal-weight masonry walls is 34.7 kips and 33.1 kips respectively.

5.5 Test Results

The most important test data are the load (sum of the two actuators) and relative displacement (AD#4 minus AD#2), or drift, of the wall. These parameters are used to discuss the overall performance of the two shear walls and for comparison with simple analytical predictions presented in the previous section.

5.5.1 Lightweight Block

As previously stated, significant problems occurred during loading of the lightweight block shear wall specimen that diminishes the value of the test and test data. The master actuator was operating under stroke control, and the slave actuator was operating to maintain essentially equal load as the master actuator. However, there was a stiffness imbalance between the two loading points, most likely caused by a slight eccentricity between the two loading points and the centerline of the wall. Whatever the cause, the slave actuator was unable to achieve the load of the master actuator. Total wall displacement reached about 0.9 in. in the first displacement cycle when the test was stopped. The actuators were then manually returned to their approximate starting positions. A permanent displacement of approximately 0.25 in. was observed in the wall.

The load versus displacement cycle for that first large cycle can be seen in Figure 5.6, which essentially represents a pushover test for the shear wall. Initial cracking occurred at a load of about 2.5 kips and a relative displacement between the top and bottom course of the wall of 0.12 in. Ultimate load is 4.1 kips at a relative displacement of 0.6 in., at that point the wall could no longer sustain any load.

After the actuators were returned to their zero point, the system was reset so that the slave actuator operated in stroke control. This prevented the actuators from "running away" in all subsequent tests. Three subsequent cycles from the first amplitude series were then run on the wall. These smaller cycles can also be seen in Figure 5.6. As shown in the figure, the wall regained some initial stiffness, most likely the effect of some friction between the units. The 0.25-in. permanent relative displacement is also evident.

Damage to the wall after the first four cycles was very evident in the crack pattern shown in Figure 5.7. Diagonal cracking consistent with shear wall failure was clearly observed. Also seen are large vertical cracks that occurred through the face shell of the ungrouted cell of the wall. A large hole actually occurred where the diagonal crack and the vertical crack converged near the compression toe of the wall, indicated by the darkly shaded area in the figure.

While the wall showed some remaining stiffness after the first large displacement, this stiffness degraded rapidly. The wall never achieved a load over 2 kips until test series LW3, when the wall ultimately fell apart. The maximum load reached in LW3C3 was 2.1 kips at relative displacement of 1.2 in. In cycles four through eight of test series LAW, the stiffness fell to zero in the positive stroke cycle, although some strength and stiffness appeared to remain in the negative stroke. The final

crack pattern can be seen in Figure 5.8. At this point, sections of face shell were totally separated from the units and were easily removed by hand. The wall appeared as if the three grouted cells were independent concrete columns coupled by the top and bottom beams.

5.5.2 Normal-Weight Block

The shear wall test of the normal-weight (designated in the tests as heavyweight, or HW) units, under the revised stroke control slave actuator control system, occurred as originally planned. Initial loading from test series HW1 through HW3 caused nearly linear elastic behavior. A single crack was observed after the first three test series in the bed joint between the seventh and eighth courses of block from the center to the north edge of the wall, as shown in Figure 5.9. From the actual data recorded it was not possible to detect at what load that crack actually occurred.

Load versus deflection curves for subsequent load series, HW4 through HW8, are shown in Figure 5.10. The wall appeared to behave elastically until a "yield" load was reached, somewhere between 14 and 16 kips. Cycle HW6C03 reached a peak load of 16 kips at a displacement of 0.07 in. Cycle HW7C03 shows a sudden change in stiffness at a load of 14 kips, and reached a maximum load of 18 kips at a relative displacement of 0.32 in. A permanent relative displacement of approximately 0.1 in. in the direction of the positive displacement was seen after cycle HW7C03. The wall completely failed during the HW8 test series, stopping after cycle HW8C05.

Crack patterns in Figure 5.11 for the normal-weight concrete block shear wall test are shown for test series HW3, HW7, and HW8. Cracking was almost exclusively within the mortar joints, which is typical of a strong block/weak mortar system. At failure, splitting occurred in the grouted cell along the southern edge of the wall, resulting in loss of bond of the vertical reinforcing bar.

5.5.3 Comparison of the Two Test Walls

As can be seen by comparing Figure 5.6 and Figure 5.10, there was a significant difference in ultimate strength between the lightweight and normal-weight unit walls. While direct comparison is difficult because of the problems with loading the lightweight block wall, some observations are significant. The lightweight wall failed at one-fourth the ultimate shear load of the normal-weight unit wall. Cracking in the lightweight unit wall occurred through the units, while the normal-weight unit wall cracked primarily through the mortar joints. While diagonal

cracking was evident in both walls, the lightweight unit wall also showed vertical cracks through the face shells of the ungrouted cells.

5.5.4 *Comparison of Test Results to Strength Predictions*

For the lightweight unit wall, tested ultimate strength was 4.1 kips versus 23.6 kips predicted. The analytical model was unable to predict the results for this test. Strength was overpredicted by a factor of 5.7 times. For the normal-weight unit shear wall, tested ultimate strength was 18 kips versus 24.8 kips predicted. In this case the ultimate load was over-predicted by a factor of 1.4. This result is considered consistent with the variation observed by Fattal in developing the empirical equation, the normal-weight unit wall performed within expectations, and the lightweight unit wall failed far below the predicted strength.

5.6 Evaluation of Results

It is difficult to draw conclusions from two tests, particularly when loading problems may have affected the results. Significant questions are raised as a result of the shear wall tests and certain precautions should be taken if using the lightweight units for in-plane shear wall applications. Crack patterns shown in Figures 5.7, 5.8 and 5.11 are considered particularly important and indicative of the potential cause for low shear values in the lightweight block wall. The normal-weight unit wall cracked in the mortar joints, typical of a strong block/weak mortar system. The lightweight unit wall cracked through the units, indicative of a weak block/strong mortar system. The mortar and grout for each of the two walls was mixed of the same materials and to the same proportions and applied by the same mason or laborer. The inconsistency is therefore suspected to be caused by the loading or the units used in this configuration.

Possible causes of the low shear load capacity of the lightweight unit wall are high concentration of shear forces in the ungrouted face shells and the inability to develop the horizontal joint reinforcing steel due to reduced bed joint area. Neither of these areas has been addressed in specific studies on the lightweight units. The 40 percent reduction in cross sectional area of the face shell resulted in significantly higher shear stresses in the material. Strength tests and beam tests have demonstrated adequate performance in compression, but premature shear failure may indicate low ultimate tensile strength in the material. A combination of reduced area and lower tensile strength can contribute to these very low ultimate shear strength results.

The second potential problem, the inability to develop the horizontal joint steel, is suggested by the significant vertical cracks that developed through the reinforced bed joints of the lightweight unit wall. It appears that the joint steel was insufficient in minimizing crack development or crack growth. While it is believed that the 7/8 in. bed joint is sufficient to provide adequate cover for corrosion protection of the joint steel, it may not properly develop the strength of the reinforcement. However, the horizontal steel cannot be the only contributor to the low shear strength of the wall, because the factors involving the horizontal steel account for only 25 percent of the predicted wall strength. Excluding consideration of any horizontal steel in the shear strength equation will still result in over predicting shear strength by a factor of 4.3 times.

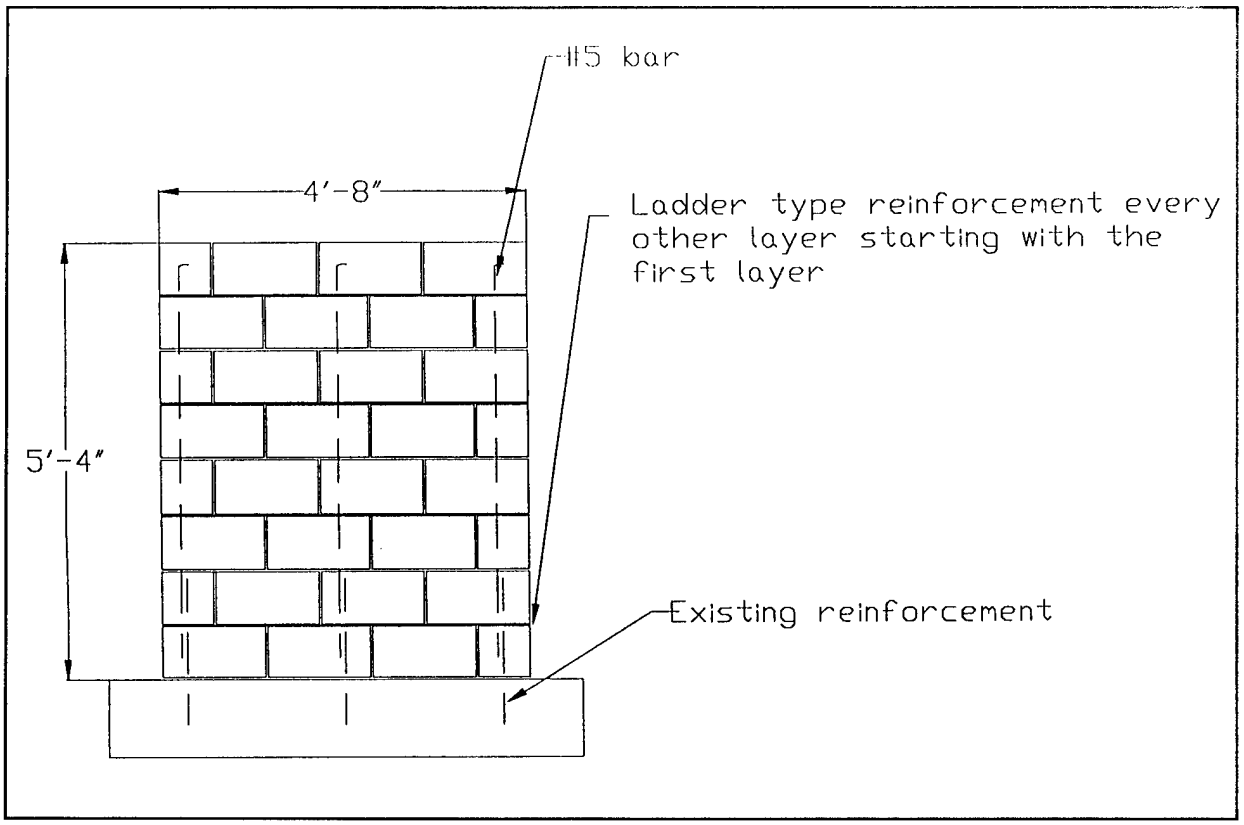

Figure 5.1. Typical test wall.

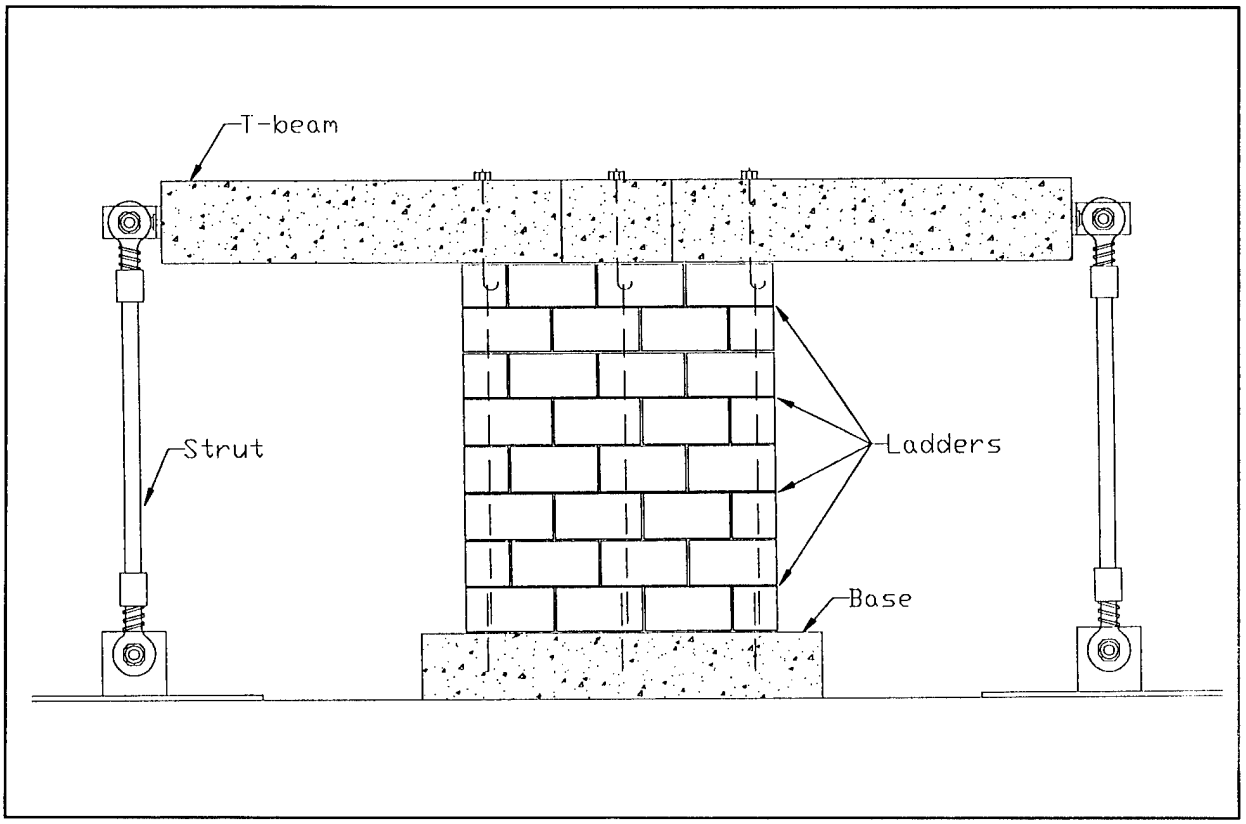

Figure 5.2. Side view of test wall and vertical restraint.

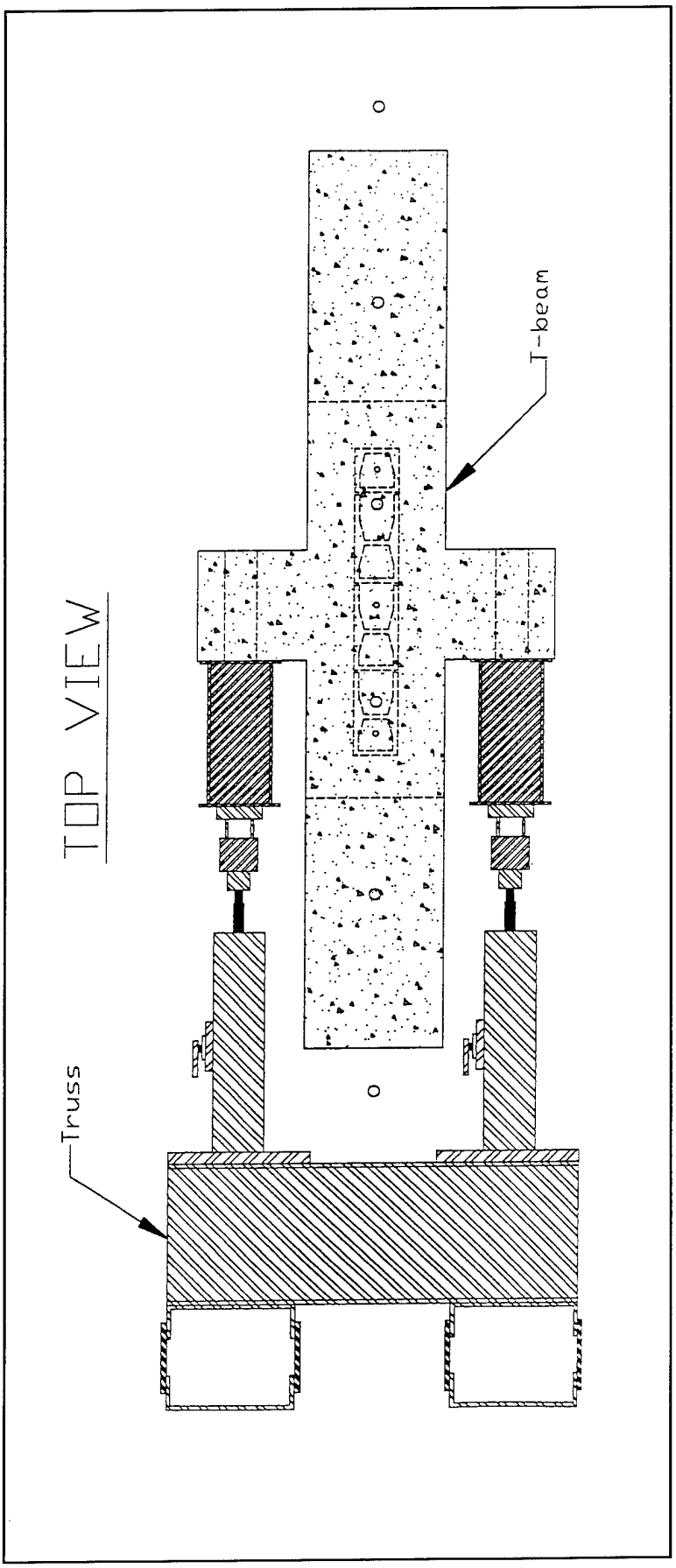

Figure 5.3. Plan view of load apparatus.

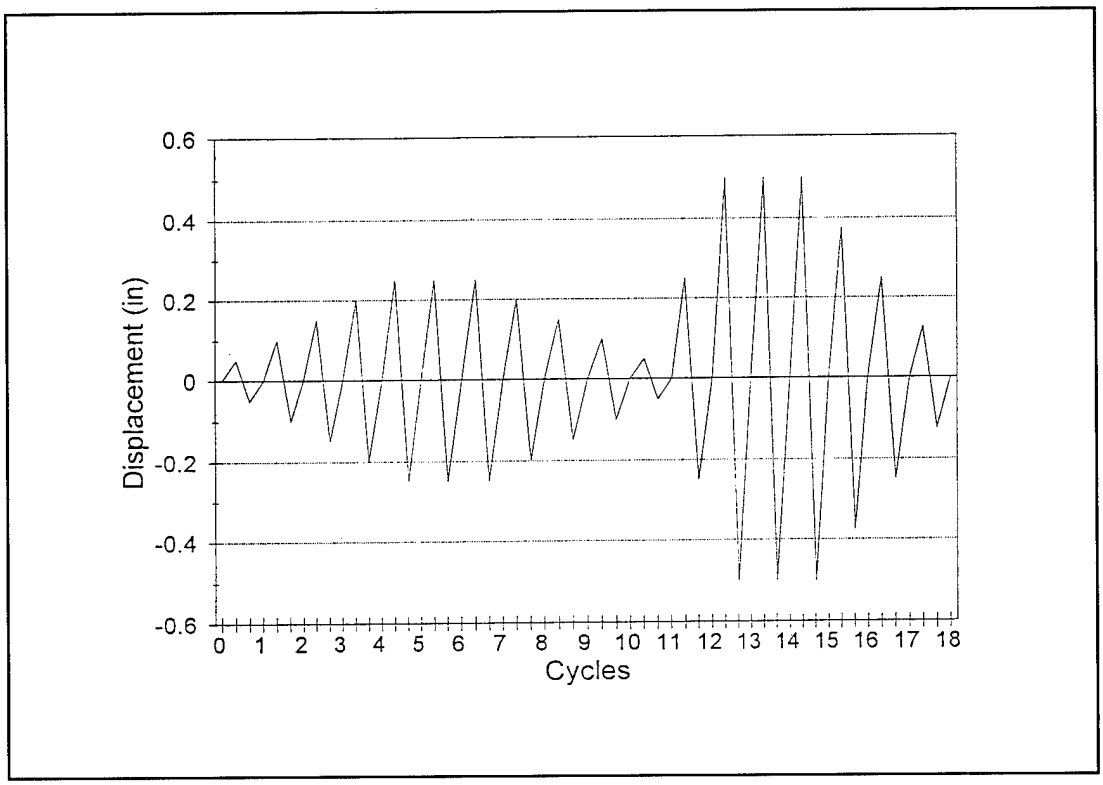

Figure 5.4. Actuator stroke displacement cycle used in test loading.

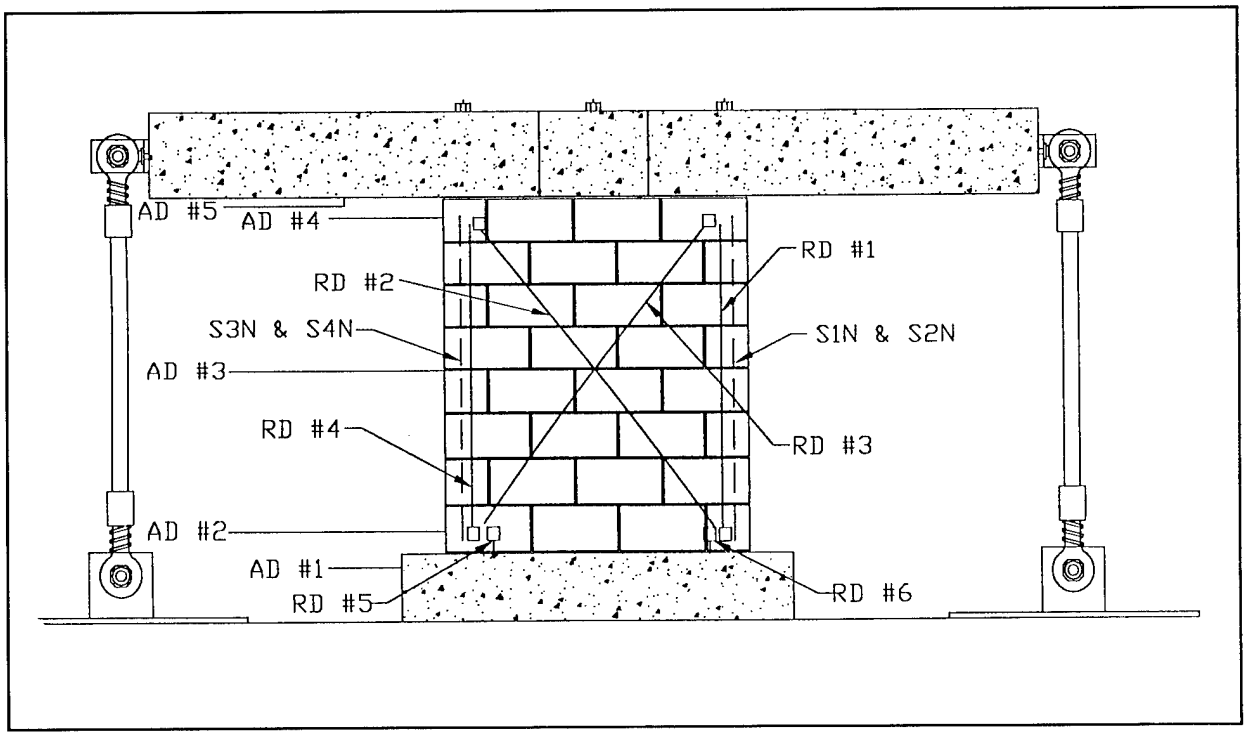

Figure 5.5. Instrumentation diagram for test setup.

Table 5.1. Parameters for shear strength predictions and results.

Wall	r	f_m (MPa)	f_{yv} (MPa)	ρ_v	f_{yh} (MPa)	ρ_h	q (MPa)	V_p (MPa)	V_p (kips)
LW	1.14	20.9	438	0.00139	417	0.00029	0.0655	0.569	34.7
NW	1.14	19.1	438	0.00139	417	0.00029	0.0655	0.542	33.1

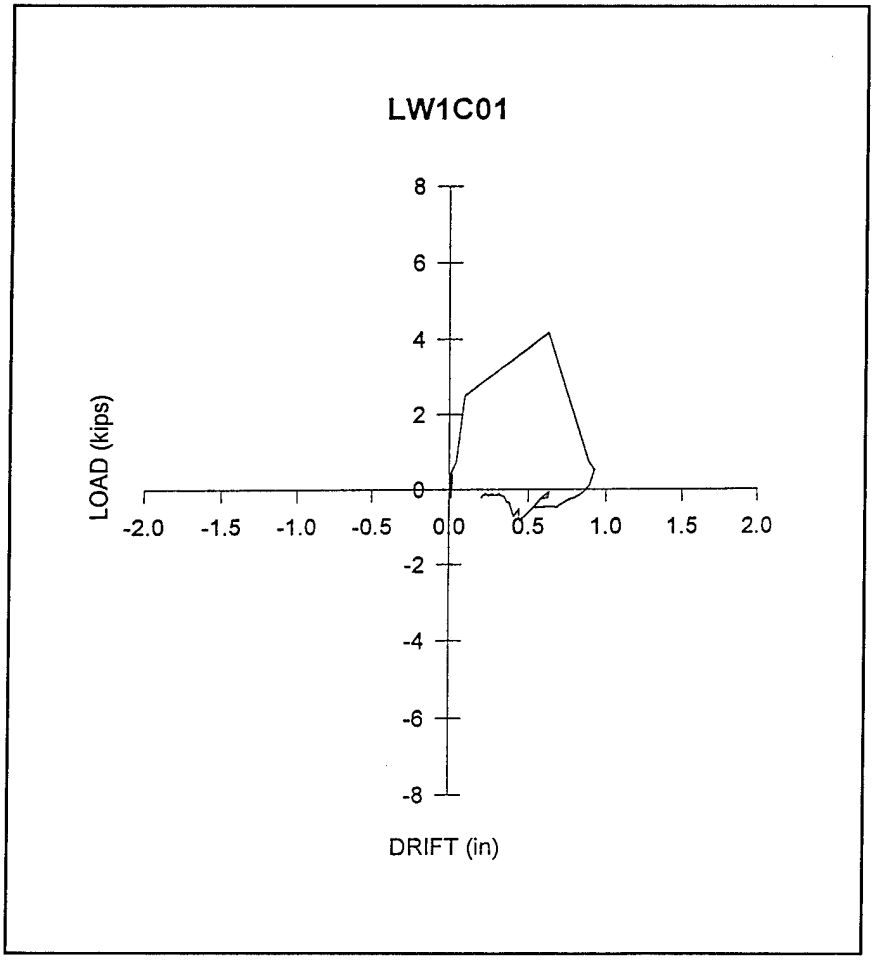

Figure 5.6. Load vs displacement for lightweight CMU test wall after first four loading cycles.

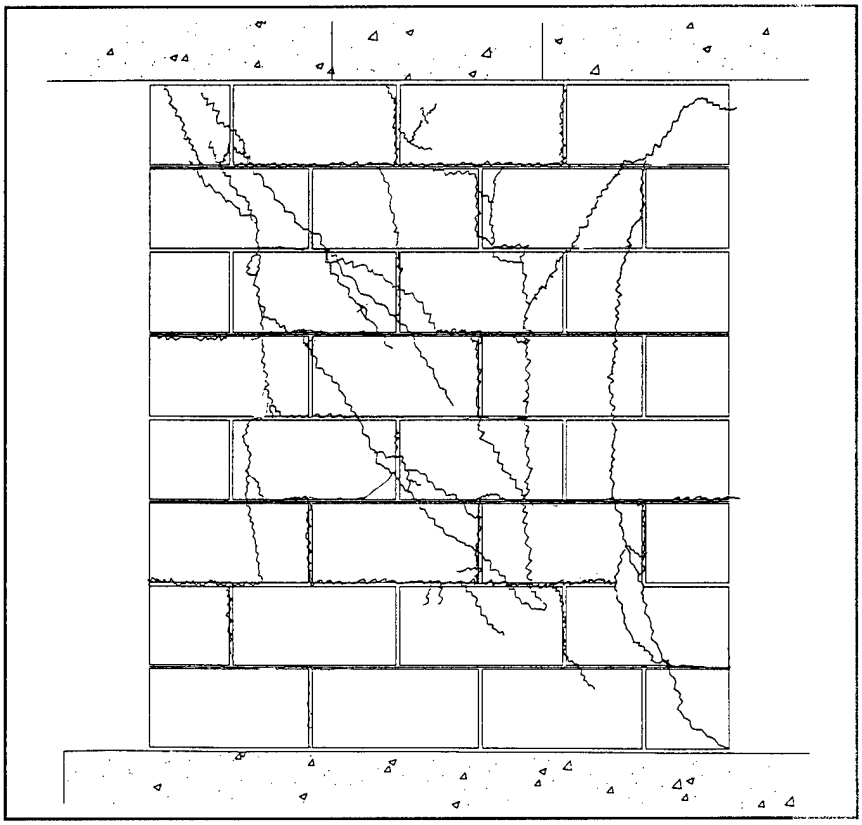

Figure 5.7. Diagram of crack pattern for lightweight CMU test wall after first four loading cycles.

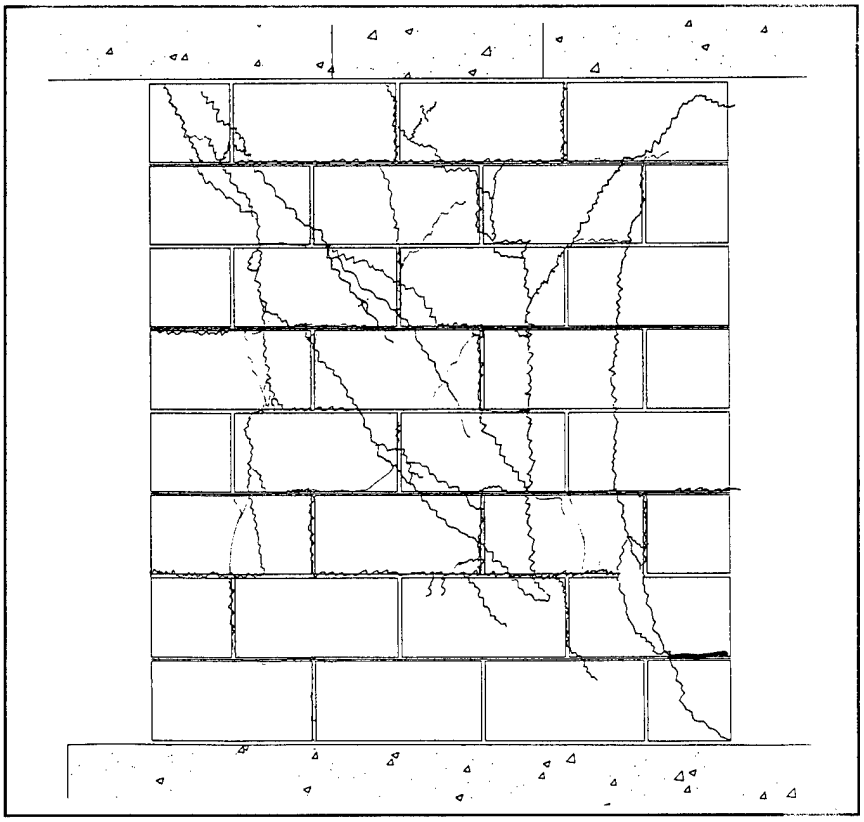

Figure 5.8. Final crack pattern representing complete failure of lightweight CMU test wall.

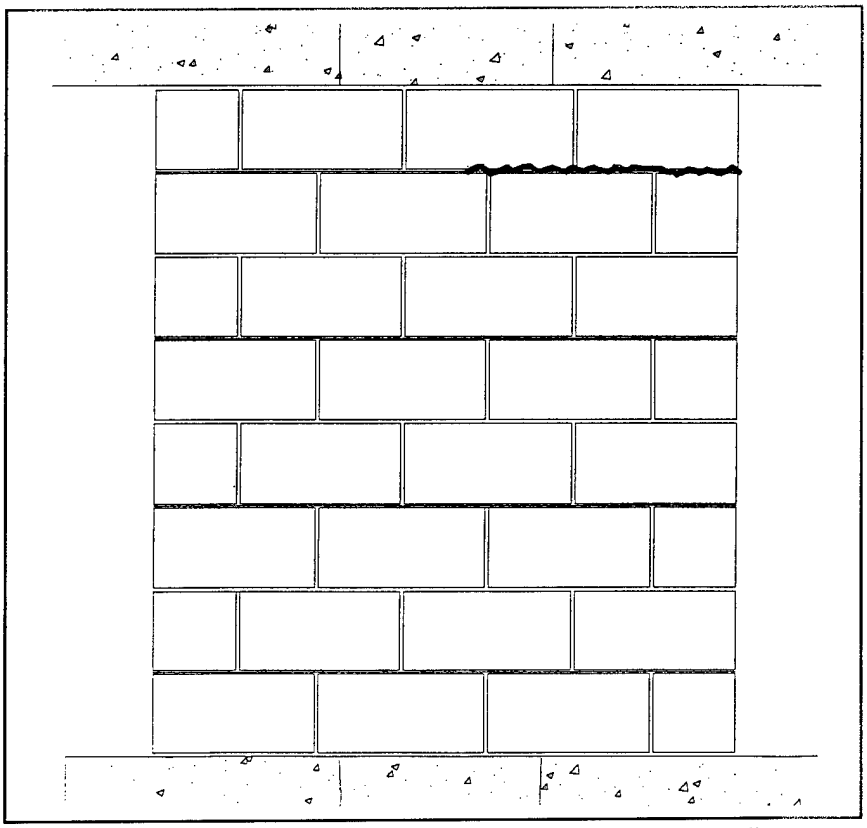

Figure 5.9. Crack in normal-weight (HW) CMU wall after three loading cycles.

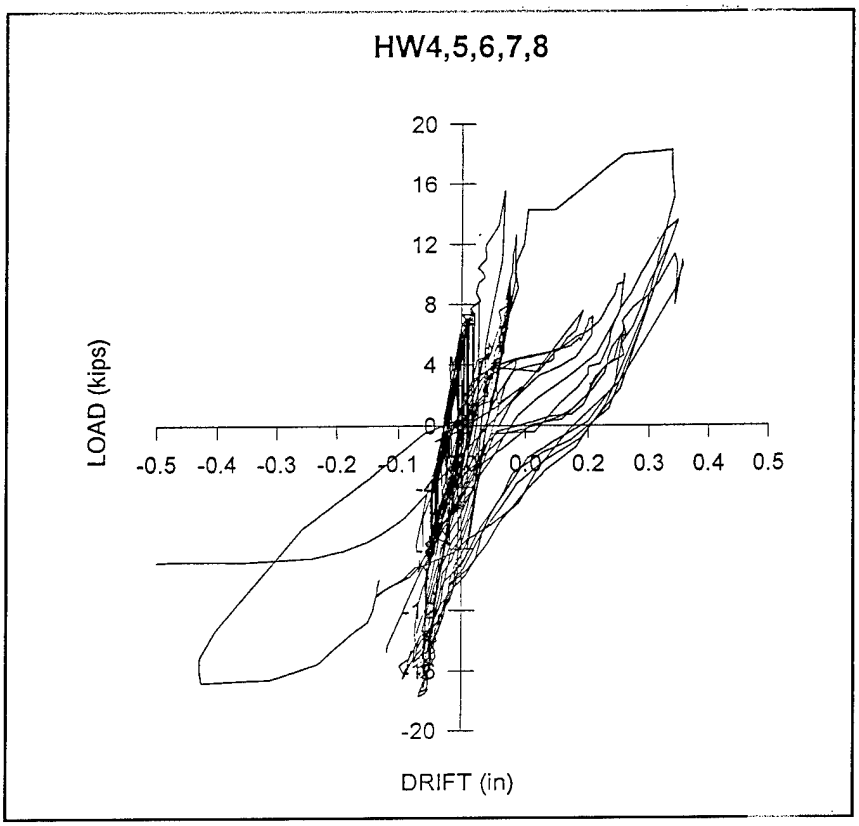

Figure 5.10. Load vs deflection graph for load series HW4 through HW8.

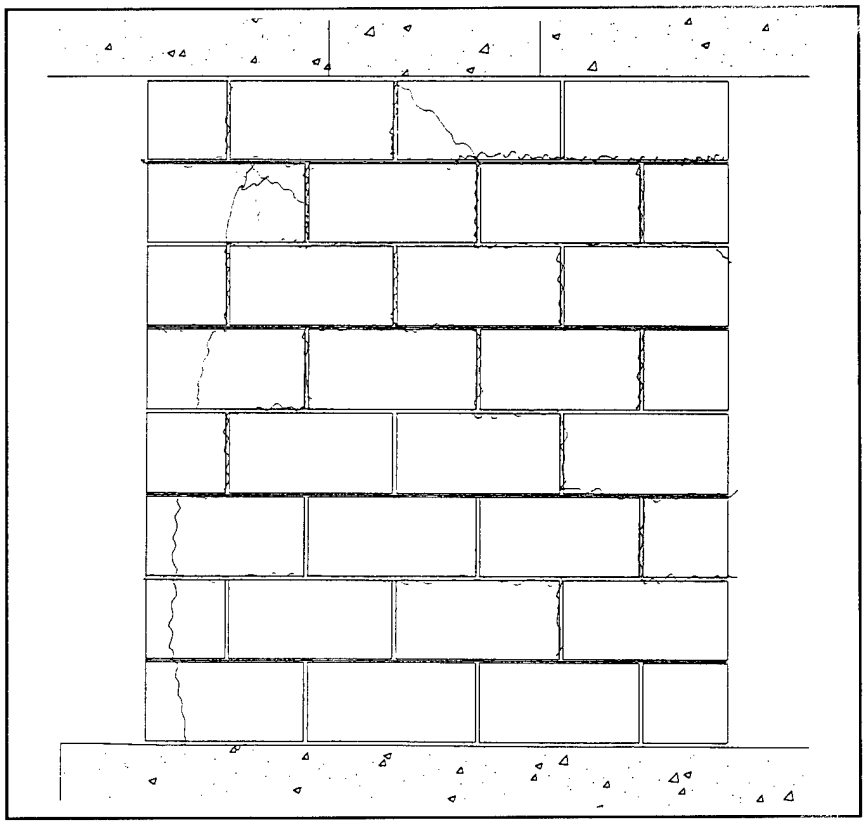

Figure 5.11. Crack patterns for test series HW3, HW7, and HW8.

6 Durability Evaluation

6.1 Introduction

No standard currently exists for the comprehensive testing of CMU durability. Therefore a major portion of this phase of the work was devoted to the development of a durability test that adequately evaluates the freeze-thaw performance of CMUs under cycling. Durability factors were calculated for each specimen, and these factors were plotted against variables such as the amount of cementitious materials in the mix to establish relationships and determine optimum ratios. The effect of various admixtures on the durability of the units is evaluated and discussed.

Durability is defined as the ability of the unit to withstand abrasion, chemical attack, weathering, or other deteriorating forces. CMUs are typically used in buildings or retaining walls, and few of these types of structures are subjected to exterior chemical attack or abrasion. The main cause of deterioration for standard CMUs is the weather. Units must be able to withstand periodic wetting and drying from the weather. The most severe weather exposure occurs when wet units are subjected to freezing temperatures. Units that are placed underground and not protected could be exposed to cyclic saturated freezing and thawing.

No standard presently exists for the testing of CMUs for freeze-thaw cycling. A relationship between absorption testing and freeze-thaw durability has not been established for CMUs. Alkali-aggregate reactions or other internal chemical deteriorations cannot be predicted by absorption test results. Therefore, it appeared necessary to test the units under actual freeze-thaw cycling to compare the durability of mixes and to evaluate the effects of internal chemical reactions on the durability of the units.

Existing standards for similar materials were examined. Conditions specific to CMUs were examined and addressed. A test method was developed and executed. Several test runs were made. Test results are provided. The correlation between absorption test results and the freeze-thaw test results is discussed.

6.2 Standard Test Method for Freeze-Thaw Evaluation

6.2.1 Existing Standards

6.2.1.1 ASTM C 666—Freeze-thaw testing of poured-in-place concrete. This test method is designed to determine the resistance of cast-in-place concrete to rapid freeze and thaw cycling. The test is performed in the laboratory by using one of two different procedures: Procedure A uses rapid freezing and thawing in water, and Procedure B uses rapid freezing in air and thawing in water.

The test results are used to compare different mix designs, aggregates, and chemical admixtures and their effect on resistance to freeze-thaw cycling. Specimens that are found to be relatively unaffected are assumed to be either not critically saturated, or are made with sound aggregate, a proper air void system, and allowed to mature properly. Specimens for comparison must be the same size and tested under the same procedure. No extrapolation from test results to field performance can be made.

The standard requires a freezing and thawing device capable of automatically and continuously exposing the specimens to reproducible cycles within the specified temperature ranges. Provisions to store specimens in a frozen condition if the test is interrupted are required. In Procedure A, each specimen is surrounded by not less than 1/32 in. (1 mm) or more than 1/8 in. (3 mm) of water at all times. In Procedure B, specimens are surrounded by water during thawing phases and surrounded by air during freezing phases of the cycling. A method to support the specimen that will not allow direct heat transmission from the bottom of the container to the specimens must be provided. A flat spiral of 1/8 in. (3 mm) wire laid on the bottom of the container is allowed. The temperature of the heat exchanging medium must be constant enough that the difference in temperature of any two points taken on any surface of any of the containers (Procedure A) or on any specimen surface (Procedure B) is within 6 °F (-3.3 °C). In Procedure B, the specimens are not kept in containers, and the supports on which the specimens rest should not be in contact with the full end or side of a specimen. Temperature measuring equipment must be accurate to within 2 °F (1.1 °C). Dynamic Testing Apparatus must conform to the requirements of ASTM C 215.

The nominal cycle consists of a temperature variation at the center of the control units from 40 °F (4.4 °C) to 0 °F (-17.8 °C) and back over a period of 2–5 hours. The thawing phase of the cycle must be at least 25 percent of the cycle for Procedure A and at least 20 percent of the cycle for Procedure B. To make a fair comparison of one mix to another, there are many specifications concerning the time required to

change the temperature at the center of the specimen and the temperature differential between the surface and the center of the specimen. Both procedures use prisms or cylinders made in accordance with ASTM C 192 and ASTM C 490.

The test is conducted using the following procedure. Immediately after curing, the specimen must be brought to within -2 °F (-16.7 °C) to +4 °F (-15.6 °C) of the target thaw temperature, tested for fundamental transverse frequency, and weighed. The cross-sectional dimensions must be measured to within the tolerances specified in ASTM C 215. If length comparison is to be made, the original length measurements must also be taken at this time. The moisture content should be kept as constant as possible during this time.

Freeze-thaw cycling can be started at the beginning of the thaw phase of the cycle. Specimens must be removed periodically, in thawed condition, and weighed, tested for fundamental frequency, and checked for length change if applicable. The interval between tests may not exceed 36 cycles. The test is continued for 300 cycles. Individual specimens have failed and are removed from the test when their relative dynamic modulus of elasticity (defined under "Calculations") reaches 60 percent of the initial modulus. When using the optional length test, ten percent expansion is the failure criteria.

The standard recommends that fundamental longitudinal frequency and fundamental transverse frequency be initially measured and used as a check on the fundamental transverse frequency and Poisson's ratio respectively.

The relative dynamic modulus of elasticity is calculated using the following equation:

$$Pc = (n12/n2) * 100 \qquad \text{[Eq 6-1]}$$

where:

Pc = the relative dynamic modulus of elasticity, after c cycles of freezing and thawing (percent)
n = the dynamic modulus of elasticity at 0 cycles (Hz), and
n1 = the dynamic modulus of elasticity at c cycles (Hz).

This calculation assumes that the weight and the dimensions of each specimen are the same, and these dimensions remain the same during cycling. The procedure is adequate for comparing different concrete formulations.

The durability factor is calculated by:

$$DF = PN/M \quad \text{[Eq 6-2]}$$

where:

DF = the durability of the test specimen
P = the relative dynamic modulus of elasticity after N cycles (percent)
N = the number of cycles at which the specimen fails, and
M = the specified number of cycles considered passing.

If the length change option is chosen, the length change (percent) is calculated as follows:

$$Lc = [(l2 - l1)/Lg] * 100 \quad \text{[Eq 6-3]}$$

where:

Lc = the length change of the test specimen after c cycles (percent)
l2 = length comparator reading at 0 cycles
l1 = length comparator reading after c cycles, and
Lg = the effective gage length between the innermost ends of the gage studs as shown in the mold diagram in Specification C490.

6.2.1.2 ***ASTM C 67—Freeze-thaw testing for brick.*** This standard covers the procedures for all necessary sampling and testing for brick and structural clay tile. Only those portions of the standard that relate to freeze-thaw testing will be covered in this review.

Brick specimens must be half bricks with approximately plane and parallel ends. Specimens must not have shattering or unsoundness from absorption or flexure tests. A minimum of five brick specimens must be tested. Five full, or 4-in. (101.6-mm) cells cut from five separate structural clay tile specimens must be used. No restrictions are made on the age of the specimens or the method of storing them before testing begins.

The procedure is similar to the procedure required for ASTM C 666 Method B. Test specimens must be dried in the drying oven for a minimum of 24 hours and until two successive weighings yield results to within ±2 percent. They are cooled in the drying room, unstacked, for a period of at least four hours. Specimens may be used when they are no longer noticeably warm. Alternatively, specimens may be cooled by setting in a ventilated room at room temperature for 4 hours if they have a current of air from a fan passing over them for at least 2 hours.

The specimens are then weighed and submerged in the thawing tank for 4 ± 1/2 hours, removed from the thawing tank, and placed on edge in the trays in such a manner that they are separated by 1/2 in. (12.7 mm). Water must be added to the tray until each specimen stands in 1/2 in. (12.7 mm) of water, and the tray is placed in the freezing chamber for 20 ± 1 hours. The trays and specimens are immersed in the thawing tank for 4 ± 1/2 hours, removed from the thawing tank, and set on edge and in water. The freezing cycle is repeated. The procedure is repeated each day of the normal work week, ending with the thawing cycle. The specimens must be removed from the thawing tank and stored in the drying room for 44 ±1 hours. They should not be stacked and must have at least 1 in. (25.4 mm) between each of them. The specimens must be inspected and the weekly cycling repeated starting and ending with the thawing cycle. The drying cycle is optional if continuous cycling is possible. If the test must be interrupted, the specimens should be kept in the drying cycle. The test must be continued for 50 cycles. Individual specimens are removed from the test when they break, or when they have lost 3 percent of their original weight as judged by visual inspection

There are two possible methods for reporting results. The loss in weight at failure may be calculated as a percentage of the original dry weight of the specimen. It is also permissible to report only the number of cycles taken to fail the specimen along with a general description of the failure.

6.2.1.3 ASTM C 671—Freeze-thaw durability testing by dilation. This standard uses dilation as a measurement of freeze-thaw durability for cast-in-place concrete. The specimen is cooled slowly from 35 to 15 °F (1.7 to -9.4 °C). The cooling must be at a rate of 5 ±1 °F/hr (2.8 ± 0.6 °C/hr). It is followed by a constant temperature bath at 35 ±2 °F (1.7 ±1.1 °C). The cycle is repeated every two weeks. Length change is measured after each cycle and a graph of the deviation from original length-vs-time is obtained. Failure is reached when the specimen achieves a specified deviation from the prefreezing length-vs-time line. This deviation is called the dilation.

The dilation method was developed to replace the rapid cycling methods of ASTM C 666. It is based on research by Powers, Helmuth, and others. These researchers have suggested that dilation may be an accurate predictor of freeze-thaw durability because actual freezing due to weather takes place at a very slow rate, so rapid freeze-thaw testing may not give an accurate indication of performance.

6.2.2 Existing Related Standards

6.2.2.1 ASTM C 140—Absorption of concrete masonry units. The ASTM C 90 standard for CMUs requires that units be tested under ASTM C 140 for strength and absorption. Only the part of the standard covering absorption testing will be discussed.

A minimum of three full sized specimens for each batch is required. The specimens must be immersed in water at room temperature for 24 hours, and then weighed while suspended by a metal wire and fully immersed in water. The specimens must be removed from the water and allowed to drain on a 3/8 in. (9.5 mm) or coarser wire mesh for one minute. The specimens are wiped with a damp cloth and weighed in the air. After saturating, the specimens must be oven dried at a temperature of 212 to 239 °F (100 to 115 °C) for a minimum of 24 hours and until two successive weightings at intervals of two hours are not different by more than 0.2 percent.

Absorption is calculated using either

$$\text{Absorption (pcf)} = [(A - B)/(A - C)] \times 62.4 \qquad \text{[Eq 6-4]}$$

or

$$\text{Absorption (\%)} = [(A - B)/B)] \times 100 \qquad \text{[Eq 6-5]}$$

where:

A = the weight of the saturated unit in air (lb),
B = the oven dry weight of the unit (lb), and
C = the suspended immersed weight of the saturated unit (lb).

It is necessary to report results for individual specimens. An average of the results of three units from each batch is also required.

ASTM C 90 sets criteria for units to be exposed to weathering or below grade, and is based on ASTM C 140 - Absorption results. These criteria are summarized in Table 6.1.

6.2.2.2 ASTM C 88—Sodium sulfide salts destruction test. This test involves soaking a presized specimen of aggregate for 16–18 hours in a solution of water and sodium sulfate or magnesium sulfate. The specimen is drained for 15*5 minutes and oven-dried at a temperature of 230 ±9 °F (110 ±5 °C) to a constant weight. This process is repeated for a specified number of cycles and the aggregate is

resieved and weighed. The percentage of initial weight retained on each sieve is reported. A drawing or description of the type of distress is also required.

According to the theory behind this test, the salt residue left in the aggregate pores after drying will expand upon rehydration. This expansion is thought to simulate the expansion of water during freezing. Although this test is specified for aggregates, the scope is broad enough that the method could be adapted for testing concrete specimens.

6.2.3 Evaluation of Existing Standards for Application to CMU

6.2.3.1 NCMA task force on freeze-thaw durability. A National Concrete Masonry Association Task Force was formed to examine cement content and the use of admixtures to enhance the freeze-thaw durability CMUs. Since there are no available standard test procedures for freeze-thaw testing of CMUs, the task force investigated current related standards and available information and proposed a new standard test procedure for CMUs. The task force's modified test procedure is summarized as follows:

1. Dry and weigh specimen utilizing ASTM C 67 as a guideline.
2. Immerse specimen for 24 hours and wet weigh, using ASTM C 140 as a guideline.
3. Once the specimen has been weighed, place in tray so head face is surrounded by 1/2 in. of water and rests on a 1/4-in. rod.
4. Freeze and thaw utilizing ASTM C 666.
5. After 15 cycles (plus or minus two cycles) of this freezing and thawing per ASTM C 666, thaw and place specimen in water (thawing tank per ASTM C 67) for 24 hours, then wet weigh using ASTM C 140 again as a guideline.
6. After weight has been determined, if the specimen has experienced a weight loss of 7 percent and is visibly deteriorating, discontinue test. Dry and weigh the specimen as per ASTM C 67.
7. Continue testing for a total of 300 cycles, making observations every 25 cycles, using the criteria described in numbers 5 and 6.
8. If the test must be interrupted, keep specimen in a frozen state.

6.2.3.2 ACI 201.2R – 3 committee report. The ACI 201.2R – 3 committee report discusses the resistance of poured-in-place concrete to freezing and thawing. It is one of several reports on durability contained in ACI 201.2R - 77, "Guide to Durable Concrete."

The report references several studies by Powers, Helmuth, and Associates from 1933 to 1961, and later studies by Powers (1945, 1965) and Helmuth (1961, 1962). Powers originally believed that frost damage was caused only by hydraulic pressures when water expanded from freezing within a capillary in the paste. This theory hypothesized that the magnitude of the pressure would be dependent on the rate of freezing, the degree of saturation, the coefficient of permeability of the paste, and the length of the flow path for the water to escape.

However, results of later studies were not consistent with this hypothesis. Powers and Helmuth found that most of the water moved toward freezing sites and not away from them. They also found that expansions during freezing decreased with an increased rate of cooling and not increased as would be expected from the hypothesis. On the basis of this evidence, they proposed the theory that the water within the concrete is really an alkaline solution. When the solution begins to freeze, a 'super cooling' of the solution occurs and the unfrozen solution is left with a high alkalinity. Because the surrounding solution has a much lower alkalinity, osmosis occurs and water migrates toward the freezing site. When the solution and the ice completely fill the capillary, hydraulic pressures cause failure. The surrounding paste shrinks as the water migrates from it.

According to Powers, air entrainment can help alleviate the problem of osmosis. If there are many bubbles and they are evenly spaced, there will be many areas where freezing and expansion can occur. These areas support 'super cooling' well, and compete with the paste capillaries and with each other for osmotic solution. In this way the solution is diffused throughout the concrete, eliminating or reducing hydraulic pressures.

Litvan (1972) continued the study on frost action in cement paste. He proposed that the difference in vapor pressure between the super cooled liquid and the surrounding bulk ice would cause water to migrate to the outside surface or large pores where it can freeze. This migration can result in both a partial desiccation of the paste and an abundance of ice in the crevices and cracks. Litvan states that failure will occur only if the redistribution of water cannot take place because there is too much water, the time available for migration is too short, or the path of migration is too long. He believes that the freezing, in these circumstances, produces a semi-amorphous solid instead of ice. The production of this semi-amorphous solid causes great internal stresses.

According to both studies, entrained air provides internal release chambers where freezing can occur with little or no damage to the paste. Therefore, the committee

states that it is generally agreed that damages to the cement paste due to hydraulic pressures in the paste can be eliminated by the correct use of entrained air.

The use of air-entrainment alone, however, does not guarantee that the concrete will not be damaged from freezing. Freezing phenomena in the aggregate particles must also be taken into account. Most aggregates have large pores in comparison to the cement paste. In tests done by Powers (1965), the aggregate pores expelled water during freezing.

Dunn and Hudec (1965) proposed that deterioration of rock during freezing was due to the expansion of unfreezable water and not to freezing. Clay bearing limestone aggregates that failed without freezing were used to support this theory. Studies by Helmuth (1961, 1962) have shown, however, that absorbed water contracts instead of expanding during freezing. Helmuth does agree that the absorption of large amounts of water by aggregates with fine pore structures can be detrimental to concrete. However, he believes that the detriment is due to the formation of ice.

Verbeck and Landgren (1960) have shown that the size of the coarse aggregate is an important factor in frost resistance. They have shown each type of natural rock has a critical size. Rocks below the critical size can be frozen without damage. For most good quality rocks, they demonstrated that the critical size was 1/4 in. (6 mm) or larger. They found that some aggregate rocks such as granite and basalt do not experience internal stress when freezing occurs regardless of the particle size.

The committee report states these general conclusions: if concrete becomes critically saturated and is frozen, it may fail if it is not air-entrained, and if the concrete is air-entrained with a bubble spacing factor of less than 0.008 in. (0.20 mm), freezing will not produce destructive stress.

Some rocks contain practically no freezable water and will withstand freezing and thawing in air-entrained concrete even if kept wet for long periods of time. This resistance to freezing may not occur if the voids in the rock become filled with water and solid matter. If absorptive aggregates are used and the concrete is continuously exposed to a wet environment, the concrete will probably fail. Popouts can result when this type of aggregate ruptures or expels water into the paste. Since concrete is not normally in a state of critical saturation and can dry out during drying seasons, air-entrained concrete is generally not damaged by frost action even when made with absorptive aggregates.

The effect of freeze-thaw cycling is dependent on the degree of saturation of the concrete. Therefore, the committee strongly recommends structural detailing that

reduces or eliminates water infiltration or standing water in contact with the structure.

The water absorption of aggregate in concrete is a function of the rate of water absorption of the cement paste. Therefore, it is recommended that the aggregate be as dry as possible and the water to cement ratio be as low as possible when the concrete is being made. Good construction and curing practices are also recommended.

As mentioned before, the use of entrained air is strongly recommended. An air content of 6 to 7 ½ percent is recommended for a 3/8 in. (mm) aggregate size. Some air entraining admixtures do not produce the necessary 0.008 in. (0.20 mm) spacing and are not recommended for use. The amount of admixture required to produce the desired air entrainment is affected by mix proportioning, slump, mixing time, temperature, amount of pozzolans in the mix, and many other factors. The committee recommends using one of the standard methods to determine the air content in the mix.

The committee states that the ASTM C 666 procedure is accepted by many agencies as the most reliable indicator of relative durability. The test has been criticized, however, because it does not duplicate actual field moisture conditions and it uses an accelerated cooling rate. Therefore, test results can be used to compare aggregates or mixes, but cannot be used to assess whether or not an aggregate or mix will give satisfactory performance under actual freeze-thaw conditions. ASTM C 671 is described and discussed. The committee concluded that this test shows promise, but takes a long time to perform and is very sensitive to moisture content. They state that most agencies have continued to use the ASTM C 666 pending improvements in the ASTM C 671 procedure.

6.3 Selection of Freeze-Thaw Test Method for CMU

6.3.1 Scope

None of the standard existing procedures for brick masonry could be applied directly to concrete masonry because brick is a ceramic, not a concrete. Differences in the failure mechanisms between the two materials are highly probable. Therefore, pass and failure criteria for brick masonry may not be adequate for concrete masonry. A few procedures unique to the ASTM C 67 standard were notable. The standard allowed specimens to be saw cut with no change in procedures or calculations. This suggested that a specimen cut from a CMU might provide a representative sample.

Also, the ASTM C 67 standard required drying the specimens to a constant water content before testing. Although not required by other standards, this appeared to be a logical requirement since initial water absorption may be a variable in freeze-thaw resistance.

The NCMA Committee procedure did not specify specimen type or size for concrete masonry. Although visible detection of deterioration as a basis for failure may be acceptable for brick, other standards for concrete insist on the monitoring of dynamic modulus. Before testing, the validity of a 7 percent weight loss was unknown. The work of Powers (1945, 1965) and Helmuth (1961, 1962) on osmosis suggests, however, that a criterion based on weight gain may be more representative.

The Sodium Sulfide Destruction Test or the Critical Dilation Test have not been fully developed. From the work of Powers and Helmuth, it is known that an osmosis of water toward the cells occurs during freezing due to the alkalinity of the solution. The Sodium Sulfide Destruction Test ignores this phenomenon and tests only the material's ability to withstand swelling in the pores. Since the rate of osmosis is also an important factor, this test was not used. The Critical Dilation Test mimics natural phenomena by requiring a slow freeze. Dilation is directly related to the rate of osmosis within the material, and the test should give very representative results. However, this test has been slow to be accepted in the industry. The concrete masonry test method selected must be easy to understand for the results to be accepted. Therefore, a more conventional approach was chosen.

Two basic approaches presently exist for testing cast-in-place concrete. One approach is to saturate the specimens during thawing phases and to partially immerse the specimens during the freezing phases. The other approach is to leave the specimens fully saturated during all phases of the cycle. The exposure of CMUs is more likely simulated by the partially saturated method, but this method is much harder to control in the laboratory. Variations in the container humidity or small variations in the level of immersing water may cause differing water contents in specimens. This can produce variations in the internal stresses between specimens. Variations caused by the rate of temperature change can also be further complicated by differing water contents. There are already many variables involved with freeze-thaw testing that are difficult or impossible to control. Therefore, the fully saturated method was chosen to eliminate the variable of moisture content.

This test method is used to determine the resistance of CMUs to rapid freeze-thaw cycling. The test is performed in the laboratory by rapid freezing and thawing in water. The results may be used to compare different mix designs, aggregates, and

concrete masonry units to freeze-thaw cycling. Specimens to be compared must be tested under the same conditions. No extrapolation from test results to field performance can be made. The test is designed for comparative purposes only and no minimum standard is available or inferred.

Criteria for passing and failing are different for each existing freeze-thaw standard. The applicability of these criteria depends to a large extent on the material, the specimen, and the possible modes of failure. The most common response of brick to freeze-thaw cycling is degradation of the surface. Because of this, visual inspection and weight loss are valid tools for monitoring performance. Concrete, on the other hand, exhibits many modes of failure other than surface degradation. It is possible for a concrete specimen to have little or no surface degradation at failure. Internal damage may leave concrete with a fraction of its original structural strength without any surface deterioration. In large specimens, those required for ASTM C 666 testing for instance, the internal expansion could cause enough swelling to make the specimens hard to remove from the container. For these reasons, ASTM C 666 requires monitoring of the dynamic modulus of elasticity as a control criterion. Specimens that drop below 60 percent of their initial dynamic modulus of elasticity, as calculated by ASTM C 215, have failed and are removed from the test. Both weight change and dynamic modulus of elasticity were used as criteria for evaluating CMU durability.

6.3.1.1 ***Weight change.*** All specimens tested under this project were monitored for change in weight at approximately 12-cycle intervals. Specimens gained weight for approximately 3/4 of the complete test time. This was largely attributed to the absorption of water into the unit. Just before failure, the units began to expel water and the weights dropped quickly. Although this behavior was consistent, it was not considered for use as a test criterion for several reasons.

Although weight gains and losses were noted, none of the weight changes represented more than 2 percent change in weight for any specimen. Precision in excess of that normally available in a standard laboratory would be required to accurately detect weight changes of this magnitude. Even with adequate equipment, no numerical correlation that could be used for failure determination could be found.

Although much information about the specimen can be derived from studying weight change during cycling, setting failure criteria from this information was impossible. Units that failed quickly often had high weight gains at the beginning of cycling and continued to gain weight for some time. This behavior was probably due to the active osmotic forces within the unit. Although initial weight gain was high in early failing units, units with high alkalinity but good void systems also had

high initial weight gains but took much longer to fail. Therefore, initial weight gain was ruled out as a failure criterion. No correlation could be found between percentage of weight loss and number of cycles to failure. Further studies of weight changes may shed more light in this area.

6.3.1.2 ***Dynamic modulus of elasticity.*** The fundamental frequency of each specimen was determined at approximately every 12 cycles. ASTM C 666 requires calculations based on the dynamic modulus of elasticity calculated by the ASTM C 215 method. Steady decrease in the modulus of elasticity was noted for nearly every specimen before failure. Failure occurred after the specimens had dropped to within 60–70 percent of the original modulus. The measurement appears to be a very good criterion for failure. Aside from use as a failure criterion, much information can be gained about the behavior of the specimen by studying the change in dynamic modulus of elasticity with increasing numbers of freeze-thaw cycling.

However, a problem does exist with the method of calculating the dynamic modulus of elasticity from the ASTM C 215 method. For convenience, the formula for transverse dynamic modulus of elasticity as presented in ASTM C 215 is repeated here.

The dynamic Young's modulus of elasticity is calculated using

$$\text{DynamicE} = CWn^2 \qquad \text{[Eq 6-6]}$$

where:

W = the weight of the specimen (lb),

n = the fundamental transverse frequency (Hz), either

$$C = 0.00416\frac{(L^3T)}{d^4}$$

for a cylinder, or

$$C = 0.00245\frac{(L^3T)}{bt^3}$$

for a prism

L = the length of the specimen (in.),

d = the diameter of the cylinder (in.),

t = the dimension in the driving direction

b = the dimension in the other cross-sectional dimension

T = a factor based on the radius of gyration, the length of the specimen and Poisson's ratio. The radius of gyration, K, is equal to d/4 for a cylinder

and t/3.464 for a prism. Table 6.2 gives values of T for a Poisson's ratio of 1/6.

These calculations do not make provisions for differing modes of vibration. To assess the validity of these equations over various modes it was first necessary to derive a general expression for the modulus of elasticity. One possible derivation for this equation comes from an analysis known as the Bernoulli method. Since the natural frequency for a damped system is nearly the same as for an undamped system, the simpler undamped system is considered. This method develops a relationship between the static modulus of elasticity and the fundamental frequency for a continuous system by modeling the system as a beam in flexure. The resulting equation for the dynamic modulus of elasticity is:

$$E = \left(\frac{\omega}{C_n}\right)^2 \frac{mL^3}{I} \qquad \text{[Eq 6-7]}$$

where:

m = specimen mass
L = specimen length
I = specimen moment of inertia
Cn = a constant chosen from Table 6.3
ω = fundamental frequency of the mode corresponding to the value used for Cn.

Equation 6-7 can be expressed as

$$\omega = C_n \sqrt{\frac{EI}{mL^3}} \qquad \text{[Eq 6-8]}$$

This equation was solved for the first 10 modes for various values of modulus of elasticity. The modulus of elasticity was calculated using the equation

$$E_s = 40000\sqrt{f_c} + 1 \times 10^6 \left(\frac{w}{145}\right)^{0.5} \qquad \text{[Eq 6-9]}$$

developed by Nilson at Cornell where f'c is the compressive strength of the concrete (psi) and is the unit weight (pcf). The equation has been shown to be valid for concrete with compressive strengths from 3000 psi to 12000 psi. Table 6.4 gives ranges of expected fundamental frequencies obtained for concrete specimens with dimensions of 3 × 7/8 × 16 5/8 in. (7.6 × 2.2 × 42.2 cm). The range represents moduli of elasticity for concrete with densities ranging from 80–145 pcf, and compressive strengths ranging from 1800–5000 psi.

of elasticity for concrete with densities ranging from 80–145 pcf, and compressive strengths ranging from 1800–5000 psi.

6.3.2 Test Specimens

Specimen selection was the biggest stumbling block to directly adapting any of the present standards. Cast-in-place or proctor-type specimens do not adequately represent the properties of CMUs manufactured with vibro-press technology. Most units are large and bulky with large voids. This fact, complicated by the multitude of sizes and shapes available, suggests that full units would not make appropriate specimens.

CMUs presently used for structural applications have hollow core areas in the units. Structural stresses are resisted mainly by the webs and face shells. If the unit is subjected to saturated freezing and thawing cycles, the webs and face shells may be surrounded by water or ice. The resistance of the unit to this cycling is dependent on the thickness of the face shell or web as well as the intrinsic properties of the unit. To model the behavior of the actual unit as closely as possible, a specimen cut from the face shell of the unit was chosen. Nearly all existing standards allow cut specimens with no added adjustments to the procedures.

The specimen size was governed by the availability of automatic cycling equipment container sizes. The cycling equipment in the laboratory was supplied with containers to accommodate a 3 × 4 × 16-in. (7.6 × 10.2 × 40.6-cm) specimen under ASTM C 666 standards. Quarter-inch (0.64-cm) plastic end blocks allowed the containers to accommodate 3 × 4 × 15-3/4-in. (7.6 × 10.2 × 40-cm) specimens. Since the most commonly used CMU on the market is 15-5/8 in. (39.7 cm) in length, a specimen size of 3 × 15-5/8 in. × the thickness of the face shell (7.6 × 39.7 cm × the thickness of the face shell) was chosen for testing.

Proportions of cement, aggregate, water and silica fume, fly ash, and hydrated lime for the mixes tested are shown in Tables 6.5 and 6.6. Although specimens were tested at various ages, most specimens tested simultaneously were the same age.

6.3.3 Test Procedure

Standardization of the environment is critical if specimens from one test are to be compared with one another. During testing, ASTM C 666 requires monitoring the temperature at the center of one of the units. The temperature change controls the length of the cycle and the control specimen is moved around in the testing apparatus to ensure that all areas of the apparatus are monitored. Automated

cycling works well for fully saturated tests and is less labor-intensive than the fixed cycle rates and narrow temperature variations called for in the ASTM C 67 method.

Internal temperature monitoring is not practical for concrete masonry specimens, however. It is impractical to produce specimens with the control sensors cast in the center, as is done for ASTM C 666. Because different units have different sized face shells, the specimens are also different in size. Some will take longer to reach the temperature in the center than others. *In situ* units exposed to the same cycling may behave differently due to the difference in temperature transmission. To overcome these problems, it was decided to control the cycles based on environmental conditions in the testing apparatus.

One of the containers in the apparatus was designated a control chamber. Quarter-inch plastic inserts were placed on the bottom of the container and the sensors placed on top. This set-up kept the sensors off the bottom of the metal container and allowed water to surround the sensors. The sensors were then covered with water. Cycle time was controlled by the temperature of the water. The control container was left in the center of the apparatus for the length of the test and the specimens were rotated at each reading. This technique maintained a constant, reproducible temperature variation within the cycling apparatus as long as the sensors remained in the center of the container and were not allowed to touch the metal sides or bottom.

A temperature range of 0–60 °F (-17.8–15.6 °C) was needed to fully freeze and thaw all specimens each cycle. The nominal freeze-thaw cycle consists of a temperature variation at sensors from 60 °F (15.6 °C) to 0 °F (-17.8 °C) and back over a 4–8 hour period. The thawing phase of the cycle must be at least 25 percent of the cycle. Temperatures above 75 °F (24 °C) or below -15 °F (-26 °C) are not allowed. The period of transition between the freezing and thawing phases of the cycle is not allowed to exceed 10 minutes except when specimens are being checked for weight and fundamental frequency. Freeze-thaw cycling can then be started at the beginning of the thaw phase of the cycle.

The specimens must initially be oven dried to a constant weight. They should be allowed to cool for a minimum of 4 hours and a maximum of 24 hours at room temperature, tested for fundamental transverse frequency, and weighed. The cross-sectional dimensions must be measured to within the tolerances specified in ASTM C 215.

Specimens must be removed periodically at the top of the thawing cycle, weighed, and tested for fundamental frequency. Fundamental torsional frequency must be

initially measured if Poisson's ratio is to be calculated. All specimens should be kept saturated except when taking readings on an individual specimen. The interval between readings should be between 10–15 cycles.

The specimen containers must be rinsed after each weighing, and the specimens returned either randomly or according to some predetermined rotation schedule to ensure that each specimen is subjected to all parts of the freezing apparatus. The test is continued for 100 cycles or until all specimens have failed. Individual specimens that have failed may be removed from the test when their relative dynamic modulus of elasticity (defined under 'Calculations') reaches 60 percent of the initial modulus. When weighing specimens, record remarks about the condition of the specimen. Replace failures with dummy specimens for the remainder of the test.

Freeze-thaw testing was carried out in accordance with the method described above. The specimens were dried to a constant weight, cooled, and submersed in water for 24 hours. The initial saturated fundamental frequency and weight were obtained for each specimen. The specimens were placed into the containers. A rod with a 1/8 in. (0.32 cm) diameter was placed in a Z shape on the bottom of the container to allow room for 1/8 in. (0.32 cm) of water beneath the specimen. All sides of the specimen were surrounded by 1/16 in. (0.16 cm) to 1/8 in. (0.32 cm) of water at all times during the test. The water level was kept at 1/8 in. (0.32 cm) to 1/4 in. (0.0.64 cm) above the top of the specimen.

The temperature of the water that contained the specimens was cycled from 0 °F (-18 °C) ±10 °F (6 °C) to 60 °F (16 °C) ±10 °F (6 °C). Temperature was monitored by reserving one container for temperature sensors. The sensors were held 1/4 in. (0.64 cm) off the bottom of the container with plastic inserts. The containers were filled to a level of 1-1/2 in. (3.8 cm) to 2-1/2 in. (6.4 cm). Temperature variations were monitored and recorded. A chart for a typical week is shown in Figure 6.1. Specimens remained in the cycling chamber until they lacked the structural integrity to continue testing.

Absorption testing was done in accordance with ASTM C 140. The units were submersed in water with a 19.5 in. (49.5 cm) hydraulic head at the base of the unit with the unit on its 16 in. (40.6 cm) side. Submersion time was a minimum of 24 hours and a maximum of 28 hours. Oven temperatures were kept constant between 200 °F (93 °C) and 230 °F (110 °C).

6.4 Test Results

Seven runs were completed. Three of the runs (1, 2, and 4) used random mixes of the same specimens. Three in. (7.6 cm) specimens were cut from the full length of the face shells of 8 × 8 × 16-in. (20.3 × 20.3 × 40.6-cm) units. This gave specimens that were 3 in. × 15-5/8 in. × the thickness of the face shell (7.6 cm × 39.7 cm × face shell thickness).

Another test (run 5) was run using the same specimen size and specimens from units produced in the laboratory. Some of the specimens for this run were cut so that their widths were slightly larger than specified. Although they originally appeared within tolerance, failure occurred prematurely for many of these specimens. For this reason, the test run was discarded as nonrepresentative.

One test (run 3) was conducted with half-sized specimens, 3 × 7-3/4-in. (7.6 × 19.7-cm) by the thickness of the face shell. Another test (run 7) was conducted with specimens that were cut from paving units and were 3 × 7-3/4× 4-in. (7.6 × 19.7 × 10.2-cm). The 7-3/4 in. (19.7 cm) specimens were placed 2 to a container during testing.

The final test (run 6) was performed to ascertain the durability factor for the units chosen to build basements for the productivity tests. Entire units were used for absorption testing.

6.4.1 Durability Data

The fundamental frequency and weight of each specimen were recorded initially and at approximately every twelfth cycle until failure. A corresponding weight was obtained for each fundamental frequency reading. Readings for some typical lightweight and normal-weight specimens can be found in Tables 6.7 and 6.8, respectively.

The transverse dynamic modulus of elasticity was calculated using the equation given in ASTM C 215. Values calculated for all readings for specimen 2-11 (mix W11) are shown in Table 6.9. It was not possible to calculate the dynamic modulus of elasticity for the 7-3/4 in. (19.7 cm) specimens.

The change in dynamic modulus was calculated for each reading by dividing the value of the dynamic modulus for that reading by the initial dynamic modulus of the specimen. The percentages for specimen 2-11 can be seen in Table 6.9. Three different methods were used to calculate the durability factors of the specimens.

The durability factor (DF') was calculated as the number of cycles that the units reached 60 percent of their original dynamic modulus or the number of cycles when the specimen failed if the specimen failed before reaching 60 percent of its original modulus. Linear interpolation was used to calculate the correct number of cycles. For specimen 2-11, the durability factor (DF') was calculated as

$$DF_{(2-11)} = 67 + \left(\frac{61-60}{61-40}\right)(77-67) = 67.5 \text{ cycles} \qquad \text{[Eq 6-10]}$$

The durability factor (DF 60) was calculated using the method given in ASTM C 666. For specimen 2-11, using 60 percent of the initial dynamic modulus as a failure criteria and 100 cycles as a criteria for passing, the relative dynamic modulus is

$$P_{2-11} = \frac{1300000^2}{2100000^2}(100) = 61.9 \qquad \text{[Eq 6-11]}$$

the durability factor (DF 60) was calculated as

$$DF(60)_{2-11} = \frac{61.9(67)}{100} = 41.5 \qquad \text{[Eq 6-12]}$$

The same procedure was used to calculate the durability factor (DF 80), but 80 percent of the dynamic modulus was used as a failure criterion. For specimen 2-11,

$$DF(80)_{2-11} = \frac{1800000^2}{2100000^2}(100)\frac{49}{100} = 36.0 \qquad \text{[Eq 6-13]}$$

The changes in modulus for the specimens in Table 6.9 are plotted in Figures 6.2 and 6.3.

6.4.2 Absorption Data

Absorption testing was carried out in accordance with ASTM C 140. Each unit was weighed while saturated, in the air and while suspended in water, and again after oven drying.

After converting weight measurements to pounds, the density, net volume, and absorption were calculated using the equations given in ASTM C 140. Average values for these properties for the mixes tested can be found in Table 6.10 and Table 6.11.

6.5 Discussion of Test Results

6.5.1 Aggregates

The type of aggregate in a mix can greatly affect the durability of the unit, and many types of aggregates are available for use with concrete block. To rule out the variable of aggregate type, only two types of aggregates were used in this experiment. The normal-weight aggregate was a Platte River block sand used in normal production by area manufacturers. The lightweight aggregate selected for this project was expanded shale. It was chosen mainly for its ready availability and low cost throughout the United States.

6.5.2 Cementitious Materials

6.5.2.1 Cementitious materials in normal-weight mixes. Using block sand (normal-weight) aggregate to produce standard CMUs results in a dense, uniform matrix with an adequate, uniform air void system. When the percentage of cementitious materials is increased in the mix, the density increases due to the increased specific gravity of the materials. Cementitious materials, being finer than the fine aggregate particles, also fill in small voids in the matrix.

An increased proportion of cement in the units is accompanied by an increase in the proportion of calcium hydroxide in the final unit. According to Powers and Helmuth, concrete matrices are subjected to internal expansions during freezing caused by osmosis due to the supercooling of the alkaline solution contained in the pores. If the proportion of calcium hydroxide is increased, the alkalinity of the solution will be proportionately increased. This increased alkalinity may tend to increase the rate and intensity of internal expansion in the concrete due to osmosis.

A graph of durability factors versus percentage of cementitious materials in normal-weight mixes is shown in Figure 6.4. The graph depicts a loss in freeze-thaw resistance with increasing percentages of cementitious material.

Although there is a correlation between increasing percentages of cementitious materials and a loss in free-thaw resistance, it is not possible to state that increased alkalinity is the cause for the loss in freeze-thaw resistance. The increase in density may also play an important part. The filling in of voids by the fine cement particles may result in an inadequate void system. Figure 6.5 shows a relationship similar to that in Figure 6.4 for density alone.

The concept of an inadequate void system is further substantiated if the type of failure is observed. Very dense normal-weight specimens retained their surface integrity throughout testing. Failure was not obvious until the specimens cracked and broke. This failure type happening at such early stages indicates that the void system was inadequate to correctly distribute internal moisture. However, the specimens generally continued to gain weight from water absorption until failure. Since the attraction of fluids into the matrix is a function of the alkalinity of the solution, the extra percentage of calcium hydroxide in mixes with high percentages of cementitious materials cannot be ruled out as a cause of reduced freeze-thaw resistance in these mixes.

6.5.2.2 Cementitious materials in lightweight mixes. As mentioned before, lightweight aggregates cause open and irregular void systems in the matrix. Surface deterioration generally begins early in these mixes. The mode of failure is a combination of surface erosion and interior deterioration due to internal pressures. Since the extra cementitious materials in lightweight mixes also fills in the voids and creates a denser, more uniform matrix, the increase in the percentage of cementitious materials in the mix should improve the freeze-thaw resistance. A strong increase in durability factor with increasing density was found for lightweight specimens. This relationship is shown in Figure 6.6.

Unlike the normal-weight mixes, an optimum did exist for the amount of cementitious materials in the mix. Figure 6.7 shows the relationship obtained. Although an extrapolated curve is not drawn, clearly an optimum must exist somewhere between 12 and 15 percent.

A peak was also suggested for the percentage of fly ash in relation to the percentage of cementitious materials. This relationship is shown in Figure 6.8. The optimum here appears to be around 0.45–0.5 percent.

A compatible optimum was found for the percentage of fly ash in the mix. This relationship is shown in Figure 6.9. The 6–8 percent suggested optimum would yield 12–16 percent of cementitious materials in the mix if a ratio of 0.5 is used for percentage of fly ash to percentage of cementitious materials.

Relationships between durability and the proportions of silica fume were not as obvious. The strongest of these relationships reflected the optimum percentage of silica fume in relation to the percentage of fly ash. This relationship is shown in Figure 6.10. Although not as strongly indicated, it is possible that an optimum may exist somewhere between 0.08 percent and 0.18 percent.

6.5.3 Admixtures

Fatty acid based waterproofer was used to precoat lightweight aggregates. The aggregates were allowed to dry before being used in the mix. Waterproofing was an attempt to seal the aggregate and make it less absorptive. The process was expected to promote better mixing and machinability during batching, and to lower the absorption of the finished unit. The use of this method in one of the lightweight mixes (W11-PC) resulted in an average decrease of absorption from the untreated unit of around 10 percent, as shown in Figure 6.11. However, the strength of the units was lowered by 12 percent. Freeze-thaw specimens that were made by this process outperformed the standard normal-weight units.

A latex-based waterproofer was added to the standard normal-weight mix. The resulting units (W15) had higher absorption results than the standard normal-weight units. Although higher in total absorption, mixes using this admixture are known to be preferred by local contractors due to the low permeability of the resulting units. Freeze-thaw durability factors for specimens manufactured with integral latex waterproofer were similar to standard normal-weight durability factors.

Externally applied waterproofers and sealants may also increase resistance to freeze-thaw deterioration. Since the emphasis of this study was to determine the differences in freeze-thaw resistance due to mix variables, the effects of externally applied substances were not investigated.

6.5.4 Statistical Analysis of Results

Descriptive statistics for mixes tested in runs 1, 2, and 4 are given in Tables 6.12 through 6.20. These three runs were performed under essentially the same conditions. Data from other runs is not included as they were not performed under the same conditions or they were not performed on the same mixes. Results for the standard units with and without fly ash represent specimens from each of the three runs. Specimens are of varying ages and from different commercial batches. Results from mix W16 include specimens from mixes with varying amounts of water in the mix and also were represented in all three runs. Data from mixes W11, W11-PC, and W20 represent specimens from one run only. Data from mixes W14, W18, and the standard lightweight mix represent specimens from the same batch but tested during more than one run.

These statistical results represent a very small number of specimens. As such, they are inadequate to formulate minimum standard deviations or other requirements. However, preliminary observations can be drawn from the statistical results. First,

the durability factor calculated according to ASTM C 666 method, DF(60), had the lowest standard deviation of the three methods for nearly all specimens. This repeatability indicates that this method of calculation may be more precise than the other two.

The standard error is reasonable for mixes tested during the same run. The range of data varied from around 5 to 20 for this type of specimen. When comparing data from more than one run, however, the standard error increases dramatically. The range increases dramatically and values may only be consistent to 15 cycles.

One-tailed student t-tests were run to compare the performance of the mixes. All t-tests were run at a confidence level of 95 percent (± 0.5) Results of the t-tests are in Table 6.21.

One interesting result was the comparison of standard units with and without fly ash. When all three runs (1, 2, and 4) were pooled, the t-test revealed that the probability that the units with fly ash outperformed the units without fly ash was 0.82. When only the data from the first two runs were considered, t-test results indicated a 93 percent probability that the units without fly ash outperformed the units with fly ash.

This contradiction was reinforced by the fact that when all data was again pooled from all three runs, the W11 specimens had a higher probability of being outperformed by the standard specimens without fly ash than by the standard specimens with fly ash. Also, the W11 - PC specimens had a higher probability of outperforming the standard units with fly ash than the standard units without fly ash. The reason for this contradiction is unknown. Possible explanations include non-representative or mismarked specimens in one of the runs or calculation errors. It is also possible that there was no experimental error and that the difference is due to natural coincidence. Statistics performed over a small number of samples may not be totally representative.

Some preliminary conclusions, however, may be drawn. First, there is insufficient probability of difference between the standard (with or without fly ash) units and the W11 units to state that one is better than the other. The conclusion from this study is, therefore, that the W11 lightweight high-performance units are comparable in freeze-thaw resistance to the commonly used standard normal-weight units. There was a probability of 0.90 within a confidence level of 95 percent that the W11 specimens performed significantly better than the standard lightweight units.

Second, there is sufficient probability to show that the W11-PC specimens outperformed all of the other specimens in this test. The only difference between the W11 and W11-PC mixes was the precoating of the aggregates with fatty acid waterproofers before mixing. These results are strong evidence that aggregate absorption during mixing and/or after the mix has cured can significantly affect freeze-thaw resistance in CMUs. Further research in the area of aggregate absorption is recommended.

6.5.5 Comparison of Absorption and Freeze-thaw Test Results

No relationship could be found between absorption test results and freeze-thaw test results in this experiment. This is not surprising because several factors other than absorption also influence the freeze-thaw resistance of a unit. These results suggest that absorption results may not be a good predictor of freeze-thaw resistance.

6.6 Summary of Durability Test Findings

6.6.1 Durability Test Procedure

The procedure chosen was thought to be the best available procedure at the time. Little or no weight loss occurred in the specimens during testing, but the dynamic modulus of elasticity of each specimen dropped significantly with repeated freeze-thaw cycling. Therefore, the suggested failure criterion of the change in dynamic modulus of elasticity appears to be preferable.

During an abandoned test, water levels in the test containers were allowed to drop well below the tops of the specimens. These specimens appeared to have an accelerated rate of degradation. This observation suggests that the saturated freeze-thaw test may not be the worst case test for CMUs. Further research using a partially saturated method is suggested.

Many specimens that had high initial weight gains had low freeze-thaw resistance. This corroborates the findings of Powers and Helmuth that deterioration is caused by the osmosis of liquids into the cells. Rapid freeze-thaw tests do not adequately model *in situ* conditions. Further development of a freeze-thaw procedure based on dilation is highly recommended.

The procedure as outlined in Chapter 3 was relatively easy to perform in the laboratory. The frequent readings make the test somewhat labor intensive, but readings can be scheduled during the course of a normal work week. Since the

freezing and thawing cycles are automatically controlled, only the weighing and the taking of fundamental frequencies are subject to operator error. Proper laboratory procedures can nearly eliminate errors due to weighing. Some skill is necessary to obtain precise readings with most fundamental frequency equipment.

In situ freezing and thawing cycles would be much slower than the 4- to 7-hr cycles used for this test. The ability of a unit to resist deterioration is a function of the rate of osmotic forces within the cell structure. This rate may be dependent on the rate of the temperature change. Present equipment is designed for the rapid cycles of the ASTM C 666 test. Rapid cycling is necessary for the ASTM C 666 test if it is to be performed in a reasonable amount of time. The method requires only 100 cycles to fail most specimens, therefore, it could accommodate longer cycles and still be performed in a reasonable amount of time. However, equipment must be designed that can automatically cycle at a much slower rate.

The thickness of the specimens did not seem to affect the rate of degradation with the exception of specimens cut 5/8 in. (cm) or less in thickness. These very thin specimens tended to break before the fundamental frequency of the specimens dropped to below 60 percent of their original dynamic modulus.

Variations in the specified temperature range affected the results of the test. One test was run with a cycle variation of -10 °F (-23.3 °C) to 60 °F (15.6 °C) instead of the standard 0 °F (-17.8 °C) to 60 °F (15.6 °C). The result was an overall loss of around 10 cycles from the durability factors. Unanticipated variations may occur in the temperature cycling due to equipment and/or operator failure and acts of nature. For this reason, mixes to be compared should be run together in the same test if possible. If this is not possible, specimens from a mix with a known durability rating should be tested along with the unknown specimens as controls. The durability factors for tests with varied standards may be approximated by the following correction factor:

$$CF = \frac{DCF(\text{Nonstandard Conditions})}{DCF(\text{Standard Conditions})} \qquad \text{[Eq 6-14]}$$

where CF is a correction factor applied to the durability factors for unknown specimens, and DCF is the durability factor of the control specimen under the given conditions.

6.6.2 Durability of Normal-weight High-performance CMU

As the percentage of cementitious materials is increased in the mix, the durability of the units in this study decreased. The addition of extremely fine pozzolans such

as fly ash and silica fume increased the density of the resulting units. As the density of normal-weight units was increased, the durability of the units decreased. Units substituting fly ash for a portion of the cement had lower durability factors than standard units. There were insufficient data in this study to determine the exact causes of the decreases in durability. Some possible mechanisms are discussed in the following paragraphs.

The alkalinity of fly ash may increase the rate of osmosis, thus decreasing the durability of the matrix. Silica fume and other silica dioxides react with the calcium hydroxide formed during hydration to form non-alkaline compounds. Proper proportioning between fly ash, silica fume, and other mix ingredients may improve durability. Further research in this area is suggested.

As the density is increased, the available air void system is reduced. The reduction in the void system, particularly the reduction in the size of voids, can have detrimental effects on durability. It is possible that air-entrainment could increase the durability of high-performance normal-weight CMUs. The use of air-entrainment has not been established for masonry. Current methods and testing procedures for cast-in-place concrete are not directly applicable. More research is needed in this area.

6.6.3 Durability of Lightweight High-performance CMUs

The durability of lightweight units improved as the amount of cementitious materials was increased to over 12 percent (by absolute volume). A sharp decline in durability factors was observed as the percentage of cementitious materials in the mix was increased above 15 percent (by absolute volume). Therefore, an optimum mix may exist somewhere between 12 and 15 percent cementitious materials by absolute volume. Insufficient data were produced in this study to determine an optimum mix.

Similar peaks were observed for the percentage of fly ash in the mix (5 to 9 percent by absolute volume). The ratio of the percentage of fly ash to the total percentage of cementitious materials in the mix (0.4 to 0.5 by absolute volume), and the ratio of the percentage of silica fume to the percentage of fly ash in the mix (around 0.1 by absolute volume). Research studying each of these relationships as independent variables may result in identifying the optimum proportions for the high-performance lightweight concrete masonry units with respect to durability.

Results of statistical t-tests indicated that, although the sample mean was slightly higher for the standard specimens than for the W11 specimens, there was

insufficient probability to support the conclusion that one was superior to the other. They also indicated that the W11 specimens significantly outperformed the standard lightweight specimens under freeze-thaw cycling.

6.6.4 Admixtures

Statistical analysis of the data indicated that the W11-PC specimens outperformed all other specimens in freeze-thaw durability. The only difference between the W11 and W11-PC mixes was the precoating of the aggregates with fatty acid water-proofers before mixing. These results are strong evidence that aggregate absorption during mixing and/or after the mix has cured can significantly affect freeze-thaw resistance in concrete masonry units. Further research in the area of aggregate absorption is recommended.

An acrylic latex waterproofer was added integrally to the normal weight mixes. The absorption results actually were slightly higher with the integral waterproofer as without. However, the durability factors were much higher for the units with the integral waterproofer. Units with the integral acrylic waterproofer are reported to be less permeable than those without, and this may account for the increase in freeze-thaw resistance.

The use of plasticizers and set retarders affects the machinability of the mix and therefore the density and uniformity of the matrix. These admixtures may affect the physical and chemical characteristics of the units. If the quantities of these admixtures change drastically from those in the units tested the relationships given in Section 6.2 may vary.

The work done on admixtures in this study was supplemental to the focus of the study and was not intended to be an in-depth evaluation. The results, however, were highly encouraging. More research with each of these admixtures is strongly suggested.

6.6.5 Requirements for Future Research

Concrete masonry technology is growing fast. The development of finite element analysis has given rise to new, easier to use, more economical shapes. Expanded natural and manmade products has provided many alternatives for aggregate selection. Research with pozzolans and admixtures has allowed the design of stronger, lighter, less permeable mixes. Structural research has developed innovative and economical uses for concrete masonry as a material.

Little research has been done, however, in the area of durability for CMUs. No standards exist that address the freeze-thaw resistance of CMUs. Absorption is the only durability test presently required for acceptance by most codes. From the results of this study, absorption does not appear to be a good predictor of freeze-thaw resistance. Many other durability problems such as the corrosion of steel reinforcement or attack by salts, acid rain, or other chemicals may have even less correlation to absorption. As new uses for CMUs become available and stronger, denser, thinner units are developed, the need for research in the area of durability becomes more and more crucial.

Table 6.1. ASTM C 90 criteria for units below grade or exposed to weather.

Weight Classification pcf (Kg/m^3)	Maximum Absorption Using ASTM C 140 pcf (Kg/m^3)
Less than 105 (1682)	18 (288)
105–125 (1682–2002)	15 (240)
Over 125 (2002)	13 (208)

Table 6.2. Values for correction factor T.

K/L	T	K/L	T
0.00	1.00	0.09	1.60
0.01	1.01	0.10	1.73
0.02	1.03	0.12	2.03
0.03	1.07	0.14	2.36
0.04	1.13	0.16	2.73
0.05	1.20	0.18	3.14
0.06	1.28	0.20	3.58
0.07	1.38	0.25	4.78
0.08	1.48	0.30	6.07

Table 6.3. Value of C_n for the first ten modes of a simple beam.

C_1	C_2	C_3	C_4	C_5	C_6	C_7	C_8	C_9	C_{10}
22.4	61.7	121	200	299	417	555	713	891	1088

Table 6.4. Range of fundamental frequencies for standard size undamaged CMU.

Mode	Fundamental Frequencies (Hz)	
	Lower Bound	Upper Bound
1	0	100
2	100	300
3	300	600
4	600	800
5	600	1000
6	1000	1500
7	1500	2000
8	2000	2500
9	2500	3000
10	3000	4000

Table 6.5. Proportioning of lightweight mixes tested.

Light-weight Mix Number	Agg. (lb/cy)	Cement (lb/cy)	Fly Ash (lb/cy)	Krete Mix (oz/cy)	Krete Plast (oz/cy)	Water (gal/cy)	Silica Fume (lb/cy)	Lime (lb/cy)
ST-LW	1619	329	58	0	1	27	0	
W11'	1534	329	153	13	5	25	27	
W11'+	1520	326	152	13	5	27	26	
W11'-PC	1587	340	159	13	6	20	27	
W16	1385	362	446	21	9	24	29	
W16+	1360	355	438	20	9	27	29	
W17	1432	374	462	21	9	19	30	
W21	1505	331	218	23	5	25	27	
W22	1471	392	415	31	9	14	30	50
W24	1478	394	416	31	9	14	30	36

Table 6.6. Proportioning of normal-weight mixes tested.

Normal Weight Mix Number	Agg. (lb/cy)	Cement (lb/cy)	Fly Ash (lb/cy)	Krete Mix (oz/cy)	Krete Plast (oz/cy)	Water (gal/cy)	Silica Fume (lb/cy)	Lime (lb/cy)
ST	3945	388	0	0	2	7		
ST-FA	3948	297	76	0	2	7		
W13	3948	297	76	0	2	7		
W15	3948	297	76	0	0	7		
W12	3565	462	215	18	8	11	36	
W14	3511	467	212	17	7	14	25	
W18	3757	451	113	0	3	9		
W20	3777	346	222	24	6	7		
W23	3878	309	194	13	6	4	22	

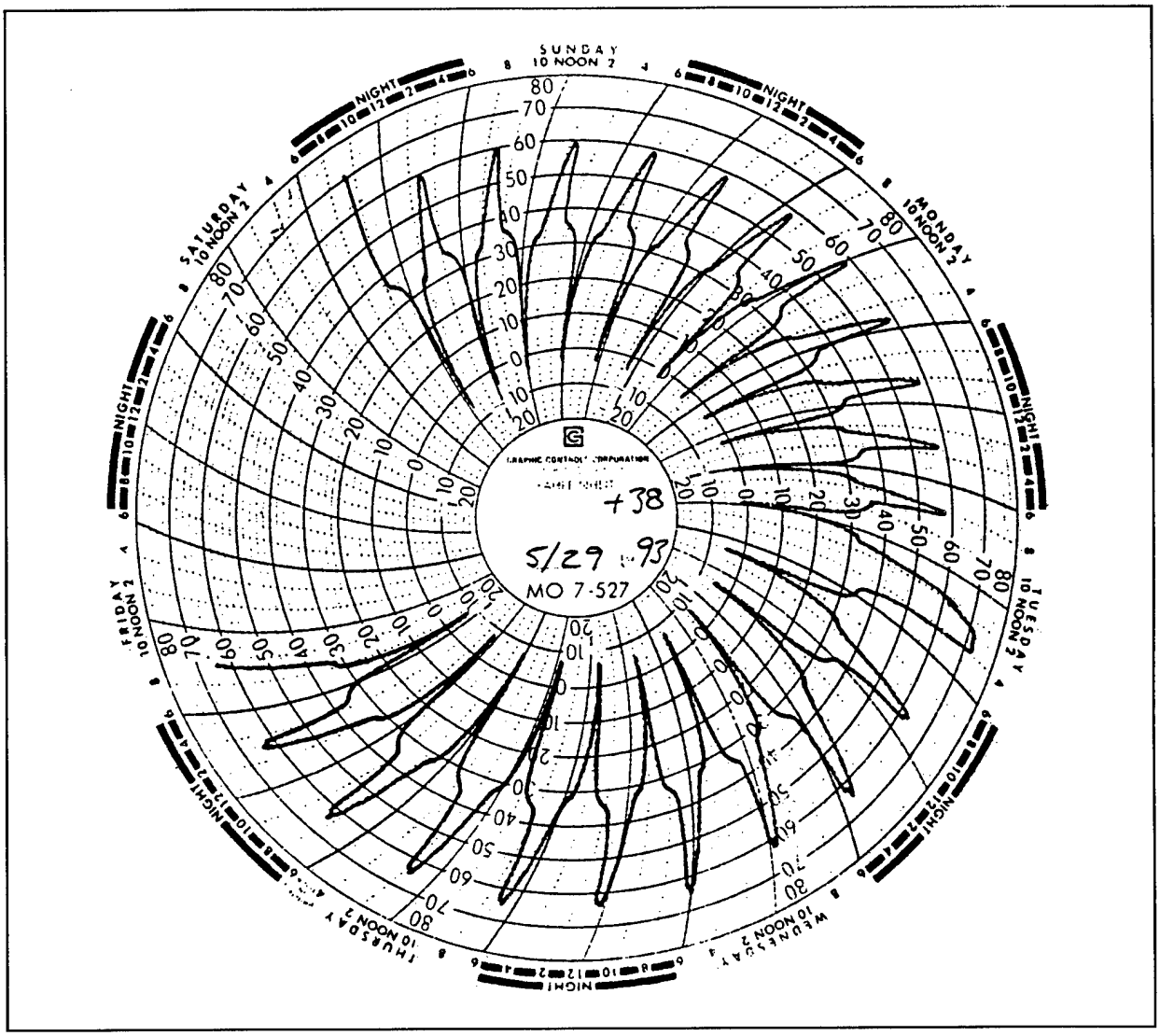

Figure 6.1. Temperature cycling chart.

Table 6.7. Lightweight block fundamental frequencies and weights.

Number of Cycles	ST-LW		W16a		W11'-PC		W11'	
	Freq.	Wt.	Freq.	Wt.	Freq.	Wt.	Freq.	Wt.
0	1065	1085	1183	1186	1331	1106	1321	1124
12	1025	1118	1173	1218	1321	1126	1292	1143
26	1075	1127	1134	1225	1331	1140	1341	1157
38	917	1133	1045	1230	1331	1136	1252	1154
49	887	1134	779	1230	1292	1142	1203	1161
67	592	1133			1262	1143	1016	1161
77					1173	1137	818	1159
88					1242	1134	532	1156
98					1163	1121		
109								

Table 6.8. Normal-weight block fundamental frequencies and weights.

Number of Cycles	ST		ST-FA		W18		W20	
	Freq.	Wt.	Freq.	Wt.	Freq.	Wt.	Freq.	Wt.
0	1430	2228	1430	2122	1479	1758	1440	1663
12	1410	2249	1371	2143	1420	1765	1390	1674
26	1489	2257	1479	2149	1410	1770	1410	1676
38	1459	2256	1410	2149	1440	1773	1311	1677
49	1420	2261	1380	2148	1351	1776	1183	1681
67	1380	2268	1233	2154	1242	1881		
77	1242	2267	1075	2139	1144	1775		
88	1065	2268	937	2133	1075	1776		
98	937	2276			996	1750		
109					917	1749		
120					868	1693		

Table 6.9. Dynamic modulus results for specimen 2-33 (Mix W11).

Number of Cycles	Fund. Frequency (Hz)	Weight (g)	Dynamic Modulus (psi)	Percent Original Dynamic Modulus
0	1321	1124	2100000	100
12	1292	1143	2100000	97
26	1341	1157	2300000	106
38	1252	1154	2000000	92
49	1203	1161	1800000	86
67	1016	1161	1300000	61
77	818	1159	850000	40
88	532	1153	360000	17

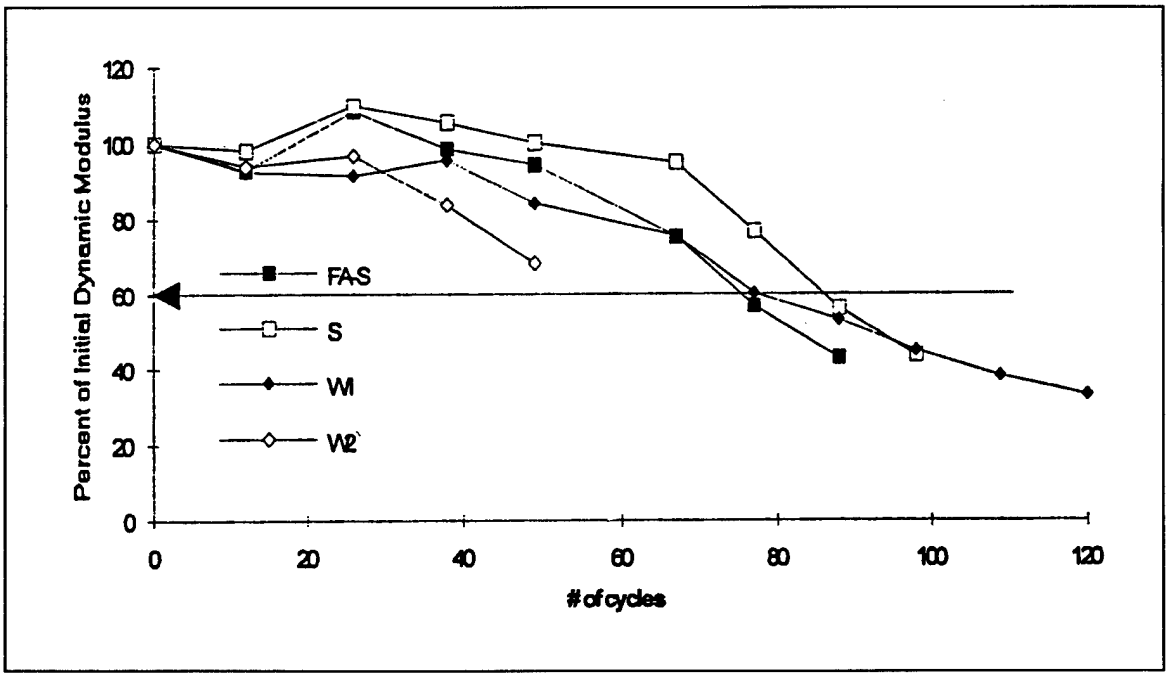

Figure 6.2. Change in dynamic modulus normal weight specimens.

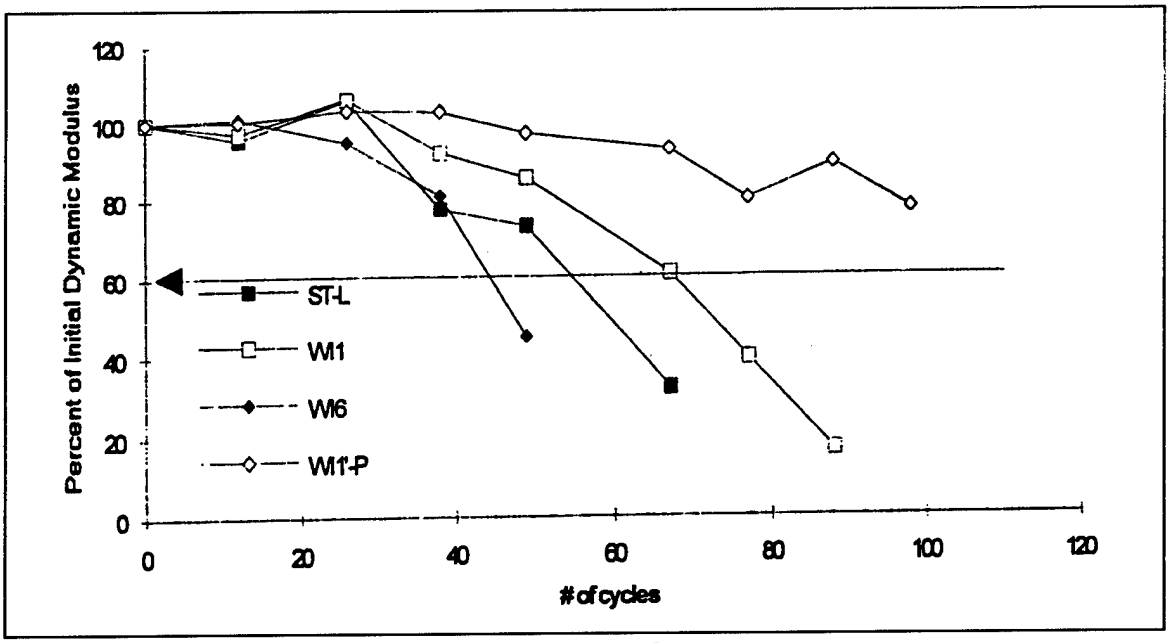

Figure 6.3. Change in dynamic modulus lightweight specimens.

Table 6.10. Results of absorption tests, lightweight units (average of three or more).

Light-weight Mix Number	Saturated. Wt. (lbs)	Dry Wt. (lbs)	Net Volume (cf)	Density (pcf)	Absorption (pcf)
ST-LW	15.7	37.9	0.18	70	17.91
W11a	21.0	37.5	0.21	87	11.77
W11b	21.2	30.1	0.22	87	11.51
W1'-PC	20.9	29.2	0.21	88	10.43
W16a	22.1	31.3	0.21	90	13.44
W16b	22.3	29.9	0.21	94	11.41
W16-PC	21.7	29.7	0.21	88	13.36
W22	22.4	28.5	0.21	91	13.97
W24	21.5	30.1	0.21	90	13.68

Table 6.11. Results of absorption tests, normal-weight units (average of three or more).

Normal Wt Mix Number	Saturated Wt (lb)	Dry Wt (lb)	Net Volume (cf)	Density (pcf)	Absorption (pcf)
ST	39.9	37.9	0.28	134	7.35
ST-FA	39.6	37.5	0.28	134	6.86
W12	31.7	30.1	0.22	140	7.66
W13	30.5	29.2	0.22	134	5.98
W14	32.6	31.3	0.22	144	6.31
W15	31.5	29.9	0.22	136	7.12
W18	31.1	29.7	0.22	137	6.66
W19	30.8	28.5	0.22	132	10.32
W23	31.6	30.1	0.22	139	6.64

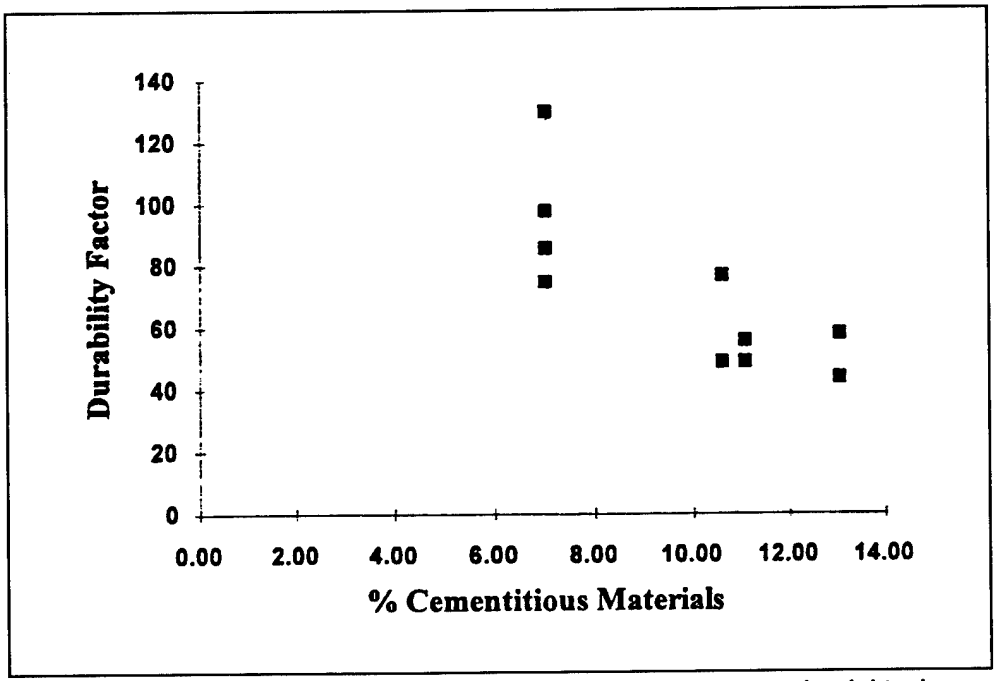

Figure 6.4. Durability factors vs percent cementitious materials normal weight mixes.

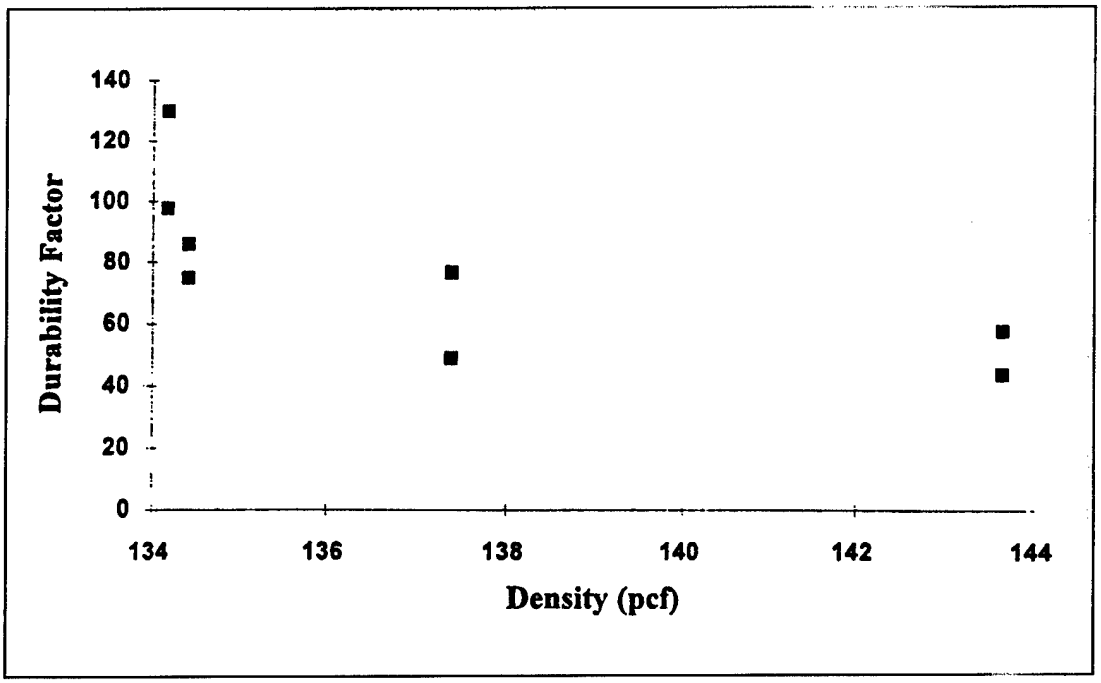

Figure 6.5. Durability factors vs density normal weight mixes.

Figure 6.6. Density vs durability lightweight mixes.

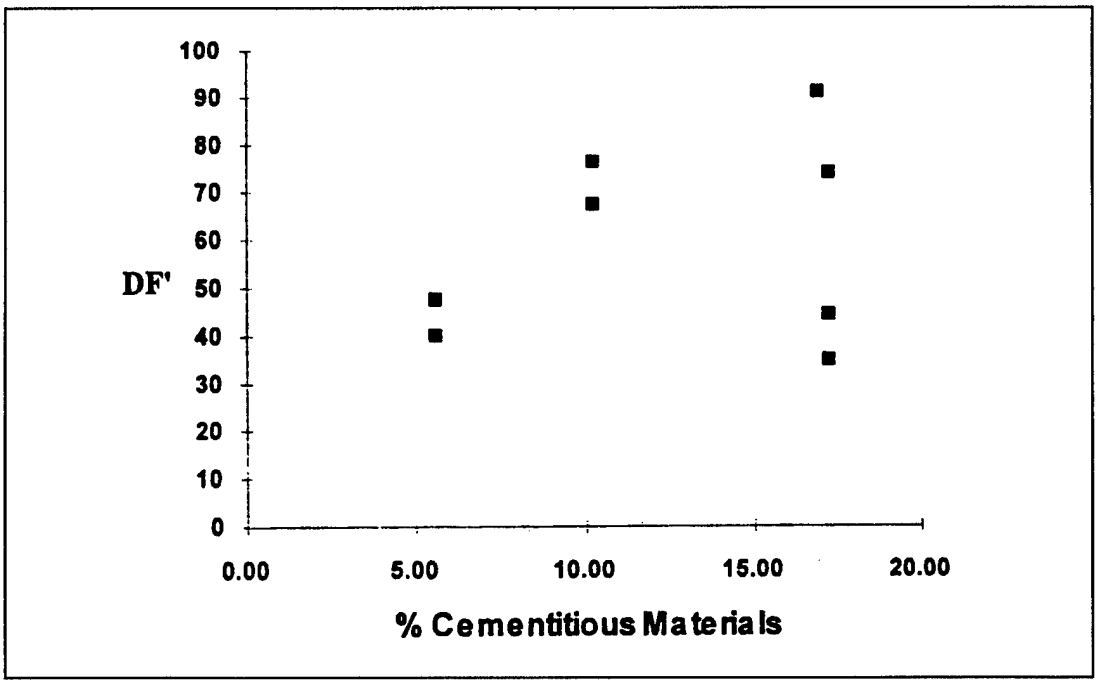

Figure 6.7. Durability factors vs percent cementitious materials lightweight mixes.

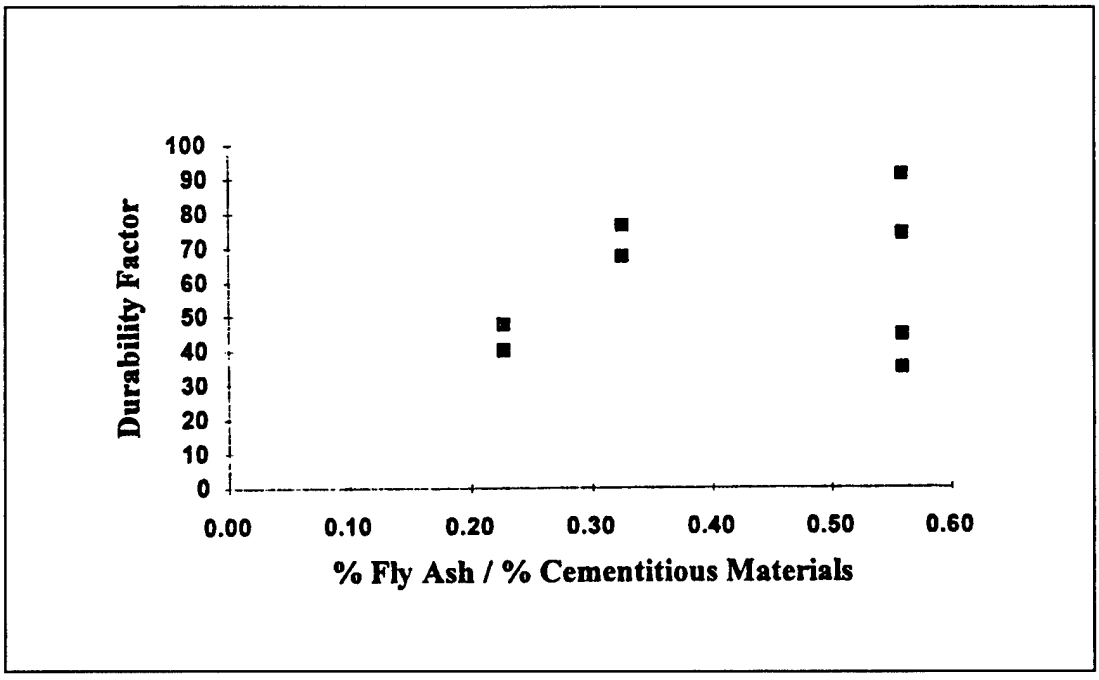

Figure 6.8. Durability factors vs percent fly ash/percent cementitious materials lightweight mixes.

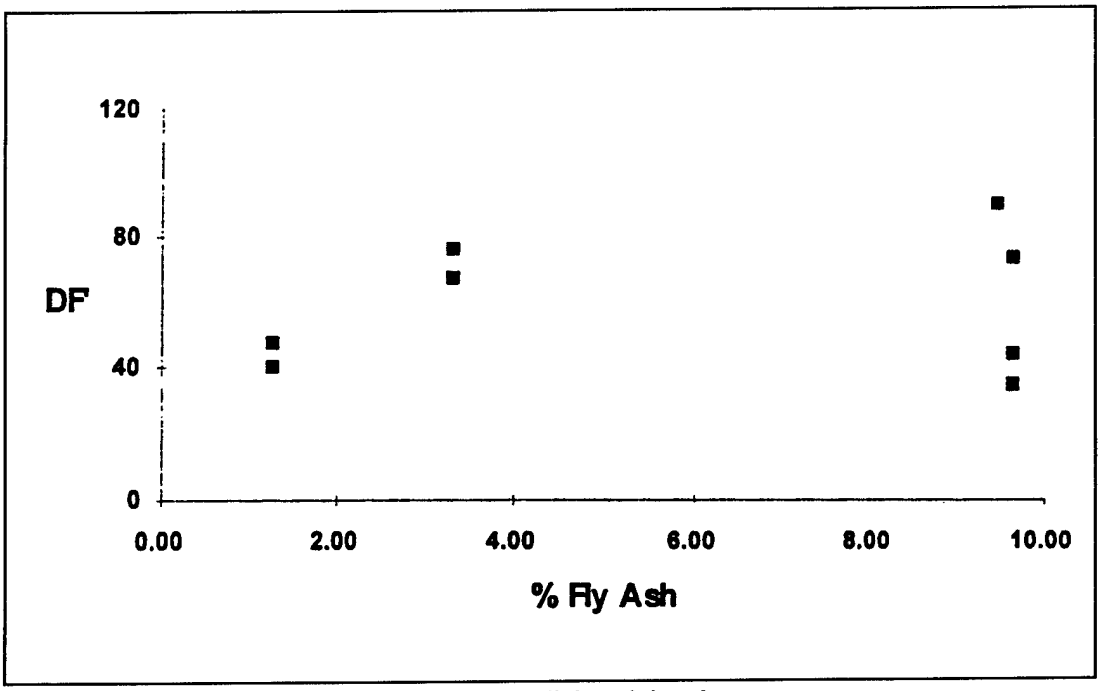

Figure 6.9. Durability factors vs percent fly ash lightweight mixes.

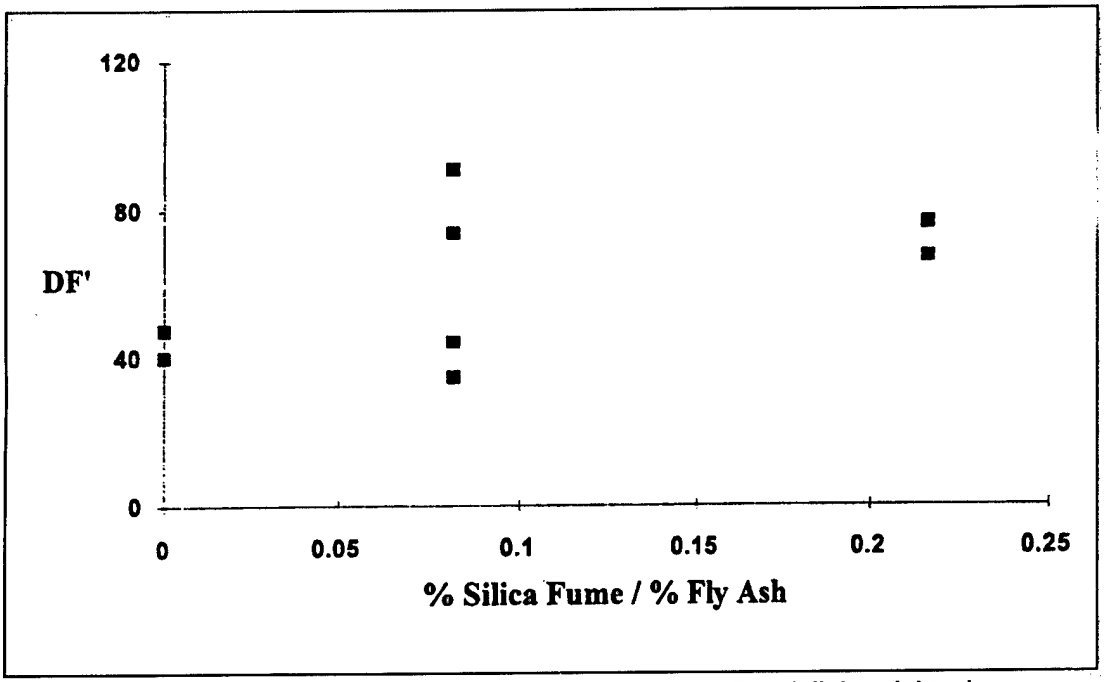

Figure 6.10. Durability factors vs percent silica fume to percent fly ash lightweight mixes.

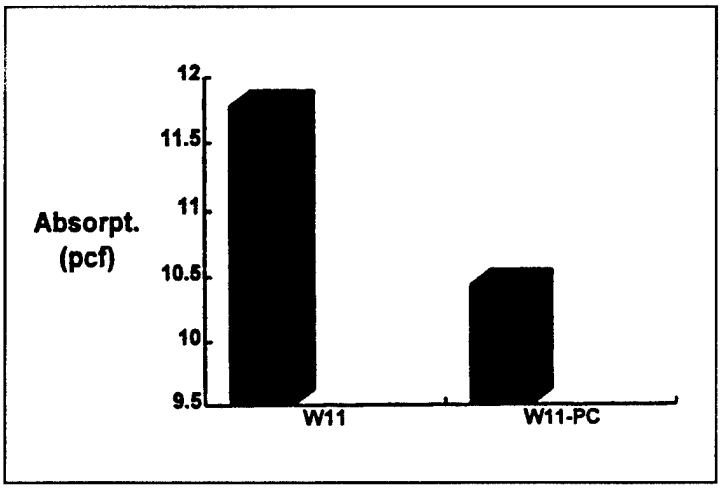

Figure 6.11. Effect of precoating on absorption.

Table 6.12. Statistics for standard units without fly ash.

	DF(60)	DF'	DF(80)
Mean	28	80	31
Standard Error	2.27	8.47	4.65
Standard Deviation	6.00	22.42	12.29
Range	18	62	31
Minimum	19	55	19
Maximum	37	117	50
Count	7	7	7

Table 6.13. Statistics for standard units with fly ash.

	DF(60)	DF'	DF(80)
Mean	22	68	33
Standard Error	3.58	8.63	6.10
Standard Deviation	8.00	19.30	13.65
Range	19	45	32
Minimum	14	41	17
Maximum	33	86	50
Count	5	5	5

Table 6.14. Statistics for standard lightweight units.

	DF(60)	DF'	DF(80)
Mean	17	54	22
Standard Error	2.08	6.78	3.89
Standard Deviation	4.17	13.56	7.78
Range	10	32	17
Minimum	11	40	16
Maximum	21	72	33
Count	4	4	4

Table 6.15. Statistics for Mix W11.

	DF(60)	DF'	DF(80)
Mean	25	67	22
Standard Error	4.37	5.48	3.32
Standard Deviation	7.57	9.50	5.75
Range	14	19	11
Minimum	17	57	16
Maximum	31	76	26
Count	3	3	3

Table 6.16. Statistics for Mix W11-PC.

	DF(60)	DF'	DF(80)
Mean	38	98	56
Standard Error	5.80	4.09	11.72
Standard Deviation	11.60	8.18	23.43
Range	28	20	51
Minimum	24	88	35
Maximum	53	108	85
Count	4	4	4

Table 6.17. Statistics for Mix W14.

	DF(60)	DF'	DF(80)
Mean	21	56	16
Standard Error	7.92	4.78	1.71
Standard Deviation	15.84	9.57	3.41
Range	33	23	8
Minimum	12	44	12
Maximum	45	67	19
Count	4	4	4

Table 6.18. Statistics for Mix W16.

	DF(60)	DF'	DF(80)
Mean	18	59	25
Standard Error	3.13	10.34	6.64
Standard Deviation	6.99	23.11	14.84
Range	17	56	31
Minimum	9	35	10
Maximum	26	91	41
Count	5	5	5

Table 6.19. Statistics for Mix W18.

	DF(60)	DF'	DF(80)
Mean	16	62	24
Standard Error	1.31	8.14	8.93
Standard Deviation	2.28	14.11	15.48
Range	4	28	31
Minimum	15	49	8
Maximum	19	77	38
Count	3	3	3

Table 6.20. Statistics for Mix W20.

	DF(60)	DF'	DF(80)
Mean	18	51	22
Standard Error	1.32	2.83	2.96
Standard Deviation	2.29	4.90	5.13
Range	5	9	10
Minimum	15	47	16
Maximum	20	56	26
Count	3	3	3

Table 6.21. t-Test comparisons of durability results.

Lightweight Mixes	p*	Normal-Weight Mixes	p*
Stnd > Stnd LW	0.97	Stnd FA > Stnd	0.82
W11 PC > Stnd	0.92	Stnd > Stnd FA (runs 1 & 2)	0.93
Stnd > Stnd FA	0.99	Stnd > W18	0.87
Stnd > W11	0.80	W18 > W14	0.74
Stnd FA >W11	0.52	W14 > W20	0.79
W11 > Stnd LW	0.90		
W11 > W16	0.71		
W16 > Stnd LW	0.64		

* p = probability of occurrence within a 95% level of confidence.

7 Cost and Productivity Evaluation

This chapter summarizes cost analyses of high-performance CMUs. The direct factors affecting CMU construction costs are unit cost and construction cost. Unit costs include materials, plant production, and transportation. Construction costs are evaluated on the basis of projected increased productivity. There are also indirect costs associated with masonry construction, including disability, workman's compensation, and lost time injuries. The effects of these cost factors are discussed below.

7.1 Basic Unit Cost Components

7.1.1 Materials

The ingredients used in normal-weight CMUs include sand and gravel, cement, fly ash, admixtures, and water. Of these, sand and gravel are naturally occurring aggregates, and fly ash is an industrial waste product. Consequently, their costs are relatively small. The costs of cement and admixtures are relatively more, depending on the type and quantity used. The ingredients used in lightweight CMUs include lightweight aggregates, cement, fly ash, admixtures, and water. Lightweight aggregates are artificially produced in high temperature kilns, so they are relatively expensive. The aggregate cost increases the costs of the units, so the material costs of lightweight units are higher than those for normal-weight units.

The costs of materials used to produce CMU mixes are given in Table 7.1. These costs were obtained from suppliers of the various materials. Different combinations of materials were used to produce both high-strength lightweight and normal-weight mixes in the laboratory and in the plant. Mix proportions are given in Chapter 3.

The material cost per unit was calculated for all mixes. The material quantities in pounds per cubic yard of a batch were calculated. The number of units produced per batch was calculated by using the following formula:

Number of Units = 0.98 weight of batch/weight of unit

The total quantity of materials used in a batch was divided by the number of units per batch to calculate the quantity of material per unit (in pounds). The cost of material per pound was then multiplied by the quantity of material in pounds to get the cost of that material per unit. Tables 7.2 and 7.3 summarize material costs for normal-weight units in the standard and optimized shapes. In Tables 7.4 and 7.5, material costs for standard all-lightweight and high-performance lightweight units are calculated.

When the material cost of a standard normal-weight unit with standard shape is taken as 100 percent, the material costs of other mixes can be compared with it. The material costs for a high-performance normal-weight unit (W12) is 21 percent greater, the cost of a standard all-lightweight unit is 98 percent more, and the cost of a high-performance lightweight unit is 166 percent more when compared to the material cost of the standard normal-weight unit. Although the material costs are higher, other expenses for these mixes are lower than the standard normal-weight unit.

The material costs of lightweight units produced from different mixes are given in Table 7.6, and those for normal-weight units are given in Table 7.7. The cost of pre-blended silica fume cement used for the lightweight and normal-weight mixes was $80 per ton. This cement was supplied by the LaFarge Corporation, Montreal, PQ, Canada. It was expected that the same cement would be available for the commercial production of the units in Omaha from the local LaFarge Corporation plant in Kansas. However, the local plant required the shipment of cement from either Montreal or Illinois. As a result, the cost was increased to $120 per ton. The new cost of the pre-blended silica fume cement is $0.06 per pound instead of $0.04 per pound. The material costs per unit thereby increased by a factor of 1.5.

7.1.2 Plant Production and Transportation

In the production process faster feeding of the mold, improved dispersion of the admixtures, and greater density of the final product help to produce a high-performance unit. To produce a dense lightweight masonry unit with extremely low absorption, the production feed time for these units could be increased 1.0 or 2.0 seconds over that of normal-weight unit feed times. However, from the manufacturer's standpoint, this increase in time is not favorable as it decreases the production rate and increases the production cost per unit. The use of admixtures optimizes the feed time of lightweight units. In addition, with the use of admixtures, mold wear will be less per unit formed, also reducing overall production costs.

The cost of plant production, transportation, and general and administrative overhead constitute other expenses. Plant production costs include labor, maintenance, repair, depreciation, utilities, and testing. The cost of transportation represents the cost of shipping the unit from the plant to the construction site. General and administrative overhead includes managers, sales, telephone, advertisements, and profit.

Unit weight has a significant effect on transportation costs. Highway load limits are governed by weight of the material to be transported and the volume of the truck used for transportation. Because of the weight limit, it is not possible to fill the available truck volume with a load of normal-weight units. The weight of a standard normal-weight unit in the standard shape is about 38 lb (17.2 kg), whereas the lightweight unit in the optimized A-shape weighs about 18 lb (8.2 kg). More of the optimized units can be transported, minimizing transportation cost per unit. Expenses for lightweight units are given in Table 7.8 and for normal-weight units in Table 7.9.

Other expenses for the standard normal-weight units in the standard shape are assumed to constitute 100 percent while other expenses for the high-performance normal-weight and lightweight units in the optimized A-shape are calculated as relative percentages. These relative values are given in Tables 7.10 and 7.11.

7.2 Cost Analysis of 16-in. Units

7.2.1 Material Cost

The material cost per unit was calculated for all mixes. The material quantities in pounds per cubic yard of a batch were calculated. The quantities of lightweight mixes with expanded shale are given in Table 7.12 and that of normal-weight mixes with sand and gravel are given in Table 7.13. The number of units produced per batch was calculated by using the following formula:

Number of Units = 0.98 weight of batch/weight of unit

The total quantity of materials used in a batch was divided by the number of units per batch to calculate the quantity of material per unit, in pounds. Then, the cost of material per pound was multiplied by the quantity of material in pounds to get the cost of that material per unit. The weight of each unit is obtained by adding the material quantities per unit. In Tables 7.4 and 7.5, material costs for standard all-lightweight and high-performance lightweight units are calculated.

The material cost of a normal-weight unit of the standard shape is taken as 100 percent and the material costs of other mixes are calculated accordingly. The material cost of a high-performance normal-weight unit (W12) is 21 percent more, the cost of a standard all-lightweight unit is 98 percent more, and the cost of a high-performance lightweight unit is 166 percent more when compared to the material cost of the standard normal-weight unit. Although the material costs are higher, other expenses for these mixes (see Section 7.2.2) are lower than for the standard normal-weight unit.

The material costs of lightweight units produced from different mixes are given in Table 7.6, and those for normal-weight units are given in Table 7.7.

7.2.2 Other Expenses

Other expenses include cost of plant production, transportation, as well as general and administrative overhead. The cost of plant production includes labor, maintenance, repair, depreciation, utilities, and testing. Transportation cost is the cost of shipping the unit from the plant to the construction site. General and administrative overhead includes managers, sales, telephone, advertisements, and profit.

The plant production cost of the high-performance units in the optimized A-shape is more than the standard normal-weight mix for the standard shape. However, the transportation cost of these units is less because of the reduction in the weight. Other expenses for lightweight units are given in Table 7.8 and for normal-weight units in Table 7.9.

Other expenses for the standard normal-weight unit in the standard shape are considered as 100 percent while other expenses for the high-performance normal-weight and lightweight units in the optimized A-shape are calculated as relative percentages. These relative values are given in Tables 7.10 and 7.11. The values of material cost and other expenses appearing in these tables cannot be added directly because each of them represents a relative value.

7.3 Cost Analysis of 24-in. Units

As discussed later in this chapter, a lightweight CMU produced in a 24-in. long configuration can achieve significant construction productivity gains. For that reason, a cost analysis for a 24-in. long unit of an optimized configuration was conducted. The same materials were used in this analysis as used for the 16-in. unit.

Net volume of 16-in. (41-cm) units is 0.22 ft^3 (6.23 E-3 m^3), and of 24-in. (61 cm) units is 0.31 ft^3 (8.8 E-3 m^3). The difference in their volumes is therefore 0.09 ft^3 (2.5 E-3 m^3). From a 1 yd^3 (0.76 m^3) mix, a smaller number of 24-in. units is produced than 16-in. units. For example, from one yd^3 of W16 mix, 127 16-in. units are produced whereas the number of 24-in. units produced is 85. Total material cost per batch of mix W16 is $50.6676. The material cost per unit is calculated as shown below:

Material Cost per Unit = $50.67/85 = $0.5961

Other expenses for a 24-in. unit are given below.

Average weight of a 24-in. lightweight unit from mix W16 is 27 lb (12.3 kg.), so shipping cost is calculated as follows:

Shipping cost = ($0.004125 per lb) * (27 lb) = $0.1114

It is assumed that the plant production and administrative costs for 24-in. units are the same for 16-in. units.

Other expenses = $0.1925 + $0.1114 + $0.3194, or $0.6233.

Final cost of 24-in. unit is = $0.5961 + $0.6233, or $1.2194.

Costs for other mixes can be calculated in the same way.

7.4 Productivity Study

The high-performance lightweight CMU costs about 25 percent more than the standard CMU. The open end and light weight of the high-performance units makes them easier and less tiring for laborers to handle. Easier handling can be translated into increased field productivity. Savings due to construction productivity are expected to more than offset the increased cost of the units.

To verify this assumption, a study was conducted to determine the effects of weight difference and optimized shape on construction productivity. One approach used to measure and compare CMU construction productivity is to control as many of the variables as possible.

7.4.1 NCMA Productivity Study

A study was performed by the National Concrete Masonry Association (NCMA 1995) to evaluate the difference in productivity due to CMU weight and size.

The study was performed in the NCMA Research and Development Laboratory. Temperature and climate were controlled. Prebuilt guides were used to anchor stringlines. End units were installed but not timed so that the entire test consisted of laying running bond in several courses over a 28 ft 0-3/8 in. length. Joints were not tooled. Strict scheduling was observed. One ten minute coffee break and one 40 minute lunch break were allowed per day. The workers performed their duties without interruption or distraction. The same mason and laborer were used for each wall section. Talking and smoking were discouraged.

Twelve different types of units were used in the study. The types of units used and their properties are given in Table 7.14. The mortar, an extended-life plastic, was chosen for its easily controllable consistency. It was premixed and delivered to the job site. A constant cone penetrometer reading was maintained for each test. Higher cone readings were allowed for lighter units. Layouts of the walls for both 24-in. and 16-in. units are shown in Figure 7.1.

A comparison of the published productivity study results is given in Tables 7.15 and 7.16. These tables illustrate the increase in productivity associated with the use of lightweight units. Table 7.17 shows a comparison of the results obtained for 16-in. units versus those obtained for 24-in. units of the same width and thickness.

As can be seen from these tables, an 8–10 percent increase in productivity was reported when comparing lightweight and normal-weight 8 x 8 x 16-in. units. When lightweight 24-in. units were used instead of 16-in. units, an additional increase in productivity of at least 24 percent was realized.

7.4.2 Productivity Based on Standard Estimation Reference Books

To operate at a profit, contractors must keep track of productivity and the factors that affect it. Accurate estimations of productivity rates ensure competitive bidding and operating within budget. Several reference books are available to assist the estimator with productivity rates for many construction operations. Productivity rates are based on completed job costs. Data are gathered from many contractors over a large area. The results are averaged and tabulated. Jobs with conditions that affect productivity are averaged separately or a factor is applied to the tabulated value to account for the varying condition.

The *Building Estimator's Reference Book*, commonly known as the "Walker Guide," is a widely used construction estimating reference. According to the Walker Guide (Siddens 1992), size, weight, class of work, openings in walls, site conditions, and whether the wall is above or below grade are the factors that most affect the productivity of concrete masonry construction. The reference states that "it is usually more economical to use lightweight units, even though they cost a few cents more per piece, because a mason can handle and lay them with less effort." The reference also states that facing walls laid in various patterns with tooled joints are more expensive. Separate tables are given for different bonds. Factors are included for type of joint required.

Table 7.18 gives the number of blocks that can be laid under average conditions by one laborer and one mason in an 8-hour day, according to the Walker Guide. The values were obtained using cement lime mortar. If Portland cement mortar is used, daily output is reduced by 5 percent. The values given are for lightweight units. A footnote states that an increase in labor and a decrease in quantities by 10 percent are required if normal-weight units are used.

The Walker Guide also gives the cost of labor for laying 100 ft^2 of standard facing block in a running or ashlar bond. Table 7.19 gives the values for 8 x 8 x 16-in. units. The rates for labor are averaged much like those for productivity. The labor cost given per square foot is $3.13. The corresponding productivity rate is 0.114 man-hours per square foot (or 0.114 m.h./SF).

Concrete and Masonry Cost Data (R.S. Means, published annually) is another popular estimator's reference. This estimating guide also takes averages from data acquired from all over the country. This reference gives a productivity rate of 0.11 m.h./SF for partition walls tooled on both sides (Means 1985). *Dodge Construction Systems Costs*, another annual publication giving overall costs for various systems, gives productivity rates in the range of 0.12 m.h./SF to 0.14 m.h./SF for tooled 8 x 8 x 16-in. CMU exterior and partition walls (Periera 1986). Based on these three references, an average productivity rate of between 0.11 m.h/SF and 0.14 m.h./SF can be expected when laying tooled block walls.

The 1993 rate in Omaha for masons was $19.65 per hour. The rate for a mason's laborer was $12.30 per hour. These rates include benefits such as health insurance and retirement, but do not include employer payments for workman's compensation, unemployment, or social security taxes. Although these expenses are somewhat

variable, 30 percent of the wage rate is considered a fair estimate. Therefore, the (1993) cost in Omaha to hire one mason and one laborer for one hour is:

$$1.3(\$19.65 + \$12.30) = \$41.54$$

Because this constitutes 2 man-hours, the cost per man-hour of a two-man mason crew in Omaha is $20.77/m.h. Using an estimated 0.125 m.h./SF as an average productivity rate, the cost of labor of laying 1 ft^2 of tooled concrete masonry wall in Omaha is approximately $2.60 per square foot. Since each unit is 0.89 ft^2, the cost of labor per unit in Omaha for laying standard 8 x 8 x 16-in. CMU walls is approximately $2.31 per unit.

Lightweight units can be handled with one hand and are less tiring to lift. Therefore, an increase in field productivity is expected when using lightweight units. This increase in productivity will vary with the type and weight of unit used, the familiarity of the crew with the unit, the type of construction, and other factors.

As productivity increases, the cost of labor per unit decreases proportionately. Since the cost of labor per unit is over twice the cost per block, this cost reduction has a dramatic effect on the total cost of the finished product. Table 7.20 shows the costs for labor and materials for lightweight blocks based on 1993 Omaha labor rates, and the decrease in costs anticipated for lightweight units due to varying increases in field productivity. The total anticipated construction costs for lightweight and normal-weight units are also shown graphically in Figure 7.2.

Table 7.17 also shows that the total cost of building with lightweight units is the same as normal-weight units if a 10 percent increase in field productivity is realized. If an increase in field productivity of over 10 percent can be achieved by the use of lightweight units, the total construction costs for lightweight units will be lower than standard-weight units.

7.4.3 Field Productivity Example

Many factors influence the field productivity of concrete masonry. The skills, knowledge, and abilities of each mason are unique, and crews are formed of many individuals. Yet the skills and abilities of the crew members, and how well those members interact with one another dramatically affects the performance of the crew and their productivity. These factors cannot be adequately addressed in a productivity study.

Familiarity with the type of work being performed is also an important factor in productivity. Although this factor is easier to control, it is still somewhat subjective. Practice with new products or systems before a study will help to decrease the discrepancy due to unfamiliarity. However, until a new product has been used extensively, the peak of the learning curve is not known, and workers will never be equally familiar with two different products. There is a degree of variance in familiarity with the work that cannot be controlled in a study.

Many factors affecting the productivity of concrete masonry construction can be identified and directly controlled. The spacing and placement method of reinforcing steel drastically changes the productivity for some types of units. The type of bond, weight and geometry of the unit, type of mortar used, and the method of finishing joints also affects productivity. These variables are usually kept constant unless they are the variable of interest.

Site conditions and variations in the structure also affect the productivity of concrete masonry construction. Running bond must be interrupted for openings. The mason must use special units or saw standard units to finish the courses. If the number of openings in a structure cannot be kept constant, productivity rates must be adjusted to account for the number and size of openings. Working conditions at field sites can never be fully controlled. However, field studies performed under similar conditions can yield adequate comparative results. If extremes in conditions such as cold weather or irregular terrain are not considered, differences in productivity due to differing site conditions may be significant.

A further demonstration of field productivity was conducted in July, 1992, when a retaining wall was constructed in Omaha, NE, using the optimized A-shape, high-performance lightweight units and the standard normal-weight units. The purpose of the wall was to test the performance of the units *in situ*. The masons that built the wall had no prior experience with the new units. Since many different mason crews were used in laying the units, conclusive productivity results were not obtained.

After building the wall, the masons were given an opportunity to comment on the new units. All of the masons were impressed with the lightweight and easy handling of the units. Several different estimates were given on how much could be saved in field productivity by using the new units instead of standard units, but the overall consensus was that 15 percent was a conservative estimate.

Table 7.1. Cost components for CMUs.

Item	Unit	Cost per Unit ($)
Expanded shale	lb	0.0197
AggreCel™	lb	0.0110
Expanded clay	lb	0.0165
3M Macrolite™	lb	0.0750
Sand and Gravel	lb	0.0021
Silica fume cement	lb	0.0400
Type-III cement	lb	0.0375
Fly ash	lb	0.0080
Condensed Silica fume	lb	0.5000
Hydrated Lime	lb	0.0495
Ultra Mix	oz	0.0570
Krete Plast	oz	0.0570
Krete Mix	oz	0.0560
Acme Shield	oz	0.0784
Dry Guard	oz	0.0680
Fiber mesh	Bag (1.5 lb)	8.000
Plant production cost	Optimized CMU	0.1925
	Standard CMU	0.1750
Transportation cost	Optimized CMU	0.0743
	Standard CMU	0.1568
General & Administration cost	Optimized CMU	0.3194
	Standard CMU	0.3194

Table 7.2. Material costs for standard normal-weight unit with standard shape.

Item	Cost ($/lb)	Quantity (lb/unit)	Cost ($/unit)
Sand and Gravel	0.0021	35.40	0.074
Type-III cement	0.0375	2.66	0.099
Fly ash	0.008	0.68	0.0054
Krete Plast	0.057 ($/oz)	0.0109	0.0006
Krete Mix	0.056 ($/oz)	----	----
Total		38.74	0.1803
Note: Number of units per yd^3 batch = 76			

Table 7.3. Material costs for high-performance normal weight mix (W12) with optimized shape.

Item	Cost ($/lb)	Quantity (lb/unit)	Cost ($/unit)
Sand and Gravel	0.0021	25.49	0.0535
Silica fume cement	0.04	3.57	0.1427
Fly ash	0.008	1.54	0.0123
Krete Plast	0.057 ($/oz)	0.054	0.0031
Krete Mix	0.056 ($/oz)	0.126	0.0070
Total		30.6	0.2186
Note: Number of units per yd^3 batch = 101			

Table 7.4. Material costs for standard all-lightweight 8-in. unit.

Item	Cost ($/lb)	Quantity (lb/unit)	Cost ($/unit)
Haydite	0.013	20.2	0.262
Type-I cement	0.035	2.42	0.085
Fly ash	0.0047	1.90	0.009
Krete Plast	0.057 ($/oz)	---	---
Krete Mix	0.056 ($/oz)	---	---
Total		24.52	0.356
Note: Number of units per yd^3 batch = 65			

Table 7.5. Material costs for high-performance lightweight mix (W11') with optimized shape.

Item	Cost ($/lb)	Quantity (lb/unit)	Cost ($/unit)
Expanded shale	0.0197	13.7	0.2707
Silica fume cement	0.04	3.17	0.1269
Fly ash	0.008	1.38	0.011
Krete Plast	0.057 ($/oz)	0.048	0.0027
Krete Mix	0.056 ($/oz)	0.12	0.0065
Total		18.25	0.4178
Note: Number of units per yd^3 batch = 106			

Table 7.6. Material cost of lightweight CMUs.

Mix No.	Expanded shale ($)	Cement ($)	Fly ash ($)	Admixture ($)	Material cost per batch ($)	Units per yd^3	Material cost per unit ($)
Std. NW	5.67	7.65	0.416	0.0714	13.8074	76	0.1803
W11(old)	39.40	18.48	1.60	1.368	60.848	145	0.4196
W11'	28.7226	13.44	1.168	0.957	44.2876	106	0.4178
W11'-PC	28.7226	13.44	1.168	4.0146	47.3452	106	0.4467
W16	28.7226	16.44	3.76	1.745	50.6676	127	0.3990
W17	28.7226	16.44	3.76	4.8026	53.7252	127	0.4230
W22	28.7226	29.05	5.763	2.249	65.7846	127	0.5180
W24	28.7226	29.05	5.025	2.249	65.0418	127	0.5121
All-LW	17.68	5.705	0.6016	---	23.9866	65	0.356

Table 7.7. Material cost of normal-weight CMUs.

Mix No.	Sand and Gravel ($)	Cement ($)	Fly ash ($)	Admixture ($)	Material cost per batch ($)	Units per yd^3	Material cost per unit ($)
Std. NW	5.67	7.65	0.416	0.0714	13.8074	76	0.1803
W12	5.67	15.08	1.304	1.069	23.123	106	0.2181
W13	5.67	7.65	0.416	0.0714	13.8074	96	0.1438
W14	5.67	23.0875	1.304	1.013	31.0745	106	0.2932
W15	5.67	7.65	0.416	4.012	17.748	96	0.1849
W18	5.67	12.1875	0.648	0.114	18.6195	102	0.1825
W19	5.67	12.1875	0.648	8.114	18.6195	102	0.1825
W23	5.67	16.0625	1.08	0.732	23.5445	100	0.2354

Table 7.8. Other expenses for lightweight CMUs.

Mix No.	Plant expenses per unit ($)	Shipping cost per unit ($)	Administration and profit ($)	Total other expenses ($)
Std. NW	0.1750	0.1568	0.3194	0.6512
W11(old)	0.1925	0.0743	0.3194	0.5862
W11'	0.1925	0.0743	0.3194	0.5862
W11'-PC	0.1925	0.0743	0.3194	0.5862
W16	0.1925	0.0743	0.3194	0.5862
W17	0.1925	0.0743	0.3194	0.5862
W22	0.1925	0.0743	0.3194	0.5862
W24	0.1925	0.0743	0.3194	0.5862

Table 7.9. Other expenses for normal-weight CMUs.

Mix No.	Plant expenses per unit ($)	Shipping cost per unit ($)	Administration and profit ($)	Total other expenses ($)
Std. NW	0.1750	0.1568	0.3194	0.6512
W12	0.1925	0.1238	0.3194	0.6357
W13	0.1925	0.1238	0.3194	0.6357
W14	0.1925	0.1238	0.3194	0.6357
W15	0.1925	0.1238	0.3194	0.6357
W18	0.1925	0.1238	0.3194	0.6357
W19	0.1925	0.1238	0.3194	0.6357
W23	0.1925	0.1238	0.3194	0.6357

Table 7.10. Relative costs for lightweight CMUs.

Mix No.	Material cost per unit ($)	Other expenses per unit ($)	Total cost per unit ($)
Std. NW	100	100	100
W11(old)	232.7	90.0	121.0
W11'	266.9	90.0	128.4
W11'-PC	282.9	90.0	131.8
W16	257.2	90.0	126.3
W17	270.5	90.0	129.6
W22	287.3	90.0	132.8
W24	284.0	90.0	132.1
All-LW	197.5	---	---

Table 7.11. Relative costs for normal-weight CMUs.

Mix No.	Material cost per unit ($)	Other expenses per unit ($)	Total cost per unit ($)
Std. NW	100	100	100
W12	121.0	97.6	105.3
W13	79.8	97.6	93.7
W14	162.6	97.6	111.7
W15	102.6	97.6	98.7
W18	101.2	97.6	98.4
W19	144.8	97.6	107.8
W23	130.6	97.6	104.8

Table 7.12. Proportions of lightweight mixes.

Mix No.	Expanded Shale lb/yd³	Silica Fume Cement lb/yd³	Fly Ash lb/yd³	Krete Plast fl oz	Krete Mix fl oz
All-LW	Haydite 1360	Type-I - 163	128	---	---
W4	Coarse 740 Fine 901	462	528	---	---
W11 (old)	Medium 1500 Fine 500	462	200	7	Ultra Mix 17
W11'	1458	336	146	5	12
W11'-PC	1458	336	146	5	12 Acme Shield 39
W16	1458	411	470	9	22
W17	1458	410	470	9	22 Acme Shield 39
W21	1458	346	212	6	22

Mix No.	Expanded Shale lb/yd³	Type-III Cement lb/yd³	Silica Fume lb/yd³	Fly Ash lb/yd³	Hydrated Lime lb/yd³	Krete Plast fl oz	Krete Mix fl oz
W22	1458	388	29	411	50	9	31
W24	1458	388	29	411	35	9	31

Table 7.13. Proportions of normal-weight mixes.

Mix No.	Sand and Gravel lb/yd³	Cement lb/yd³	Fly Ash lb/yd³	Krete Plast fl oz	Krete Mix fl oz
W12	2700	Silica fume cement - 377	163	5	14
W13 (Std. NW)	2700	Type III - 204	52	1.3	---
W14	2700	Type III - 349 Silica fume - 20	163	5	13
W15	2700	Type III - 204	52	Dry guard - 62	---
W18	2700	Type III - 325	81	2	---
W19	2700	Type III - 325	81	2	Fiber mesh 1 bag (1.5 lb)
W20	2700	273	160	4	17

Mix No.	Sand and Gravel lb/yd³	Type-III cement lb/yd³	Silica Fume lb/yd³	Fly Ash lb/yd³	Krete Plast fl oz	Krete Mix fl oz
W23	2700	215	16	135	4	9

Table 7.14. Size and properties of CMUs tested by NCMA.

Size (in.)	Lightweight		Normal weight	
	Weight (lb)	Unit Weight (pcf)	Weight (lb)	Unit Weight (pcf)
4 x 8 x 16	17.0	88.9	24.3	130.1
6 x 8 x 16	19.1	84.1	32.6	129.7
8 x 8 x 16	25.3	90.5	34.3	128.1
12 x 8 x 16	35.6	89.0	48.4	126.6
4 x 8 x 24	26.1	93.9	36.6	133.8
8 x 8 x 24	46.4	101.6	52.9	131.8

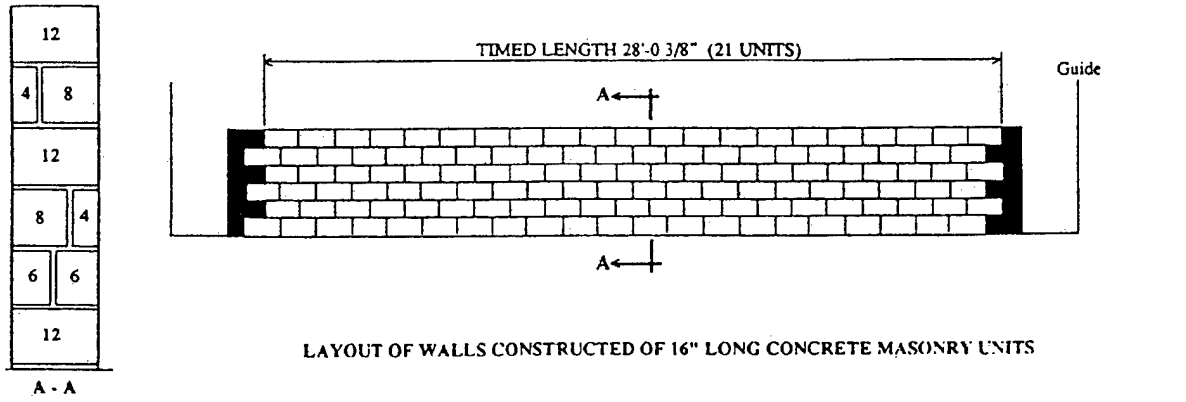

Figure ©1987 NCMA. Reprinted with permission.

Figure 7.1. Layout of walls constructed of 24-in. long concrete masonry units.

Table 7.15. Comparison of productivity findings for 16-in. units.

Unit Size	Unit Type	Course	Line Placement	Time (min:sec)	Blocks/hr	Ft^2/hr	% Change
	HW			15:28	81.4	72.9	
	LW	3	Inside	13:21	86.7	86.7	+18.9
	HW			19:16	65.3	58.5	
4x8x16	LW	5	Outside	15:36	80.7	72.2	+23.4
	HW			15:04	83.5	74.8	
	LW	2	Outside	14:32	86.7	77.5	+3.6
	HW			15:15	82.6	73.9	
6x8x16	LW	2	Inside	14:01	89.8	80.4	+8.8
	HW			16:26	76.6	68.6	
	LW	3	Outside	15:12	82.9	74.1	+8.0
	HW			16:08	78.1	69.8	
8x8x16	LW	5	Inside	14:40	85.9	76.8	+10.0
	HW			16:08	78.1	69.8	
	LW	1	Inside	13:21	94.5	84.4	+20.9
	HW			16:09	78.1	69.8	
	LW	4	Outside	14:51	85.1	75.9	+8.7
	HW			20:36	61.1	54.7	
12x8x16	LW	6	Inside	15:35	80.9	72.3	+32.1

Source: NCMA Research and Development Laboratories, ©1987. Reprinted courtesy of NCMA.

Table 7.16. Comparison of productivity results for 24-in. units.

Unit Size	Unit Type	Course	Line Placement	Time (min:sec)	Blocks/hr	Ft^2/hr	% Change
	HW			13:07	64.1	85.9	
	LW	2	Outside	9:41	86.7	116.4	+35.5
	HW			11:36	72.4	97.1	
	LW	2	Inside	9:03	92.8	124.5	+28.2
	HW			11:36	72.4	97.1	
	LW	4	Outside	9:49	85.5	114.8	+16.2
	HW			10:52	77.3	103.7	
4x8x24	LW	4	Inside	9:34	87.7	117.8	+13.6
	HW			11:52	73.9	95.0	
	LW	1	Inside	9:52	89.8	114.2	+20.2
	HW			10:49	77.6	104.2	
	LW	3	Outside	10:16	81.8	109.8	+5.4
	HW			12:57	64.9	87.0	
	LW	5	Inside	11:28	73.3	98.3	+13.0
	HW			13:57	60.2	80.8	
8x8x24	LW	6	Outside	11:57	70.3	94.3	+16.7

Source: NCMA Research and Development Laboratories, ©1987. Reprinted courtesy of NCMA.

Table 7.17. Comparison of results for 16-in. vs 24-in. units.

Unit		Course	Line Placement	Time/Course (Min:Sec)	Time/Unit (Sec)	No. Blk. (Hr)	Rate (Ft^2/Hr)	Rate (% Change)
Size	Type							
8 x 8 x 16	H.W.	3	Outside	16:26	47.0	76.6	68.6	
8 x 8 x 24	H.W.			10:49	46.4	77.6	104.2	+51.9
8 x 8 x 16	L.W.	3	Outside	15:12	43.4	82.9	74.1	
8 x 8 x 24	L.W.			10:16	44.0	81.8	109.8	+48.2
8 x 8 x 16	H.W.	5	Inside	16:08	46.1	78.1	69.8	
8 x 8 x 24	H.W.			12:57	55.5	64.9	87.0	+24.6
8 x 8 x 16	L.W.	5	Inside	14:40	41.9	85.9	76.8	
8 x 8 x 24	L.W.			11:28	49.1	73.3	98.3	+28.0
Source: NCMA Research and Development Laboratories, ©1987. Reprinted courtesy of NCMA.								

Table 7.18. Number of lightweight units laid in one day (one laborer and one mason).

	Number of Units	Mason Hours	Labor Hours
Size	(8 hr)	(100 pieces)	(100 pieces)
8 x 8 x 16	150 - 170	5.0	5.0
Source: Walker 1982.			

Table 7.19. Cost of laying 100 ft^2 of facing block in a running or ashlar bond.

	Hours	Labor Rate	Total Cost ($)
Mason	7	25.62	179.34
Laborer	7	19.13	133.91
		Total Cost	313.25
Source: Walker 1982.			

Table 7.20. Material and labor cost ($) with increased field productivity (8 x 8 x 16 units in Omaha, NE, 1993).

	Percent Increase in Field Productivity						
	0%	5%	10%	12%	15%	20%	25%
Material - NW	0.82	0.82	0.82	0.82	0.82	0.82	0.82
Material - LW	1.05	1.05	1.05	1.05	1.05	1.05	1.05
Labor - NW	2.31	2.31	2.31	2.31	2.31	2.31	2.31
Labor - LW	2.31	2.19	2.08	2.03	1.96	1.85	1.73
Total Cost - LW	3.36	3.24	3.13	3.08	3.01	2.90	2.78
Total Cost - NW	3.13	3.13	3.13	3.13	3.13	3.13	3.13

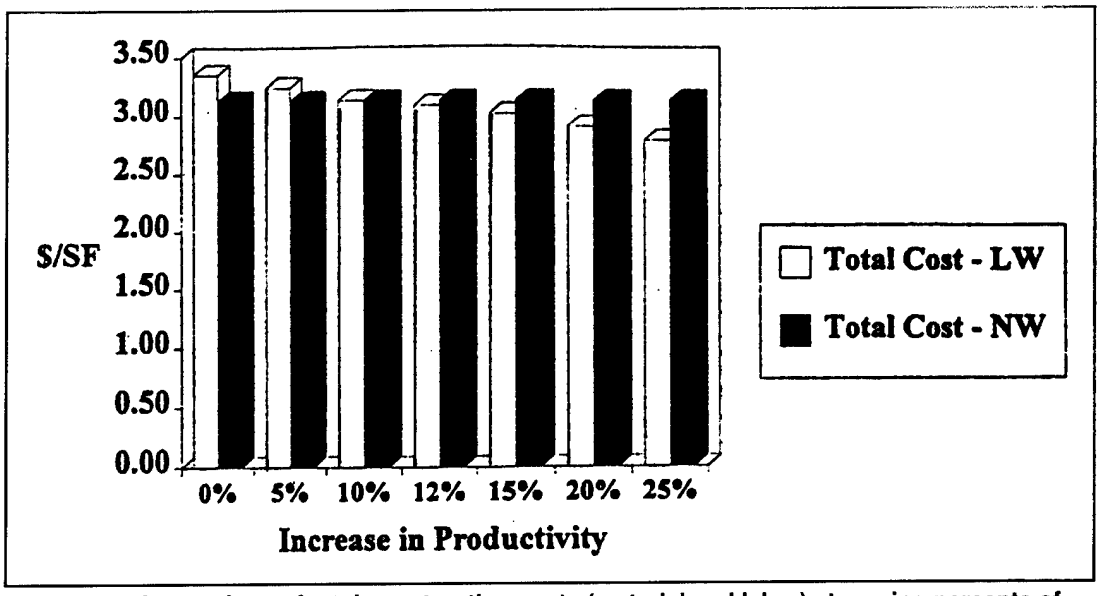

Figure 7.2. Comparison of total construction costs (material and labor) at varying percents of increased productivity due to the use of lightweight units.

8 Conclusions, Recommendations, and Commercialization

8.1 Conclusions

A new type of high-strength lightweight CMU has been designed, engineered, and tested in this CPAR project. In the testing reported here the new CMU has met or exceeded all performance-based requirements for block masonry. Using expanded shale aggregates and an optimized unit shape as the primary innovative components, the high-performance lightweight CMUs weighed about 19 lb (8.6 kg) and had average net compressive strength of 4000 lb/in.^{2} (28 MPa). The minimum void gradation of the expanded shale was modified to provide high strength, good durability, and a smooth, uniform texture as specified in the research objective.

Using a standard brick durability test modified for application to CMUs, the durability of lightweight units was shown to improve as the amount of cementitious materials was increased to over 12 percent (by absolute volume). However, a sharp decline in durability indicators was observed as the percentage of cementitious materials in the mix was increased above 15 percent (by absolute volume). Based on these findings, it is concluded that an optimum mix exists somewhere between 10 and 15 percent cementitious materials by absolute volume. This study produced insufficient data to determine the optimum mix, however.

Similar durability peaks were observed for the percentage of fly ash in the mix (5 to 9 percent by absolute volume). The ratio of the percentage of fly ash to the total percentage of cementitious materials in the mix ranged from 0.4 to 0.5 by absolute volume, and the ratio of the percentage of silica fume to the percentage fly ash in the mix was around 0.1 by absolute volume. Research studying each of these relationships as independent variables may result in identifying optimal mix proportions for high-performance lightweight CMUs with respect to durability.

Results of statistical t-tests on the durability data indicated that, although the sample mean was slightly higher for the standard CMU specimens than for the specimens made from mix W11, there was insufficient probability to support the conclusion that one was superior to the other. The t-tests also indicated that the

W11 specimens significantly outperformed the standard lightweight specimens under freeze-thaw cycling.

It is concluded that the durability test procedure developed in this project now represents the best available procedure for testing CMU durability. Little or no weight loss occurred in the specimens during testing, but the dynamic modulus of elasticity of each specimen dropped significantly with repeated freeze-thaw cycling. Therefore, change in dynamic modulus of elasticity appears to be preferable to weight loss as a CMU durability criterion.

During an abandoned test, water levels in the test containers were allowed to drop well below the tops of the specimens. These specimens exhibited an accelerated rate of degradation. This observation suggests that the saturated freeze-thaw test may not represent the worst-case test for concrete masonry units.

Many specimens that had high initial weight gains also exhibited low freeze-thaw resistance. This corroborates the findings of Powers (1945, 1965) and Helmuth (1961, 1962) that deterioration is caused by the osmosis of liquids into the cells. Rapid freeze-thaw tests do not adequately model *in situ* conditions.

It is concluded that admixtures have a significant impact on the durability and production of the new lightweight units. Statistical analyses of the data indicated that the W11-PC specimens outperformed all other specimens in freeze-thaw durability. The only difference between the W11 and W11-PC mixes was the precoating of the aggregates with fatty acid waterproofers before mixing. These results are strong evidence that aggregate absorption during mixing and/or after the mix has cured can significantly affect freeze-thaw resistance in CMUs.

The use of plasticizers and set retarders affects the machinability of the mix and therefore the density and uniformity of the matrix. These admixtures may affect the physical and chemical characteristics of the units. If the quantities of these admixtures change drastically from those in the units tested, the relationships given in section 6.2 may vary.

Mix W14 had the highest strength of the normal-weight mixes. Net compressive strengths for the W14 units were over 7000 psi and the surface was nearly impenetrable. However, the cost was over 12 percent higher than the standard unit and the freeze-thaw resistance of the mix was low. Mix W23 was a successful attempt to lower the price and increase durability, but Mix W18—a mix with high cement content, very little fly ash, and no silica fume—had higher strength and durability at a still lower cost.

Choosing the optimum lightweight mix is difficult. Mixes with lower percentages of fly ash and cementitious materials had higher strengths and lower absorption results, but texture was far superior in mixes using higher percentages of fly ash and cementitious materials. Some of the mixes that included lime yielded very high strengths and reasonable absorption rates, but these mixes proved to be expensive and were difficult to machine in the plant—even with the addition of large quantities of admixtures. This research has identified several good choices for lightweight mix, however, depending on the intended use:

- The W11 mix design produces a unit with high strength, reasonable absorption, low efflorescence, and acceptable freeze-thaw durability. Even with its more open texture and somewhat higher cost, it is the prime choice for retaining walls and structural footings.
- The W16 mix produces smooth-surfaced blocks that may be preferred for basements and interior facing walls. This unit is also the least expensive of the high-performance lightweight units.
- If freeze-thaw resistance is critical to design, the optimum choice is the W11-PC unit. Although this unit is somewhat more expensive than the others, it is superior to standard CMUs in freeze-thaw resistance.

The final production cost of units from these three mixes was 32 percent higher than the production cost for standard normal-weight CMUs. However, the productivity analysis conducted in this work indicates that a 10 percent increase in field labor productivity would offset the higher per-unit production cost. After field productivity tests using lightweight units, participating masons determined that a 15 percent field productivity increase was a reasonable, conservative expectation. Such an improvement would lower net direct construction costs by 3.8 percent. Furthermore, significant intangible cost benefits could be expected to accrue in the form of reduced labor-related losses due to injuries, workmans compensation, and disability.

In a peripheral investigation conducted by the National Concrete Masonry Association (NCMA) during this study, some of the experimental mixes were used to produce a limited quantity of 24-in. normal-weight and lightweight high-performance CMUs. Masonry contractors who participated in the NCMA study expressed interest in the potential productivity gains that could arise from the use of 24-in. high-performance CMUs. In this productivity study, productivity using a lightweight 24-in. unit was 60 percent higher than when using the 16 in. normal-weight unit (NCMA 1995).

8.2 Recommendations

The results of this study demonstrate that the new high-strength lightweight CMU provides a cost-effective and safer alternative for most concrete masonry construction. The units are recommended for use in all load-bearing wall applications. In addition, the units are recommended for shear wall applications when the walls are fully grouted. The units are not recommended at this time for partially grouted shear wall applications. When using the new lightweight CMU, all standard masonry design and construction practices for either above- or below-grade use, as applicable, should be followed.

During the course of this investigation, several masonry testing and performance issues were determined by the researchers to require additional research, but such research was beyond the scope of the CPAR objective. Nevertheless, these issues should be studied by the science and engineering community within the masonry industry. Specifically, it is recommended that: (1) further research on CMU durability be conducted using a partially saturated test method that simulates the worst-case scenario for CMUs in freeze-thaw cycling, (2) that a freeze-thaw CMU durability test procedure based on dilation be developed as a follow-up to the correlation identified between initial CMU weight gains in saturation and low freeze-thaw resistance, and (3) that further research be conducted on the impact of admixtures and aggregate absorption on CMU durability.

8.3 Technology Transfer and Commercialization

Army Corps of Engineers-recommended masonry details have been revised to include the A-shaped CMU for all reinforced masonry applications. These details are shown in Drawing No. 00-90-04 and are available from U.S. Army Engineer Division Huntsville, AL. Information on lightweight units has also been integrated into the Corps PROSPECT course on Masonry Design.

The high-strength lightweight CMU produced in this project corresponds to all performance-based criteria in ASTM C 90. However, it does not conform to the empirical-based face shell thickness requirements, so local waiver of this requirement by building officials may be required.

The high-strength lightweight CMU can be manufactured by most modern block manufacturing plants in the world that use the standard vibro-press block-making technology. Any prospective manufacturer of these CMUs needing information on mix design, mold design, or manufacturing beyond what is documented in this

technical report should contact the University of Nebraska Center for Infrastructure Research, Omaha, NE.

Results of this effort have been disseminated to industry professionals through several technical papers, conference presentations, press releases, and trade shows. Articles presenting this new CMU have been published in *Masonry Construction* magazine, and a promotional videotape is available in limited quantities from USACERL.

The Nebraska Masonry Institute and the Masonry Contractors Association of Northern Nebraska—both of which were partner participants in this CPAR research—have disseminated product information to their members and national parent organizations. These two organizations will continue to promote the use of the product, which is commercially available in the Omaha metropolitan area.

References

ACI 201, *Guide to Durable Concrete* (American Concrete Institute, 1977).

American Concrete Institute [ACI] Committee 318, Building Code Requirements for Structural Concrete and Commentary, ACI 318-95 (ACI, 1995).

ACI 530-92/ASCE 5-92/TMS 402-92, *Building Code Requirements for Masonry Structures* (American Concrete Institute Standards, Detroit, MI, 1992).

ACI 530.1-92/ASCE 6-92/TMS 402-92, *Specifications for Masonry Structures* (American Concrete Institute Standards, Detroit, MI, 1992).

ACI 530-92/ASCE 5-92/TMS 402-92, *Commentary on Building Code Requirements for Masonry Structures* (American Concrete Institute, Detroit, MI, 1992).

ACI 530-92/ASCE 5-92/TMS 402-92, *Commentary on Specifications for Masonry Structures* (American Concrete Institute Standards, Detroit, MI, 1992).

Amrhein, James J., *Reinforced Masonry Engineering Handbook* (Masonry Institute of America, 2550 Beverly Boulevard, Los Angeles, CA, 90057, 1992).

American Society for Testing and Materials. *Standard Test Methods for Compressive Strength of Masonry Prisms* (Annual Book of ASTM Standards, Philadelphia, PA, 1990).

ASTM C 90-96, *Standard Specification for Loadbearing Concrete Masonry Units* (ASTM, Philadelphia, PA, 1996), section 4, vol 4.05.

ASTM C 666-80, *Standard Test Method for Resistance of Concrete to Rapid Freezing and Thawing* (ASTM, Philadelphia, PA, 1996), section 4, vol 4.02.

Amiri, Babrak, G.L. Krause, and M.K. Tadros, "Lightweight High-performance Concrete Block Mix Design," *ACI Materials Journal* (June 1993).

Amiri, B., "Mix Design of Lightweight Masonry Blocks"; *Proceedings of the Fifth North American Masonry Conference* (Philadelphia, PA, 1993).

Afshari, Farhad, and Movses J. Kaldjian, "Finite Element Analysis of Concrete Masonry Prisms," *ACI Materials Journal*, vol 86, no. 5 (Sep.-Oct. 1989), pp 525-530.

Aitein, Pierre Claude, *Condensed Silica Fume* (Les Editions de l'Universite de Sherbrooke, 1983).

Atkinson, R.H., "Effect of Loaden Platting Thickness on Masonry Units and Prism Strengths," *The Masonry Society Journal*, vol 10, no. 1 (August 1991), pp 86-87.

BS 5628 Part 1, *Code of Practice for Structural Use of Masonry. Part I : Unreinforced Masonry* (British Standard Institution, London, England, 1992).

Bexton, Karen A., Maher K. Tadros, and Richard T. Horton, "Compression Strength of Masonry," *5th Canadian Masonry Symposium*, vol 2 (Vancouver: University of British Columbia, 1989), pp 629.

Bowser, J.D., "Water Penetration and Absorption of High-performance Lightweight Concrete Masonry Units"; *Sixth North American Masonry Conference* (Philadelphia, PA, 1993).

Bowser, J.D., S.M. Kulkarni, M.K. Tadros, G.L. Krause, and S.C. Sweeney, "Water Penetration and Absorption of High-performance Lightweight Concrete Masonry Units," *The Sixth North American Masonry Conference Proceedings* (Philadelphia, PA, June 1993).

Buildex Inc., *A Unique Combination of Quality & Economy* (Buildex Publication #141, P.O. Box #15, Ottawa, KS).

Butler, Steven M., "Preliminary Study on the Chemical Composition and Utilization of Fly Ash," *Special Problems Report - University of Nebraska at Omaha* (August 1992).

Cheema, T.S., and R.E. Klinger, "Compressive Strength of Concrete Masonry Prisms." *ACI Materials Journal*, vol 86, no. 5 (Sep.-Oct. 1989), pp 525-530.

Chahine, G.N., and R.G. Drysdale, "Influence of Test Conditions on the Compressive Strength and Behavior of Face Shell Mortar Bedded Concrete Block Prisms," *5th North American Masonry Conference*, vol 2 (Urbana: University of Illinois, 1990), pp 663.

Concrete International, "Products & Practice" (July 1991).

Dhir, K., R.G.C. Mays, and H.C. Chua, "Lightweight Structural Concrete With Aglite Aggregate; Mix Properties," *International Journal of Cement Composite and Lightweight Concrete*, vol 6, no. 4 (November 1984).

Drysdale, Robert G., and Ahmed A. Hamid, "Behavior of Concrete Block Masonry Under Axial Compression," *ACI Journal*, vol 76 (June 1979), pp 707.

Dunn, J.R., and P.P. Hudec, "The Influence of Clays on Water and Ice in Rock Pores" Report No. RR65-5 (New York State Dept. of Public Works, 1965).

Expanded Shale Clay & Slate Institute, *Construction with the Speed of Light* (Expanded Shale Clay & Slate Institute, Salt Lake City, UT).

Ganesan T.P., and K. Ramamurthy "Behavior of Concrete Hollow-Block Masonry Prisms Under Axial Compression," *Journal of Structural Engineering*, vol 118, no. 7 (July 1992).

Gmb H Maschinenfabric, "Mix Compositions for the Production of Hollow Concrete Blocks" (KNAUER Information No. 2/74, Germany).

Hamid, Ahmed E., and Ambrose O. Chukwunenye,"Compression Behavior of Concrete Masonry Prisms," *Journal of Structural Engineering*, vol 112, no. 3 (March 1986), pp 605-613.

Hamid, Ahmed E., and Ambrose O. Chukwunenye, "Effect of Type of Mortar Bedding on the Behavior of Axially Loaded Hollow Block Masonry Prisms," *Proceedings of the Third North American Masonry Conference*, University of Texas at Arlington, Arlington, TX (June 1985), pp 16.1–16.11.

Helmuth, R.A., "Dimensional Changes of Hardened Portland Cement Pastes Caused by Temperature Changes," *Proceedings, Highway Research Board*, vol 40 (1961), pp 315-336.

Helmuth, R.A., "Capillary Size Restrictions on Ice Formation in Hardened Portland Cement Pastes," *Proceedings. Fourth International Symposium on the Chemistry of Cement*, Monograph No. 43 (National Bureau of Standards, vol 2 (Washington, D.C., 1962), pp 829-833.

Hirata, S.K., and M.I. Hanunons, "The Positive Effect of Class C Fly Ash on Creep in Mass Concrete Structures," *Proceedings: Ninth International Ash Use Symposium Volume 1: Concrete and Related Products* (American Coal Ash Association, Washington, D.C., January 1991).

Holm, T.A., *Engineered Masonry with High-strength Lightweight Concrete Masonry Units* (Solite Corporation).

Huang, R., S.T. Kuo, C.M. Liu, and J.J. Cfbang, "The Properties of High Fly Ash Concrete," *Proceedings: Ninth International Ash Use Symposium Volume 1: Concrete and Related Products* (American Coal Ash Association, Washington, D.C., January 1991).

Idorn, G.M., "Research and Development for the Use of Fly Ash in Cement and Concrete," *Workshop Proceedings: Research and Development Needs for Use of Fly Ash in Cement and Concrete* (Electric Power Research Institute,1982).

Khalaf, F., A. Handry, and D. Fairbairn, "Concrete Block Masonry Prisms Compressed Normal and Parallel to Bed Face," *5th North American Masonry Conference*, vol 1. (Urbana-Champaign: University of Illinois, 1990), pp. 595.

Khalifa, Magdi A., Maher K. Tadros, Say-Gunn Low, and Ahmed E. Magzoub, "Shape Optimization of an Ultra Lightweight CMU," *The Masonry Society Journal* (April, 1993).

Khalil, M.R.A., N.G. Shrive, and P. Ameny, "Three Dimensional Stress Distribution in Concrete Masonry Prisms And Walls," *Magazine of Concrete Research*, vol 39, no. 139 (June 1987), pp 73-82.

Klieger, P., "Recommended Practice for Selecting Proportions for No-Slump Concrete," *ACI 211 - 65, Subcommittee 2 Committee 211.*

Koski, J.A., "High-strength Structural Load Bearing Masonry in Tall Buildings" (Masonry Construction, February 1992).

Kosmatka, Steven H., and William C. Panarese, *Design and Control of Concrete Mixtures - Thirteenth Edition* (Portland Cement Association, Skokie, IL, 1988).

Kulkarni, S.M., *High-performance Concrete Masonry Unit Mix Design*, Thesis (University of Nebraska at Lincoln, 1993).

Larsen, T.J., and J.M. Armghani, "Quality Concrete with Fly Ash," *Proceedings: Eight International Ash Utilization Symposium*, vol 1 (American Coal Ash Association, Washington, D.C. 1987).

Litvan, G.G., "Phase Transitions of Adsorbates: IV, Mechanism of Frost Action in Hardened Cement Paste," *Journal, American Ceramic Society*, vol 55, no. 1 (January 1972), pp 38-42.

Low, Say-Gunn, M.K. Tadros, A. Einea, M.A. Khalifa, A.E. Magzoub, and E. Staab, "Shape Optimization of Concrete Masonry Units," *The Sixth North American Masonry Conference Proceedings* (Philadelphia, PA, June 1993).

Low, S.G., "Shape Optimization of Concrete Masonry Units," *Proceedings of the Fifth North American Masonry Conference* (Philadelphia, PA, 1993).

Malhotra, V.M., V.S. Ramachandran, and R.F. Feldman, Pierre-Claude Aitcin, *Condensed Silica Fume in Concrete* (Florida, 1987).

Maurenbrecher, A.H.P., "Axial Compression Tests on Masonry Walls and Prisms," *Proceedings of the Third North American Masonry Conference* (University of Texas at Arlington, Arlington, TX (June 1985), pp 19.1- 19.14.

Means, R.S., *Concrete and Masonry Cost Data* (R.S. Means Publishing Co, Kingston, MA, 1985).

Naik, T.R., and B.W. Ramme, "Setting and Hardening of High Fly Ash Content Concrete," *Proceedings: Eight International Ash Utilization Symposium, vol. 1* (American Coal Ash Association, Washington, D.C., 1987).

National Concrete Masonry Association (NCMA) Research and Development Laboratories, *Research Investigation of Mason Productivity* (NCMA, Herndon, VA, 1987).

NCMA High-Strength Block Task Force, *Special Considerations for Manufacturing High-strength Concrete Masonry Units* (NCMA, Herndon, VA 22070, 1971).

NCMA, "Discussion of Concrete Block Mix Volume and Yield," Technical Bulletin #6 (2009 14th Street North, Arlington, VA 22201, December 1955).

NCMA, "Aggregate Gradation for Concrete Block," Technical Bulletin #5 (P.O. Box 135, 6845 Elm Street, Maclean, VA 22101, August 1955).

Paz, M., *Structural Dynamics Theory and Computation* (Van Nostrand Reinhold, NY, 1991).

Periera, P.E., *Dodge Construction Systems Costs* (McGraw Hill Information Systems Co., Princeton, NJ, 1986).

Ping, Goo, and R.G. Drysdale, "Stress Strain Relationship for Hollow Concrete Block in Compression," *5th Canadian Masonry Symposium* (Department of Civil Engineering, University of British Columbia, Vancouver, B.C., Canada, vol 2, 1990), pp 599-608.

Powers, T.C., "A Working Hypothesis for Further Studies of Frost Resistance of Concrete," *ACI Journal*, Proceedings vol 41, no. 4 (245272) (February 1945).

Powers, T.C., "The Mechanism of Frost Action in Concrete," *Stanton Walker Lecture No. 3* (National Sand and Gravel Association/National Ready Mixed Concrete Association, Silver Spring, MD, 1965).

Prestera, J.R., D.E. Dixon, and D.A. Crodker, "Standard Practice for Selecting Proportions for Structural Lightweight Concrete," ACI 211-2, *ACI Material Journal*, vol 87, no. 6, Nov.–Dec. 1990.

Roberts, J.J. (1973). "The Effect of Different Tests Procedures upon the Indicated Strength of Concrete Block in Compression," *Magazine of Concrete Research*, 25 (June), pp 87-98.

Schultz, A.G., *NIST Research Program on the Seismic Resistance of Partially Grouted Masonry Shear Walls*, NISTIR 5481 (National Institute of Standards and Technology [NIST], Gaithersburg, MD, June 1994).

Shrive, N.G., and E.L. Jessop, (19n. "Hollow Concrete Blocks with Enhanced Structural Efficiency and Compatible Grout," *Magazine of Concrete Research*, 25 (June), pp 133-140.

Siddens, S., *The Building Estimator's Reference Book* (Frank R. Walker Company, Lisle, IL, 1992).

Tadros, M.K., G.L. Krause, Baabrak Amiri, and S.C. Sweeney, *State of-the-Art of Concrete Masonry Units* (University of Nebraska–Lincoln, March 1992).

Tadros, Maher K., "Flexural Behavior of Reinforced Concrete Masonry Member," *Proceedings of the Third North American Masonry Conference*, University of Texas at Arlington, Arlington, TX (June 1985), pp 31.1–31.17.

Ukita, K., and M. Ishii, "A Fundamental Study on Applicability of Classified Fly Ash for Use as a High-strength Concrete Admixture," *Proceedings: Ninth International Ash Use Symposium, Volume 1* (Concrete and Related Products, American Coal Ash Association, Washington, D.C., January 1991).

Uniform Building Code (International Conference of Building Officials, 5360 South Workman Mill Road, Whittier, CA 900601, 1991).

Verbeck, G. and R. Landgren, "Influence of Physical Characteristics of Aggregates on the Frost Resistance of Concrete." *Proceedings* (ASTM, vol 60, 1960), pp 1063-1079.

Abbreviations and Acronyms

ACI	American Concrete Institute
ASTM	American Society for Testing and Materials
CMU	concrete masonry unit
FEA	finite element analysis
kips	kilopounds
ksi	kilopounds per square inch
lb/ft^3	pounds per cubic foot
MPa	megapascal
NCMA	National Concrete Masonry Association
psi	pounds per square inch
pcf	pounds per cubic foot

USACERL DISTRIBUTION

Chief of Engineers
ATTN: CEHEC-IM-LH (2)
ATTN: CEHEC-IM-LP (2)
ATTN: CECC-R
ATTN: CEMP-ET
ATTN: CERD-L

US Army Engr District
ATTN: Library (40)

US Army Engr Division
ATTN: Library (11)

Defense Tech Info Center 22304
ATTN: DTIC-O (2)

60
6/97